

An integrative taxonomic revision of Pareineae slug-eating snakes (Squamata: Pareidae) reveals unprecedented diversity in Indochina (#64561)

1

First submission

Guidance from your Editor

Please submit by **28 Aug 2021** for the benefit of the authors (and your \$200 publishing discount) .



Structure and Criteria

Please read the 'Structure and Criteria' page for general guidance.



Custom checks

Make sure you include the custom checks shown below, in your review.



Author notes

Have you read the author notes on the [guidance page](#)?



Raw data check

Review the raw data.



Image check

Check that figures and images have not been inappropriately manipulated.

Privacy reminder: If uploading an annotated PDF, remove identifiable information to remain anonymous.

Files

Download and review all files from the [materials page](#).

24 Figure file(s)

18 Table file(s)

3 Raw data file(s)

! Custom checks



DNA data checks

- ! Have you checked the authors [data deposition statement](#)?
- ! Can you access the deposited data?
- ! Has the data been deposited correctly?
- ! Is the deposition information noted in the manuscript?

Vertebrate animal usage checks

- ! Have you checked the authors [ethical approval statement](#)?
- ! Were the experiments necessary and ethical?
- ! Have you checked our [animal research policies](#)?



Field study

- ! Have you checked the authors [field study permits](#)?
- ! Are the field study permits appropriate?

New species checks



- ! Have you checked our [new species policies](#)?
- ! Do you agree that it is a new species?
- ! Is it correctly described e.g. meets ICZN standard?

For assistance email peer.review@peerj.com



Structure your review

The review form is divided into 5 sections. Please consider these when composing your review:

1. **BASIC REPORTING**
2. **EXPERIMENTAL DESIGN**
3. **VALIDITY OF THE FINDINGS**
4. General comments
5. Confidential notes to the editor

You can also annotate this PDF and upload it as part of your review

When ready [submit online](#).

Editorial Criteria

Use these criteria points to structure your review. The full detailed editorial criteria is on your [guidance page](#).

BASIC REPORTING

- Clear, unambiguous, professional English language used throughout.
- Intro & background to show context. Literature well referenced & relevant.
- Structure conforms to [PeerJ standards](#), discipline norm, or improved for clarity.
- Figures are relevant, high quality, well labelled & described.
- Raw data supplied (see [PeerJ policy](#)).

EXPERIMENTAL DESIGN

- Original primary research within [Scope of the journal](#).
- Research question well defined, relevant & meaningful. It is stated how the research fills an identified knowledge gap.
- Rigorous investigation performed to a high technical & ethical standard.
- Methods described with sufficient detail & information to replicate.

VALIDITY OF THE FINDINGS

- Impact and novelty not assessed. *Meaningful* replication encouraged where rationale & benefit to literature is clearly stated.
- All underlying data have been provided; they are robust, statistically sound, & controlled.
- Conclusions are well stated, linked to original research question & limited to supporting results.



The best reviewers use these techniques

Tip

Example

Support criticisms with evidence from the text or from other sources

Smith et al (J of Methodology, 2005, V3, pp 123) have shown that the analysis you use in Lines 241-250 is not the most appropriate for this situation. Please explain why you used this method.

Give specific suggestions on how to improve the manuscript

Your introduction needs more detail. I suggest that you improve the description at lines 57- 86 to provide more justification for your study (specifically, you should expand upon the knowledge gap being filled).

Comment on language and grammar issues

The English language should be improved to ensure that an international audience can clearly understand your text. Some examples where the language could be improved include lines 23, 77, 121, 128 - the current phrasing makes comprehension difficult. I suggest you have a colleague who is proficient in English and familiar with the subject matter review your manuscript, or contact a professional editing service.

Organize by importance of the issues, and number your points

- 1. Your most important issue*
- 2. The next most important item*
- 3. ...*
- 4. The least important points*

Please provide constructive criticism, and avoid personal opinions

I thank you for providing the raw data, however your supplemental files need more descriptive metadata identifiers to be useful to future readers. Although your results are compelling, the data analysis should be improved in the following ways: AA, BB, CC

Comment on strengths (as well as weaknesses) of the manuscript

I commend the authors for their extensive data set, compiled over many years of detailed fieldwork. In addition, the manuscript is clearly written in professional, unambiguous language. If there is a weakness, it is in the statistical analysis (as I have noted above) which should be improved upon before Acceptance.

An integrative taxonomic revision of Pareinae slug-eating snakes (Squamata: Pareidae) reveals unprecedented diversity in Indochina

Nikolay A Poyarkov^{Corresp., 1, 2}, Tan Van Nguyen³, Parinya Pawangkhanant⁴, Platon V. Yushchenko², Peter Brakels⁵, Linh Hoang Nguyen⁶, Hung Ngoc Nguyen⁶, Chatmongkon Suwannapoom⁴, Nikolai L. Orlov⁷, Gernot Vogel⁸

¹ Laboratory of Tropical Ecology, Joint Russian-Vietnamese Tropical Research and Technological Center, Hanoi, Hanoi, Vietnam

² Faculty of Biology, Department of Vertebrate Zoology, Moscow State University, Moscow, Moscow, Russia

³ Department of Species Conservation, Save Vietnam's Wildlife, Ninh Binh, Ninh Binh, Vietnam

⁴ Division of Fishery, School of Agriculture and Natural Resources, University of Phayao, Phayao, Phayao, Thailand

⁵ IUCN Laos PDR, Vientiane, Vientiane, Lao PDR

⁶ Department of Zoology, Southern Institute of Ecology, Vietnam Academy of Science and Technology, Ho Chi Minh City, Ho Chi Minh City, Vietnam

⁷ Department of Herpetology, Zoological Institute, Russian Academy of Sciences, St. Petersburg, St. Petersburg, Russia

⁸ Society for Southeast Asian Herpetology, Heidelberg, Germany

Corresponding Author: Nikolay A Poyarkov

Email address: n.poyarkov@gmail.com

Slug-eating snakes of the subfamily Pareinae are an insufficiently studied group of snakes specialized in feeding on terrestrial mollusks. Currently Pareinae encompass three genera with 34 species distributed across the Oriental biogeographic region. Despite the recent significant progress in understanding of Pareinae diversity, the subfamily remains taxonomically challenging. Here we present an updated phylogeny of the subfamily with a comprehensive taxon sampling including 30 currently recognized Pareinae species and several previously unknown candidate species and lineages. Phylogenetic analyses of mtDNA and nuDNA data yielded a well-resolved phylogeny, and supported the monophyly of the three genera *Asthenodipsas*, *Aplopeltura*, and *Pareas*. Within both *Asthenodipsas* and *Pareas* our analyses recovered deep differentiation with each genus being represented by two morphologically diagnosable clades, which we treat as subgenera. We further apply an integrative taxonomic approach, including analyses of molecular and morphological data, along with examination of available type materials, to address the longstanding taxonomic questions of the subgenus *Pareas*, and reveal the high level of hidden diversity of these snakes in Indochina. We restrict the distribution of *P. carinatus* to southern Southeast Asia, and recognize two subspecies within it, including one new subspecies proposed for the populations from Thailand and Myanmar. We further revalidate *P. berdmorei*, synonymize *P. menglaensis* with *P. berdmorei*, and recognize three subspecies within this taxon, including the new subspecies erected for the populations from Laos and

Vietnam. Furthermore, we describe two new species of *Pareas* from Vietnam: one belonging to the *P. carinatus* group from southern Vietnam, and a new member of the *P. nuchalis* group from the central Vietnam. We provide new data on *P. temporalis*, and report on a significant range extension for *P. nuchalis*. We review the diversity, distribution, conservation status and biogeography of slug-eating snakes. Our phylogeny, along with molecular clock and ancestral area analyses, reveal a complex diversification pattern of Pareinae involving a high degree of sympatry of widespread and endemic species. Our analyses support the “upstream” colonization hypothesis and, thus, the Pareinae appears to have originated in Sundaland during the middle Eocene and then colonized mainland Asia in early Oligocene. Sundaland and Eastern Indochina appear to have played the key roles as the centers of Pareinae diversification. Our results reveal that both vicariance and dispersal are responsible for current distribution patterns of Pareinae, with tectonic movements, orogeny and paleoclimatic shifts being the probable drivers of diversification. Our study further highlights the importance of comprehensive taxonomic revisions not only for the better understanding of biodiversity and its evolution, but also for the elaboration of adequate conservation actions.

1 **An integrative taxonomic revision of Pareinae Slug-eating Snakes**
2 **(Squamata: Pareidae) reveals unprecedented diversity in Indochina**

3
4 **Nikolay A. Poyarkov^{1,2,*}, Tan Van Nguyen³, Parinya Pawangkhanant⁴, Platon V.**
5 **Yushchenko¹, Peter Brakels⁵, Linh Hoang Nguyen⁶, Hung Ngoc Nguyen⁶, Chatmongkon**
6 **Suwannapoom⁴, Nikolai L. Orlov⁷, Gernot Vogel⁸**

7
8 ¹ *Faculty of Biology, Department of Vertebrate Zoology, Moscow State University,*
9 *Moscow, Moscow, Russia*

10 ² *Laboratory of Tropical Ecology, Joint Russian-Vietnamese Tropical Research and*
11 *Technological Center, Hanoi, Hanoi, Vietnam*

12 ³ *Department of Species Conservation, Save Vietnam's Wildlife, Ninh Binh, Ninh Binh,*
13 *Vietnam*

14 ⁴ *Division of Fishery, School of Agriculture and Natural Resources, University of Phayao,*
15 *Phayao, Phayao, Thailand*

16 ⁵ *IUCN Laos PDR, Vientiane, Vientiane, Lao PDR*

17 ⁶ *Department of Zoology, Southern Institute of Ecology, Vietnam Academy of Science and*
18 *Technology, Ho Chi Minh City, Ho Chi Minh City, Vietnam*

19 ⁷ *Department of Herpetology, Zoological Institute, Russian Academy of Sciences, St.*
20 *Petersburg, St. Petersburg, Russia*

21 ⁸ *Society for Southeast Asian Herpetology, Heidelberg, Germany*

22 * *Corresponding author: Nikolay A. Poyarkov: n.poyarkov@gmail.com.*

23
24 **ABSTRACT**

25
26 Slug-eating snakes of the subfamily Pareinae represent an insufficiently studied group of
27 Asian colubroid snakes specialized in feeding on terrestrial mollusks. Currently Pareinae
28 encompass three genera with 34 species widely distributed across the Oriental biogeographic
29 region. Despite the recent significant progress in understanding of Pareinae diversity, the
30 subfamily remains a taxonomically challenging group due to the wide distribution of
31 morphologically similar cryptic taxa. Here we present an updated phylogeny of the subfamily

32 with a comprehensive taxon sampling including 30 currently recognized Pareinae species and
33 several previously unknown candidate species and lineages. Phylogenetic analyses of 3561 bp of
34 both mtDNA and nuDNA data yielded a well-resolved phylogeny of the subfamily, and
35 recovered three well-supported groups, corresponding to the genera *Asthenodipsas*, *Aplopeltura*,
36 and *Pareas*. Within both *Asthenodipsas* and *Pareas* our analyses recovered deep differentiation
37 with each genus being represented by two reciprocally monophyletic and morphologically
38 diagnosable groups, which we propose to treat as subgenera. Therefore we recognize two
39 subgenera within *Asthenodipsas*: *Asthenodipsas* sensu stricto including the *A. malaccanus*
40 species group, and *Spondylodipsas* **subgen. nov.** which we establish to encompass the *A.*
41 *vertebralis* species group. Within the genus *Pareas* we recognize six species groups in two
42 subgenera: *Pareas* sensu stricto includes the *P. carinatus* and *P. nuchalis* groups; we also
43 revalidate the subgenus *Eberhardtia* **stat. nov.**, which includes the *P. hamptoni*, *P.*
44 *margaritophorus*, *P. chinensis*, and *P. monticola* species groups. We further apply an integrative
45 taxonomic approach, including analyses of molecular and morphological data, along with
46 examination of available type materials, to address the longstanding taxonomic **questions** of the
47 subgenus *Pareas*, and reveal the high level of hidden diversity of these snakes in Indochina. We
48 restrict the distribution of *P. carinatus* to southern Southeast Asia, and recognize two subspecies
49 within it, including one new subspecies proposed for the populations from Tenasserim in
50 **Thailand** and Myanmar (*P. c. tenasserimicus* **ssp. nov.**). We further revalidate *P. berdmorei*,
51 synonymize *P. menglaensis* with *P. berdmorei*, and recognize three subspecies within this taxon,
52 distributed from eastern Myanmar across the Indochina to southern China, including the new
53 subspecies erected for the populations from the northern Annamites in Laos and Vietnam (*P. b.*
54 **annamiticus** **ssp. nov.**). Furthermore, we describe two new species of *Pareas* from Vietnam: one
55 belonging to the *P. carinatus* group from the Langbian Plateau (*P. kuznetsovorum* **sp. nov.**), and
56 a new member of the *P. nuchalis* group from the Kon Tum – Gia Lai Plateau of central Vietnam
57 (*P. abros* **sp. nov.**); **provide** new data on the recently described *P. temporalis* from the Langbian
58 Plateau of southern Vietnam, and report on a significant range extension for *P. nuchalis*. Based
59 on our new data we review the diversity, distribution, conservation status and biogeography of
60 slug-eating snakes. Our phylogenetic results, along with molecular clock and ancestral area
61 analyses, reveal a complex diversification pattern of Pareinae involving a high degree of
62 sympatry of widespread and endemic species. Our analyses support the “upstream” colonization

63 hypothesis and, thus, the Pareinae appears to have originated in Sundaland during the middle
64 Eocene and then colonized mainland Asia in early Oligocene. Sundaland and Eastern Indochina
65 appear to have played the key roles as the centers of Pareinae diversification. Our results reveal
66 that both vicariance and dispersal are responsible for current distribution patterns of Pareinae,
67 with tectonic movements, orogeny and paleoclimatic shifts being the probable drivers of
68 diversification. Our study further highlights the importance of comprehensive taxonomic
69 revisions not only for the better understanding of biodiversity and its evolution, but also for the
70 elaboration of adequate conservation actions.

71

72 **Subjects:** Biodiversity, Biogeography, Evolutionary Studies, Taxonomy, Zoology

73

74 **Keywords:** *Pareas*, *Asthenodipsas*, *Aplopeltura*, *Eberhardtia*, *Spondylodipsas*, molecular
75 phylogeny, biogeography, Southeast Asia, Sundaland, cryptic species

76

77 INTRODUCTION

78

79 The snakes of the family Pareidae Romer, 1956 (Squamata, Serpentes) currently
80 encompassing 39 species inhabiting the Oriental biogeographic region are divided into two
81 subfamilies: Pareinae Romer, 1956 in Southeast Asia and Xylophiinae Deepak, Ruane & David,
82 2019 in southern India (Deepak *et al.*, 2019; Uetz, Freed & Hošek, 2021). Slug-eating snakes (or
83 snail-eating snakes) of the subfamily Pareinae are widely distributed throughout the tropical and
84 subtropical areas of Southeast and East Asia. Its members are mainly small-sized, arboreal,
85 nocturnal snakes, and are regarded as dietary specialists of terrestrial pulmonates *i.e.* slugs and
86 snails (You, Poyarkov & Lin, 2015; Cundall & Greene, 2000). Snail-eating species of Pareinae
87 are unique among terrestrial vertebrates in having asymmetric lower jaws, with more teeth on the
88 right mandible than on the left (Hoso *et al.*, 2007, 2010). Due to the specialized feeding habit and
89 foraging behaviour, the evolutionary biology of *Pareas* has received much attention in recent
90 years (Götz, 2002; Hoso & Hori, 2006, 2008; Hoso, 2007; Hoso *et al.*, 2007, 2010; You,
91 Poyarkov & Lin, 2015; Danaisawadi *et al.*, 2015, 2016; Kojima *et al.*, 2020; Chang *et al.*, 2021).

92 The subfamily Pareinae had a turbulent taxonomic history (David & Vogel, 1996; Rao &
93 Yang, 1992) with recent works (Grossmann & Tillack, 2003; Guo *et al.*, 2011; Ding *et al.*, 2020;

94 *Vogel et al., 2020, 2021*) recognizing three genera: *Pareas* Wagler, 1830 with 24 species (type
95 species: *Pareas carinatus* Wagler, 1830); *Asthenodipsas* Peters, 1864 with nine species (type
96 species: *Asthenodipsas malaccanus* [Peters, 1864]), and a monotypic genus *Aplopeltura* Duméril,
97 1853 (type species: *Aplopeltura boa* [Boie, 1828]). Two genus-level nomens, namely
98 *Eberhardtia* Angel, 1920 (type species: *Eberhardtia tonkinensis* Angel, 1920, regarded as a
99 synonym of *Pareas formosensis* [Van Denburgh, 1909] by *Ding et al., 2020*) and *Internatus*
100 Yang & Rao, 1992 (type species: *Asthenodipsas leavis* [Boie, 1827]) are presently considered as
101 junior synonyms of the genera *Pareas* and *Asthenodipsas*, respectively (see *Grosmann & Tillack,*
102 *2003; Wallach, Williams & Boundi, 2014; Ding et al., 2020; Vogel et al., 2020, 2021*). Several
103 recent phylogenetic studies suggested that the genus *Pareas* consists of two highly divergent
104 major clades and is paraphyletic with respect to *Aplopeltura* or *Asthenodipsas* (*Guo et al., 2011;*
105 *Pyron et al., 2011; Wang et al., 2020*). At the same time, other multilocus studies recovered
106 *Pareas* as a monophyletic group though with moderate or low node support values, and
107 suggested the genus *Aplopeltura* as its sister taxon (*Pyron, Burbrink & Wiens, 2013; You,*
108 *Poyarkov & Lin, 2015; Figueroa et al., 2016; Deepak et al., 2019; Zaher et al., 2019*). The genus
109 *Asthenodipsas* was also shown to include two major lineages (*Loredo et al., 2013; Figueroa et*
110 *al., 2016; Deepak et al., 2019; Wang et al., 2020*), though its monophyly got only moderate
111 support based on the concatenated analysis of mitochondrial and nuclear DNA markers (*Wang et*
112 *al., 2020; Ding et al., 2020; Vogel et al., 2021*). Therefore, despite the recent significant progress
113 in evolutionary studies on Pareinae, the phylogenetic relationship among the major genus-level
114 lineages of the subfamily still remain debated and unclear.

115 Several recent taxonomic studies have demonstrated that the species diversity of Pareinae
116 is still underestimated (e.g., *Vogel, 2015; Hauser, 2017; Quah et al., 2019, 2020, 2021; Le et al.,*
117 *2021*). The high degree of morphological similarity among closely related taxa of Pareinae often
118 makes species delineation in slug snakes quite challenging (*Guo & Deng, 2009; Vogel, 2015;*
119 *Yang et al., 2021*), suggesting that the molecular data represent an effective tool to help untangle
120 taxonomic controversies when morphological analyses yield inconsistent results (*You, Poyarkov*
121 *& Lin, 2015; Loredo et al., 2013; Vogel et al., 2020, 2021; Bhosale et al., 2020; Wang et al.,*
122 *2020; Ding et al., 2020; Liu & Rao, 2021; Yang et al., 2021*). Application of the integrative
123 taxonomic approach combining evidence from morphological and molecular data resulted in the
124 discovery of several previously unnoticed taxa and allowed to revise several species complexes,

125 including the *Pareas hamptoni* complex (You, Poyarkov & Lin, 2015; Bhosale et al., 2020; Ding
126 et al., 2020; Liu & Rao, 2021; Yang et al., 2021), the *P. margaritophorus* complex (Vogel et al.,
127 2020; Suntrarachun et al., 2020), and the *P. monticola* complex (Vogel et al., 2021).

128 On the other hand, the Keeled slug snake, *Pareas carinatus*, has received comparatively
129 little attention in most recent revisions. This species was originally described by Wagler (1830)
130 from Java, Indonesia, and was later reported to be widely distributed throughout Southeast Asia,
131 from southern China, southern Myanmar, Laos, south-western and eastern Cambodia, Vietnam,
132 Thailand, southwards to Peninsular Malaysia, and islands of Borneo, Sumatra, Java and Bali
133 (Wallach, Williams & Boundi, 2014). However, since geographic variation of this species has
134 never been examined across the different regions, its taxonomic status remained controversial
135 and a number of misidentifications were made in the past (e.g., Das, 2012, 2018). Recently,
136 Wang et al. (2020) demonstrated *P. nuchalis* (Boulenger, 1900) to be closely related to *P.*
137 *carinatus* complex, and divided the latter by describing *P. menglaensis* Wang, Che, Liu, Li, Jin,
138 Jiang, Shi & Guo, 2020, as a sister species of *P. carinatus* sensu stricto. However, in this revision
139 the authors did not examine type specimens of *P. carinatus*, and also have neglected to re-
140 evaluate the status of two available species names currently considered as junior synonyms of *P.*
141 *carinatus*: *Pareas berdmorei* Theobald, 1868, and *Amblycephalus carinatus unicolor* Bourret,
142 1934 (see Nguyen, Ho & Nguyen, 2009; Wallach, Williams & Boundi, 2014; Uetz, Freed &
143 Hošek, 2021). The most recent addition to the taxonomy of the group is the discovery of a new
144 species from southern Vietnam – *P. temporalis*, which was suggested as a sister species to *P.*
145 *nuchalis* from Borneo (Le et al., 2021); the authors also provided the most complete phylogeny
146 for the genus *Pareas* published up to date, generally concordant with the earlier results (Wang et
147 al., 2020; Vogel et al., 2021). The taxonomic history of the *P. carinatus* – *P. nuchalis* complex is
148 summarized in Table 1. Overall, the taxonomic status of *P. carinatus*, its synonyms, and *P.*
149 *menglaensis* remains unclear pending an integrative study combining data on molecular and
150 morphological variation of this group throughout its range.

151 In the present study, we provide an updated phylogeny for the subfamily Pareinae based on
152 the analysis of mitochondrial and nuclear DNA markers, and re-assess the genus-level taxonomy
153 of the group. Based on an extensive sampling we also report on a previously unrecognized
154 diversity of the genus *Pareas* in Indochina. We examine name-bearing types and re-assess
155 taxonomy of the *P. carinatus* complex using an integrative taxonomic approach, combining

156 morphological and molecular data from the newly collected and older specimens preserved in
157 herpetological collections. We also provide an updated identification key for the members of the
158 subfamily Pareinae and species of the *P. carinatus* complex. Finally, we conduct a divergence
159 time estimation analysis for the subfamily Pareinae and discuss evolution and the historical
160 biogeography of this peculiar group of snakes.

161

162 MATERIALS AND METHODS

163

164 Species concept

165 In the present study, we follow the **general lineage concept** (GLC: *De Queiroz, 2007*) which
166 suggests that a species constitutes a population of organisms independently evolving from other
167 such populations owing to a lack of gene flow. By “independently”, it is meant that new
168 mutations arising in one species cannot spread readily into another species (*Barraclough et al.,*
169 *2003; De Queiroz, 2007*). However, integrative studies on the nature and origins of species are
170 increasingly using a wider range of empirical data to delimit species boundaries, rather than
171 relying solely on traditional taxonomic procedure (*Coyne & Orr, 1998; Knowles & Carstens,*
172 *2007; Fontaneto et al., 2007*). Under the GLC herein, we follow the framework of integrative
173 taxonomy (*Padial et al., 2010; Vences et al., 2013*) that combines multiple independent lines of
174 evidence to assess the taxonomic status of the lineages in question: DNA-based molecular
175 phylogenies were used to infer species boundaries, while univariate (ANOVA) and multivariate
176 (PCA) morphological analyses were used to describe those boundaries.

177

178 Nomenclatural acts

179 The electronic version of this article in **portable document format** will represent a published
180 work according to the International Commission on Zoological Nomenclature (ICZN), and
181 hence the new names contained in the electronic version are effectively published under that
182 Code from the electronic edition alone (see Articles 8.5–8.6 of the Code). This published work
183 and the nomenclatural acts it contains have been registered in ZooBank, the online registration
184 system for the ICZN. The ZooBank Life Science Identifiers (LSIDs) can be resolved and the
185 associated information can be viewed through any standard web browser by appending the
186 LSID to the prefix <http://zoobank.org/>.

187 The LSID for this publication is as follows: urn:lsid:zoobank.org:pub:192CDD83-E08C-
188 40B1-92EB-3DB2C3E63CFA. The online version of this work is archived and available from
189 the following digital repositories: PeerJ, PubMed Central and CLOCKSS.

190

191 **Taxon sampling**

192 We used tissues from the herpetological collections of Zoological Museum of Moscow
193 University (ZMMU; Moscow, Russia); **California Academy of Sciences Museum (CAS;**
194 **California, USA); Southern Institute of Ecology Zoological Collection (SIEZC; Ho Chi**
195 **Minh City, Vietnam);** School of Agriculture and Natural Resources, University of Phayao
196 (AUP; Phayao, Thailand); and National Museum of Natural Science (NMNH, Taichung, Taiwan)
197 (summarized in Supplementary Table S1 and Appendix I). For alcohol-preserved voucher
198 specimens stored in museum collections, we removed a small sub-sample of muscle, preserved it
199 in 96% ethanol, and stored samples at -70°C . Altogether we analyzed 48 tissue samples
200 representing 20 nominal taxa of the genus *Pareas*. Geographic location of sampled populations
201 of the members of the subgenus *Pareas* is presented in Fig. 1.

202 Permissions to conduct fieldwork and collect specimens were granted by the Department of
203 Forestry, Ministry of Agriculture and Rural Development of Vietnam (permit numbers
204 #547/TCLN-BTTN; #432/TCLN-BTTN; #822/TCLN-BTTN; #142/SNgV-VP; #1539/TCLN-
205 DDPH, #1700/UBND.VX); the Forest Protection Departments of the Peoples' Committees of
206 Gia Lai Province (permit numbers #530/UBND-NC; #1951/UBND-NV), Phu Yen Province
207 (permit number #05/UBND-KT); Phu Tho Province (permit number #2394/UBND-TH3); Thanh
208 Hoa Province (permit number #3532/UBND-THKH); and Quang Nam Province (permit number
209 #308/SNgV-LS), Vietnam; by the Biotechnology and Ecology Institute Ministry of Science and
210 Technology, Lao PDR (permit no. 299); and by the Institute of Animals for Scientific Purpose
211 Development (IAD), Bangkok, Thailand (permit numbers U1-01205-2558 and UP-AE59-01-04-
212 0022). Specimen collection protocols and animal operations followed the Institutional Ethical
213 Committee of Animal Experimentation of University of Phayao (permit number 610104022).

214

215 **DNA isolation, PCR, and sequencing**

216 To infer the phylogenetic relationships among the Pareinae we obtained partial sequence
217 data of cytochrome *b* (*cyt b*) and NADH dehydrogenase subunit 4 (*ND4*) mtDNA genes, as well

218 as two nuclear genes: oocyte maturation factor *mos* (*c-mos*) and recombination activating gene 1
219 (*RAG1*). These genetic markers have been widely applied in studies of Pareidae diversity and
220 phylogenetic relationships (e.g., *Guo et al., 2011; You, Poyarkov & Lin, 2015; Deepak et al.,*
221 *2019; Wang et al., 2020; Vogel et al., 2020, 2021; Ding et al., 2020*). Total genomic DNA was
222 extracted from muscle or liver tissue samples preserved in 95% ethanol using standard phenol-
223 chloroform-proteinase K (final concentration 1 mg/ml) extraction procedures with consequent
224 isopropanol precipitation (protocols followed *Russell & Sambrook, 2001*). DNA amplification
225 was performed in 20 ml reactions using ca. 50 ng genomic DNA, 10 nmol of each primer, 15
226 nmol of each dNTP, 50 nmol of additional MgCl₂, Taq PCR buffer (10 mM of Tris-HCl, pH 8.3,
227 50 mM of KCl, 1.1 mM of MgCl₂, and 0.01% gelatine) and 1 U of Taq DNA polymerase.
228 Primers used for PCR and sequencing are summarized in Supplementary Table S2. PCRs were
229 run on a Bio-Rad T100™ Thermal Cycler. PCR protocols for *cyt b* and *ND4* gene fragments
230 followed *De Queiroz et al. (2002)* and *Salvi et al. (2013)*, respectively; the cycling parameters for
231 *c-mos* gene were identical to those described in *Slowinski & Lawson (2002)*, and for *RAG1* to
232 those described in *Groth & Barrowclough (1999)* and *Chiari et al. (2004)*. Sequence data
233 collection and visualization were performed on an ABI 3730xl automated sequencer (Applied
234 Biosystems, Foster City, CA, USA). PCR purification and cycle sequencing were done
235 commercially through Evrogen Inc. (Moscow, Russia).

236

237 **Phylogenetic analyses**

238 Sequences were managed and edited manually using Seqman in Lasergene.v7.1
239 (DNASTAR Inc., Madison, WI, USA), MEGA 7 (*Kumar, Stecher & Tamura, 2016*), and BioEdit
240 v7.0.5.2 (*Hall, 1999*). For individuals which were detected to be heterozygous in nuclear gene
241 sequences, they were phased using the software program PHASE with default sets of iterations,
242 burn-in, and threshold (*Stephens et al., 2001*), on the web-server interface SEQPHASE (*Flot,*
243 *2010*). One of the phased copies was selected at random to represent each individual in
244 subsequent analyses. All sequences were deposited in GenBank (see Supplementary Table S1 for
245 accession numbers).

246 To reconstruct the phylogenetic relationships within the Pareinae, we aligned the newly
247 obtained *cyt b*, *ND4*, *c-mos*, and *RAG1* sequences together with representative sequences from 32
248 specimens of approximately 16 nominal *Pareas* species and seven other Pareinae representatives,

249 retrieved from GenBank (see Supplementary Table S1). Two species of the genus *Xylophis*
250 (Pareidae: Xylophinae) were added to the alignment and used as outgroups for rooting the
251 phylogenetic tree following the phylogenetic data of *Deepak et al. (2019, 2020)*. In total, we
252 obtained molecular genetic data for 81 samples representing 38 taxa of Pareinae including all
253 currently recognized species of the genus *Pareas*, five species of *Asthenodipsas*, and the single
254 species of the genus *Aplopeltura (A. boa)*. Details on taxonomy, localities, GenBank accession
255 numbers, and associated references for all examined specimens are summarized in
256 Supplementary Table S1.

257 The nucleotide sequences were initially aligned in MAFFT v.6 (*Katoh et al., 2002*) with
258 default parameters; the alignment was subsequently checked by eye in BioEdit 7.0.5.2 (*Hall,*
259 *1999*) and slightly adjusted. The mean uncorrected genetic *p*-distances between sequences were
260 calculated with MEGA 7 (*Kumar, Stecher & Tamura, 2016*). Phylogenetic trees were estimated
261 for the combined mitochondrial DNA fragments (cyt *b* and *ND4*) and nuclear gene (*c-mos* and
262 *RAG1*) datasets. The total evidence analysis was performed as the approximately unbiased tree-
263 selection test (AU-test; *Shimodaira, 2002*) conducted using Treefinder v.March 2011 (*Jobb,*
264 *2011*) did not reveal statistically significant differences between mtDNA and nuDNA topologies.

265 Phylogenetic relationships of Pareinae were inferred using Bayesian Inference (BI) and
266 Maximum Likelihood (ML) approaches. The optimum partitioning schemes for alignments were
267 identified with PartitionFinder 2.1.1 (*Lanfear et al., 2012*) using the greedy search algorithm
268 under an AIC criterion, and are presented in Supplementary Table S3. When the same model was
269 proposed to different codon positions of a given gene, they were treated as a single partition.

270 BI was performed in MrBayes v3.1.2 (*Ronquist & Huelsenbeck, 2003*) with two
271 simultaneous runs, each with one cold chain and three heated chains for 200 million generations.
272 Two independent Metropolis-coupled Markov chain Monte Carlo (MCMCMC) runs were
273 performed and checked for the effective sample sizes (ESS) were all above 200 by exploring the
274 likelihood plots using TRACER v1.6 (*Rambaut & Drummond, 2007*). We discarded the initial
275 10% of trees as burn-in. Confidence in tree topology was assessed by posterior probability for
276 Bayesian analysis (BI PP) (*Huelsenbeck & Ronquist, 2001*). Nodes with BI PP values of 0.95 and
277 above were considered strongly supported, nodes with values of 0.90–0.94 were considered as
278 well-supported, and the BI PP values below 0.90 were regarded as no support (*Wilcox et al.,*
279 *2002*).

280 A Maximum Likelihood (ML) analysis was implemented using the IQ-TREE webserver
281 (*Nguyen et al., 2015; Trifinopoulos et al., 2016*). One-thousand bootstrap pseudoreplicates via
282 the ultrafast bootstrap (ML UB; *Hoang et al., 2018*) approximation algorithm were employed,
283 and nodes having ML UB values of 95% and above were considered strongly supported, while
284 nodes with values of 90%–94% we regarded as well-supported, and the ML UB node values
285 below 90% were considered as no support (*Minh et al., 2013*).

286

287 **Divergence times estimation**

288 The time-calibrated Bayesian Inference analysis was implemented in the program Bayesian
289 Evolutionary Analysis Utility (BEAUti) version 2.4.7 and run on BEAST v1.8.4 (*Drummond et*
290 *al., 2012*), including the concatenated mtDNA + nuDNA dataset. We used hierarchical likelihood
291 ratio tests in PAML v4.7 (*Yang, 2007*) to test molecular clock assumptions separately for
292 mtDNA and nuDNA markers. Based on PAML results, which indicated that there was very little
293 rate variation among the sites of mtDNA markers and so a strict clock model was used for the
294 final analysis employing unlinked site and linked tree models for the nuDNA, and an
295 uncorrelated lognormal relaxed clock for mtDNA genes. We also used these models and
296 partitioning schemes from the ML analysis with empirical frequencies estimated so as to fix them
297 to the proportions observed in the data. A coalescent exponential population prior was employed
298 as the tree prior because intraspecific relationships among many individuals were being assessed
299 and it was not known *a priori* which individuals would be grouped as species. Under the
300 coalescent model, the default priors for population growth (Laplace Distribution) and size ($1/X$)
301 were left unchanged because these parameters were not being estimated. We conducted two runs
302 of 100 million generations each in BEAST v1.8.4. We also assumed parameter convergence in
303 Tracer and discarded the first 10% of generations as burn-in. We used TreeAnnotator v1.8.0 (in
304 BEAST) to create our maximum credibility clades. Since no paleontological data for the Pareidae
305 are known to exist, we relied on four recently estimated calibration priors for this family obtained
306 from recent large-scale phylogeny of the group (*Deepak et al., 2019*) as primary calibration
307 points. Calibration points and priors are summarized in Supplementary Table S4.

308

309 **Biogeographic analyses**

310 The biogeographic range evolution history of Pareinae was reconstructed by a model-

311 testing approach in a common ML framework to find the best statistical fit using AIC in RASP
312 v3.2 (Ree *et al.*, 2005; Ree & Smith, 2008; Yu *et al.*, 2015). The models allow testing alternative
313 biogeographic hypotheses, such as dispersal, vicariance, and extinction. Six areas were defined
314 that are covered by our ingroup sample (see Fig. 2A): (A) Mainland East Asia; (B) Eastern
315 Indochina; (C) Western Indochina; (D) Indo-Burma, including eastern Himalaya and the Arakan
316 Mountains of Myanmar; (E) Sundaland; and (F) East Asian islands (Taiwan + the Ryukyus)
317 following Gorin *et al.* (2020), Chen *et al.* (2018), and Nguyen *et al.* (2020a). This coding scheme
318 reflects the complex palaeogeographic history of Southeast Asia, because Borneo, Java, Sumatra
319 and the Thai-Malay Peninsula constituted the connected landmass of Sundaland until recently
320 (Hall, 2012; Morley, 2018). Maximum areas per species were set to three, as no extant species
321 occurs in more than three biogeographical regions. Matrices of modern distributions of species
322 across the areas are presented in Supplementary Table S5; transition matrices between
323 biogeographic regions are given in Supplementary Table S6. Discrete state transitions for ranges
324 were estimated using ML framework on branches as functions of time, suggesting the best fit
325 model for ancestral ranges at the times of cladogenesis using the Akaike Information Criterion
326 (AIC) and Akaike weights (Ree & Smith, 2008; Matzke, 2013). Two models were compared:
327 Langrange Dispersal-Extinction-Cladogenesis (DEC; Ree & Smith, 2008), and the ML version of
328 Statistical Dispersal-Vicariance Analysis (S-DIVA; Ronquist, 1997).

329

330 **Morphological characteristics and analyses**

331 For this study, a total of 270 preserved specimens of the subfamily Pareinae, including 82
332 specimens of the subgenus *Pareas*, were examined for their external morphological characters
333 (see Table 2, Appendix II).

334 A total of 46 morphological and chromatic characters were recorded for each specimen
335 (following Vogel, 2015). Morphological measurements (all in mm) included: snout-vent length
336 (SVL); tail length (TaL); total length (TL); relative tail length (TaL/TL); horizontal eye diameter
337 (ED); distance from the anterior edge of orbit to nostril (Eye-nos); minimal distance from the
338 ventral edge of orbit to the edge of upper lip (Eye-mouth); head length (HL); maximal head
339 width (HW). Meristic characters evaluated were the number of dorsal scale rows counted at one
340 head length behind head (ASR), at mid-body (MSR), and at one head length before vent (PSR);
341 number of enlarged vertebral scales (VSE); presence of keeled dorsal scale rows (DORkeel);

342 number of keeled dorsal scale rows at midbody (KMD); number of ventral scales (VEN); number
343 of preventral scales (preVEN); number of subcaudal scales (SC); number of cloacal (anal) plates
344 (AN); number of supralabials (SL); number of supralabials touching the orbit (SL-eye); number
345 of supralabials touching subocular (SL-suboc); number of infralabials (IL); numbers of
346 infralabials touching each other (IL-touch); number of nasals (NAS); number of anterior
347 temporals (At); number of posterior temporals (Pt); number of loreals (LOR); loreal touching the
348 orbit or not (LOR-eye); number of preoculars (Preoc); number of presuboculars (Presuboc);
349 prefrontal touching the orbit or not (Prefr-eye); number of suboculars (SoO); subocular fused
350 with postocular or not (SoO-PoO); number of postoculars (PoO). Coloration and pattern
351 characters evaluated were the background body dorsal coloration; presence or absence of
352 ornamentation on neck; presence or absence of dark blotch or chevron on neck and nuchal areas;
353 coloration of head dorsal surface; presence and number of postorbital stripes; presence or
354 absence of a dark blotch on 7th supralabial; presence or absence of transverse bands on body;
355 number of transverse bands on body; number of discontinuous dorsal bands comprised of dark
356 dots; presence or absence of body ornamentation others than bands; dorsal bands continue on
357 belly or not; belly pattern (no pattern, banded, mottled or dotted).

358 When possible, color notes were taken from living specimens and digital images of living
359 specimens of all possible age classes prior to preservation. Measurements were taken with a
360 slide-caliper to the nearest 0.1 mm, except body and tail lengths, which were measured to the
361 nearest of one millimeter with a measuring tape. The number of ventral scales was counted
362 according to *Dowling (1951)*. Half ventrals were counted as one. The first enlarged shield
363 anterior to the ventrals was regarded as a preventral and was present in all examined specimens.
364 The first scale under the tail meeting its opposite was regarded as the first subcaudal, and the
365 terminal scute was not included in the number of subcaudals. In the number of supralabials
366 touching the subocular, those only touching the presubocular were not included. Infralabials were
367 considered being those shields that were completely below a supralabial and bordering the mouth
368 gap. Usually the last supralabial shield was a very large shield, much larger than other
369 supralabials. Smaller shields behind this enlarged shield do not border the mouth gap (only the
370 connecting muscle) and were excluded in the sublabial scales count, despite the fact that they
371 were covered by the supralabials. The first sublabial was defined as the scale that starts between
372 the posterior chin shield and the infralabials and that borders the infralabials. Values for paired

373 head characters were recorded on both sides of the head, and were reported in a left / right order.
374 The sex was determined by dissection of the ventral tail base or by the presence of everted
375 hemipenes. The hemipenial morphology was studied on specimens with hemipenial structures
376 everted before preservation; terminology and description followed *Keogh (1999)*.

377 An analysis of variance (ANOVA) was performed to ascertain if statistically significant
378 mean differences among meristic characters ($p < 0.05$) existed among the discrete populations
379 delimited in the phylogenetic analyses. ANOVAs having a p-value less than 0.05 indicating that
380 statistical differences existed were subjected to a Tukey HSD test to ascertain which population
381 pairs differed significantly ($p < 0.05$) from each other. Principal Component Analysis (PCA) was
382 used to determine if populations from different localities occupied unique positions in
383 morphospace and the degree to which their variation in morphospace coincided with potential
384 species boundaries predicted by the molecular phylogenetic and univariate analyses. PCA
385 searches for the best overall low-dimensional representation of significant morphological
386 variation in the data. Juvenile specimens, as well as the specimens with incomplete or damaged
387 tails were excluded from the PCA. Characters used in the PCA were continuous mensural data
388 from SVL, TaL, TL, ED, Eye-nos, Eye-mouth, HL, and HW, and the discrete meristic data from
389 the scale counts VSE, KMD, DORkeel, VEN, preVEN, SC, SL, SL-eye, IL, At, Pt, LOR, Preoc,
390 Presuboc, Prefr-eye, SoO, SoO-PoO, and PoO. All PCA data were natural log-transformed prior
391 to analysis and scaled to their standard deviation in order to normalize their distribution so as to
392 ensure characters with very large and very low values did not over-leverage the results owing to
393 intervariable nonlinearity and to transform meristic and mensural data into comparable units for
394 analysis. When a high correlation between certain pairs of characters was found, we omitted one
395 of them from the analyses to exclude possible overweighting effects. Statistical analyses were
396 carried out using Statistica 8.0 (Version 8.0; StatSoft, Tulsa, OK, USA).

397 Morphological and coloration characters of the examined specimens were compared in
398 detail to other species of the genus the *Pareas*. The examined comparative material is listed in
399 Appendix II. For comparison with other taxa, we also relied on previously published data (e.g.,
400 *Theobald, 1868; Bourret, 1934; Pope, 1935; Smith, 1943; Taylor, 1965; Guo & Rao, 2004; Guo*
401 *& Deng, 2009; Stuebing et al., 2014; You, Poyarkov & Lin, 2015, Vogel, 2015; Hauser, 2017;*
402 *Wang et al., 2020; Vogel et al., 2020, 2021; Ding et al., 2020; Bhosale et al., 2020; Liu & Rao,*
403 *2021; Le et al., 2021*). Other abbreviations used: Prov.: Province; Mt.: Mountain; N.P.: National

404 Park; N.R. Natural Reserve; Is.: Island; asl: above sea level.

405

406 RESULTS

407

408 Partitions, substitution models, and sequence characteristics

409 Our combined dataset was composed of 1804 bp of *cyt b* and *ND4* mtDNA genes, 1757 bp
410 of nuDNA (including 734 bp of *c-mos*, and 1023 bp of *RAG1*), and 3561 bp (mtDNA + nuDNA),
411 respectively. The concatenated mtDNA + nuDNA dataset included 81 samples, representing ca.
412 29 *Pareas* taxa, including all 24 currently recognized species of the genus (*Uetz, Freed & Hošek,*
413 *2021*), one species of the monotypic genus *Aplopeltura*, five species of the genus *Asthenodipsas*
414 (of nine currently recognized species, 56%), and two outgroup taxa (see Supplementary Table
415 S1). Information on fragment lengths and variability is summarized in Supplementary Table S3.
416 PartitionFinder 2.1.1 proposed the partition schemes and substitution models which resulted in
417 nine partitions in total (Supplementary Table S3).

418

419 Phylogenetic relationships and distribution

420 Phylogenetic trees obtained with ML and BI analyses of the three data partitions (mtDNA
421 + nuDNA, mtDNA, nuDNA) are congruent apart from the generally lower resolution of nuDNA
422 trees (see Supplementary Figures S2–S3). Overall, since the mtDNA + nuDNA phylogenetic tree
423 was mostly better resolved and had greater node support than the mtDNA and nuDNA trees, we
424 relied on the combined mtDNA + nuDNA topology for inferring phylogenetic relationships and
425 biogeographic history of *Pareinae*. The BI tree resulted from the analysis of the concatenated
426 mtDNA + nuDNA data (Fig. 3) inferred the following set of phylogenetic relationships:

- 427 1) The subfamily *Pareinae* was subdivided into five major strongly supported deeply
428 divergent groups, including two groups within the genus *Pareas* sensu lato (clades A
429 and B, see Fig. 3), the genus *Aplopeltura* (clade C, see Fig. 3), and two groups
430 corresponding to the genus *Asthenodipsas* sensu lato (clades D and E, see Fig. 3).
- 431 2) The monophyly of the genus *Asthenodipsas* got strong support in mtDNA + nuDNA
432 analysis (1.0/100; hereafter node support values are given for BI PP/ML UB,
433 respectively; see Fig. 3), while it was rendered paraphyletic in the analysis of the
434 mtDNA dataset alone, though with no significant node support. The two clades within

435 *Asthenodipsas* correspond to the *A. malaccanus* species group (clade E, in our analysis
436 represented by *A. laevis* and *A. borneensis*; 1.0/100), and to the *A. vertebralis* species
437 group (clade D, in our analysis including *A. vertebralis*, *A. tropidonotus*, and *A.*
438 *lasgalenensis*; 1.0/100).

439 3) The monophyly of the clade joining *Pareas* + *Aplopeltura* was strongly supported
440 (1.0/99). The monotypic genus *Aplopeltura* (1.0/100) in our analysis was represented
441 with two samples of *A. boa* from Peninsular Malaysia and Borneo (Sabah, Malaysia),
442 which were assigned into two highly divergent lineages (see Fig. 3).

443 4) The monophyly of the genus *Pareas* sensu lato was strongly supported by all analyses
444 (1.0/99); the genus comprised two reciprocally monophyletic highly supported groups:
445 clade A, including the members of the *P. carinatus* – *P. nuchalis* complex (1.0/100);
446 and clade B, including the remainder of *Pareas* species (1.0/100) (see Fig. 3).

447 5) Within the clade B, encompassing the majority of the genus *Pareas* diversity, four
448 subclades were recovered corresponding to the following species groups:

449 a. ***Pareas hamptoni* species group** (subclade B1; 1.0/100) including *P.*
450 *formosensis*, *P. xuelinensis*, *P. geminatus*, *P. hamptoni*, *P. niger*, *P.*
451 *mengziensis*, *P. iwasakii*, *P. atayal*, *P. komaii*, *P. vindumi*, *P. kaduri*, and *P.*
452 *nigriceps*. *Pareas kaduri* and *P. nigriceps* from East Himalaya formed a well-
453 supported monophylum (1.0/99). The three species of *Pareas* from the East
454 Asian Islands also formed a well-supported clade (1.0/100); with *P. komaii*
455 reconstructed as a sister species with respect to *P. atayal* + *P. iwasakii* though
456 with a low nodal support (0.56/88). Phylogenetic position of *P. vindumi* from
457 Myanmar within the subclade B1 remained essentially unresolved (Fig. 3). The
458 remaining species of the subclade B1 formed a well-supported clade,
459 corresponding to the *P. hamptoni* species complex (1.0/100). Within the latter,
460 *P. niger* and *P. mengziensis* from Yunnan Province of China grouped together
461 (1.0/100) and were represented with almost identical haplotypes. *Pareas*
462 *hamptoni* from Myanmar and Northern Indochina was suggested as a sister
463 taxon with respect to the clade joining *P. xuelinensis* from Yunnan and *P.*
464 *geminatus* from Northern Indochina; the latter species was recovered as
465 paraphyletic with respect to *P. xuelinensis* (1.0/100). *Pareas formosensis* was

466 represented in our analysis with five major lineages from Taiwan and Hainan
467 islands, southern mainland China and Eastern Indochina; the sample of topotype
468 *P. tonkinensis* from northern Vietnam was placed within the *P. formosensis*
469 radiation with strong support (0.99/98; see Fig. 3).

470 b. ***Pareas margaritophorus* species group** (subclade B2; 1.0/100) included four
471 species from Indochina and Indo-Burma: *P. andersonii*, *P. modestus*, *P.*
472 *macularius*, and *P. margaritophorus*. *Pareas andersonii* and *P. modestus* from
473 Myanmar and Northeast India formed a well-supported clade (1.0/100), to
474 which *P. macularius* (1.0/100) was recovered as a sister taxon. The latter
475 species was represented in our analysis with two samples from Myanmar and
476 Laos, which were assigned into two highly divergent lineages (see Fig. 3).
477 Subclade B2 was suggested as a sister lineage with respect to subclade B1
478 though with significant nodal support (0.99/89; see Fig. 3).

479 c. ***Pareas chinensis* species group** (subclade B3; 1.0/100) included *P. stanleyi*, *P.*
480 *boulengeri*, and *P. chinensis* from mainland China; the latter two species
481 formed a strongly supported monophyletic group (1.0/100). Subclade B3 was
482 suggested as a sister lineage with respect to the clade joining B1+B2 with strong
483 nodal support (1.0/92; see Fig. 3).

484 d. ***Pareas monticola* species group** (subclade B4; 1.0/100) included two species
485 from East Himalaya and Indo-Burma: *P. monticola* and *P. victorianus*.
486 Subclade B4 was suggested as a sister taxon with respect to other species
487 groups B1–B3 with strong node support (1.0/100; see Fig. 3).

488 6) Within the remainder of the genus *Pareas* (clade A; Fig. 3), unexpectedly high numbers
489 of divergent evolutionary lineages were detected. Present taxonomy recognizes three
490 species within this group: *P. carinatus*, *P. menglaensis* and *P. nuchalis*. Altogether,
491 nine divergent lineages were distinguished by robust BI PP and ML UB node support in
492 analyses of the combined mtDNA + nuDNA dataset (Fig. 3). Of these lineages, those
493 which are presently assigned to *P. carinatus*, were recovered as paraphyletic with
494 respect to both *P. menglaensis* and *P. nuchalis*. The nine evolutionary lineages revealed
495 within clade A were distributed across two major clades, which we name herein: the *P.*
496 *carinatus* species group (A1, lineages 1–6), and the *P. nuchalis* species group (A2,

497 lineages 7–9; see Fig. 3):

- 498 a. ***Pareas carinatus* species group** (subclade A1; 1.0/100) comprised six lineages
499 formerly assigned to *P. carinatus*, including the populations from Peninsular
500 Malaysia southwards from the Isthmus of Kra, corresponding to *P. carinatus*
501 sensu stricto (1.0/100; lineage 5, see Fig. 3). Two samples from Tenasserim
502 Mountains in Peninsular Thailand and Myanmar northwards from the Isthmus
503 of Kra formed a monophyletic group (1.0/100; lineage 6, see Fig. 3), which
504 represented the sister clade to the Malayan *P. carinatus* sensu stricto (1.0/100).
505 The populations of *P. carinatus* from the mainland Indochina formed a
506 monophyletic group (1.0/100), including three well-supported subgroups: (1)
507 populations from lowlands of southern Vietnam, corresponding to the
508 subspecies *P. carinatus unicolor* (Bourret, 1934) (1.0/100; lineage 1, see Fig.
509 3); (2) populations from the northern portion of Annamite (Truong Son)
510 Mountains in central Vietnam and Laos (1.0/100; lineage 2, see Fig. 3); (3)
511 populations from montane areas of Western Indochina (1.0/100; lineage 3, see
512 Fig. 3), including the recently described *P. menglaensis* from southern Yunnan
513 (locality 22, samples 39–43), and the topotypic specimen of *P. bermorei*
514 Theobald, 1868 from Mon, Myanmar (locality 17, sample 45). Finally, a single
515 specimen initially identified as *P. cf. carinatus* from Phu Yen Province in
516 southern part of Central Vietnam formed a divergent lineage with sister
517 relationships with all other populations of *P. carinatus* species group members
518 from the mainland Indochina (1.0/94; lineage 4, see Fig. 3).
- 519 b. ***Pareas nuchalis* species group** (subclade A2; 0.99/80) got moderate node
520 support level in the ML analysis since *P. nuchalis* from Borneo was only
521 represented in our work by the single partial sequence of ND4 mtDNA gene
522 (lineage 9, see Fig. 3). The two reciprocally-monophyletic lineages from
523 montane areas of Vietnam initially identified as *P. cf. carinatus* formed a well-
524 supported clade (1.0/100) which is unexpectedly only distantly related to other
525 mainland Southeast Asian members of *Pareas* and supposedly more closely
526 related to *P. nuchalis*: the lineage from Kon Tum – Gia Lai Plateau in Central
527 Annamites (1.0/100; lineage 7, see Fig. 3), and the lineage from Langbian

528 Plateau in Southern Annamites, corresponding to the recently described *P.*
529 *temporalis* (1.0/100; lineage 8, see Fig. 3).

530 Distribution of the phylogenetic lineages within the clade A is presented in Figure 1. Most
531 lineages that cluster together in each of our two major subclades A1 and A2 are allopatrically
532 distributed within the clade (Fig. 1). Two lineages from different subclades are found
533 sympatrically: *P. nuchalis* (lineage 9) occurs in sympatry with *P. carinatus* sensu stricto (lineage
534 5) in Borneo and Sumatra, while *P. cf. carinatus* (lineage 1) occurs syntopically with lineage 8 of
535 *P. temporalis* in Langbian Plateau of southern Vietnam (locality 37, Fig. 1). The only case of
536 distribution overlap of lineages belonging to the same species group includes the lineages 3 and 6
537 of *P. carinatus* which are occur sympatrically in Suanphueng area of Ratchaburi Province in
538 western Thailand (locality 14, Fig. 1). However in Suanphueng the co-occurring lineages of
539 *Pareas* have clearly different habitat preferences and are not syntopically distributed: vouchers of
540 lineage 3 were recorded in lowland bamboo forest at 300 m asl., while the voucher of lineage 6
541 was collected in the montane forest at ca. 800–1000 m asl.

542

543 **Sequence divergence**

544 The interspecific uncorrected genetic *p*-distances in *cyt b* and *ND4* mtDNA genes within
545 the genus *Pareas* are summarized in Supplementary Tables S7 and S8, respectively. For *cyt b*
546 gene genetic divergence varied from $p=4.1\%$ (between *P. geminatus* sensu stricto and *P.*
547 *xuelinensis*) to $p=25.2\%$ (between *P. kaduri* and lineage 7 of *P. cf. carinatus* from Central
548 Annamites) (Supplementary Table S7). For *ND4* gene *p*-distances varied from $p=5.2\%$ (between
549 lineages 1 and 2 of the *P. carinatus* complex) to $p=23.7\%$ (between *P. nuchalis* and *P. komaii*)
550 (Supplementary Table S8). In several cases the intraspecific distances within *Pareas* species
551 were greater than the minimal interspecific divergence values, which is likely explained with the
552 **incomplete** taxonomy of the group: lineage 6 of the *P. carinatus* complex from Tenasserim
553 (5.0/4.2, hereafter values correspond to intraspecific distances for *cyt b*/*ND4* genes), *P.*
554 *geminatus* sensu lato (7.2/-), *P. macularius* (11.5/10.4), *P. margaritophorus* (5.2/4.9), and *P.*
555 *monticola* (3.7/5.7).

556

557 **Divergence times estimation**



558 The time-calibrated BEAST analysis recovered a phylogeny with well-supported nodes
559 (BPP \geq 90) throughout the tree, topologically identical to the BI tree (Fig. 2; Supplementary Fig.
560 S1). The phylogeny indicates that the most recent common ancestor (MRCA) of Pareinae
561 originated in late Eocene (Fig. 2). Basal radiation of Pareinae likely happened during the late
562 Eocene at approximately 39.3 mya, the group continued to radiate across Asia up until the
563 Pleistocene (Fig. 2). Diversification of the genera *Asthenodipsas* and *Pareas* started during the
564 early Oligocene (30.0 mya and 31.3 mya, respectively). The major lineages (i.e. species groups)
565 within the genus *Pareas* diversified between approximately 24.0–12.4 mya with species-level
566 radiations evolving up until 5.0–2.0 mya (Fig. 2). Estimated node-ages and the 95% highest
567 posterior density (95% HPD) for the main nodes are summarized in detail in Supplementary
568 Table S9.

569

570 **Biogeography**

571 All the trees generated in RASP analyses generally recovered the same ancestral range for
572 each node, thus converging on the same biogeographical scenario (Fig. 2). Model comparisons
573 showed that the Langrange Dispersal-Extinction-Cladogenesis (DEC) model is the best fit to the
574 data and most likely to infer the correct ancestral range at each node being the it had the highest
575 and lowest log likelihood and AIC scores, respectively. Our analyses unambiguously suggested
576 that the MRCA of Pareinae (node 3; Supplementary Fig. S1; Fig. 2) most likely inhabited
577 Sundaland, which is also reconstructed as an ancestral range for the genera *Asthenodipsas* and
578 *Aplopeltura* (nodes 4 and 9, respectively; Supplementary Fig. S1; Fig. 2). The split between
579 *Pareas* and *Aplopeltura* is likely explained by a vicariant event between Sundaland and West
580 Indochina (Fig. 2). The divergence between the two major clades within the genus *Pareas*
581 coincides with a vicariance between Indo-Burma and Eastern Himalaya (ancestral range for clade
582 A) and West Indochina (ancestral range for clade B) (Fig. 2). Major ancestral nodes within the
583 *Pareas* clade A remained within Indo-Burma and Eastern Himalaya, from where its members at
584 least three times widely dispersed to the mainland East Asia and further southwards to Indochina
585 and independently twice eastwards to Taiwan and the Ryukyus (Fig. 2). *Pareas* clade B
586 expanded its range to East Indochina and at least twice dispersed to Sundaland (see Fig. 2).
587 Overall, our analysis suggests an “upstream” colonization hypothesis for the Pareinae (from
588 island to continent; see *Filardi & Moyle, 2005; Jönsson et al., 2011*), and, thus, the subfamily

589 appears to have originated in Sundaland and then colonized the mainland Asia.

590

591 **Morphological differentiation**

592 The PCA of the morphological dataset on *P. carinatus* – *P. nuchalis* complex revealed that
593 the most distant morphospacial separation occurs in *P. nuchalis* (lineage 9), *P. temporalis*
594 (lineage 8), *P. cf. carinatus* lineages from Kon Tum – Gia Lai Plateau (lineage 7), from Phu Yen
595 Province (lineage 4), and from Tenasserim (lineage 6); followed with general separation of the *P.*
596 *cf. carinatus* lineage from northern Annamites (lineage 2) and cluster consisting of the lineages
597 of *P. carinatus* sensu stricto from Sundaland (lineage 5), and *P. cf. carinatus* from western
598 Indochina and Yunnan (lineage 3) and southern Vietnam (lineage 1) (Fig. 4). PC1 accounted for
599 18.5% of the variation in the data set and loaded most heavily for relative tail length, number of
600 subcaudal scales, number of ventral scales, and number of prefrontals bordering eye (TaL/TL,
601 SC, VEN, and Prefr-eye; Supplementary Table S10). PC2 accounted for 14.8% of the variation
602 in the data set and loaded most heavily for number of keeled dorsal scale rows, total length, head
603 length, and tail length (KMD, TL, HL, and TaL; Supplementary Table S10). The univariate and
604 multivariate morphological analyses further support results of the molecular analyses by
605 indicating that the lineages within the *P. carinatus* – *P. nuchalis* complex are well-separated
606 from each other in morphospace and bear a number of statistically significant mean differences
607 in varying combinations of meristic and color pattern characters, thus providing reliable
608 diagnostic character differences among the species (Table 1; Supplementary Tables S11–13).

609

610 **Systematics**

611

612 **Genus-level taxonomy of Pareinae**

613 All recent phylogenetic studies on caenophidian snakes agree on the monophyly of
614 Pareidae (Pyron, Burbrink & Wiens, 2013; Figueroa et al., 2016; Zaher et al., 2019) and of the
615 subfamily Pareinae with respect to Xylophiinae (Deepak et al., 2019). Most works on
616 phylogenetic relationships of this group agreed that the genus *Apolpeltura* is a sister taxon of
617 *Pareas* sensu lato, however, the monophyly of the genera *Pareas* and *Asthenodipsas* has been
618 questioned for a long time.

619 Several earlier studies demonstrated that the *P. carinatus* complex (including *P. nuchalis*)

620 is phylogenetically distant from other members of the genus, which was recovered as
621 paraphyletic (e.g., *Guo et al., 2011; Pyron et al., 2011*). It was noted that these genetic
622 divergence are concordant with differences in a number of external morphology and scalation
623 characters (*Guo et al., 2011*) and scale ultrastructure (*He, 2009; Guo et al., 2020*) (see Fig. 5).
624 *Guo et al. (2011, 2020)* suggested that *P. carinatus* and *P. nuchalis* are different from other
625 *Pareas* species in morphological, ultrastructural and molecular characteristics, and therefore,
626 they “might be removed from the genus *Pareas*”; this idea was further supported by *Wang et al.*
627 (*2020*). However, due to incomplete sampling and insufficient morphological data *Guo et al.*
628 (*2011, 2020*) and *Wang et al. (2020)*, refrained from making a formal taxonomic decision on the
629 division of *Pareas* [Note - *Wang et al. (2020)* applied a new genus name ‘*Northpareas*’ to the
630 clade including all *Pareas* species except *P. carinatus*, *P. nuchalis*, and *P. menglaensis*, however
631 this name is only used in Appendix S3 of their paper and is not used in the text of their
632 manuscript, and thus should be considered a nomen nudum]. At the same time, both *Guo et al.*
633 (*2011, 2020*) and *Wang et al. (2020)* have overlooked two taxonomic issues:

- 634 1) *Pareas carinatus* Wagler, 1830 is the type species of the genus *Pareas* Wagler, 1830,
635 and hence it cannot be placed to a different genus; in our analyses the name *Pareas*
636 Wagler, 1830 corresponds to the *Pareas* clade A (see Fig. 3).
- 637 2) *Eberhardtia* Angel, 1920 is an available genus-level name, erected for *Eberhardtia*
638 *tonkinensis* Angel, 1920, which was considered a junior synonym of *Pareas*
639 *formosensis* (Van Denburgh, 1909) by *Ding et al. (2020)*; in our analyses it corresponds
640 to the *Pareas* clade B (see Fig. 3).

641 Our phylogenetic analyses confirmed the existence of two highly divergent reciprocally
642 monophyletic clades within *Pareas* sensu lato, while strongly supporting the monophyly of the
643 genus.

644 The genus *Asthenodipsas* Peters, 1864 (type species – *Asthenodipsas malaccana* Peters,
645 1864) was for the long time considered a junior synonym of *Pareas*. *Rao & Yang (1992)*
646 examined morphological differences and placed two species *laevis* Boie, 1827, and *malaccanus*
647 Peters, 1864 (that time members of the genus *Pareas*) to a newly erected genus *Internatus* Rao &
648 Yang, 1992 (type species – *Amblycephalus laevis* Boie, 1827). Further studies have also added
649 the taxa *tropidonotus* van Lidth de Jeude, 1923 and *vertebralis* Boulenger, 1900 to this genus
650 (*David & Vogel, 1996; Grossmann & Tillack, 2003*). However, *Iskandar & Colijn (“2001”*

651 2002) noted that *Rao & Yang (1992)* had clearly overlooked an available name for the taxa
652 assigned to their new genus *Internatus*, i.e., *Asthenodipsas* (*Grossmann & Tillack, 2003*). A
653 number of recent works described five additional species within the genus *Asthenodipsas*,
654 without addressing questions of genus-level taxonomy of the group (*Loredo et al., 2013; Quah et*
655 *al., 2019, 2020, 2021*). Several studies demonstrated that *Asthenodipsas* includes two major
656 highly divergent clades, one including *A. laevis* and *A. borneensis* (belonging to the *A.*
657 *malaccanus* species complex) (clade E in our analyses, see Fig. 3), and another including *A.*
658 *vertebralis*, *A. tropidonotus*, and *A. lasgalenensis* (clade D in our analyses, see Fig. 3). Hence,
659 both names *Asthenodipsas* and *Internatus* are referred to the members of clade E, while clade D
660 has no available genus-level name. In previous phylogenetic studies, monophyly of the genus
661 *Asthenodipsas* sensu lato was not supported (*Guo et al., 2011*) or got only moderate level of node
662 support (*Wang et al., 2020; Ding et al., 2020; Vogel et al., 2021*). In our analyses, monophyly of
663 *Asthenodipsas* sensu lato was strongly supported in the concatenated analysis of mtDNA +
664 nuDNA data (Fig. 3), while the analysis of mtDNA genes alone suggested paraphyly of the genus
665 with respect to *Pareas + Aplopeltura* (Supplementary Fig. S2). This genetic divergence among
666 two clades of *Asthenodipsas* is concordant with significant differences in taxonomically valuable
667 scalation characters, such as the number of chin shields and the number of infralabials in contact
668 (see Fig. 5).

669 In summary, in the molecular phylogenetic analysis, Pareinae is obviously divided into five
670 major branches: (A) *Pareas carinatus* + *P. nuchalis* complex, (B) other species of *Pareas*, (C)
671 *Aplopeltura*, (D) *Asthenodipsas vertebralis* group, and (E) other species of *Asthenodipsas* (Fig.
672 3). Monophyly of both *Pareas* sensu lato (clades A + B) and *Asthenodipsas* sensu lato (clades
673 D+E) is strongly supported, while *Asthenodipsas* does not seem to be monophyletic according to
674 mtDNA data alone. Should all five major lineages of Pareinae be recognized as distinct taxa?

675 As we argue below, we find there to be substantial evidence supporting the treatment of the
676 major clades within *Pareas* sensu lato and *Asthenodipsas* sensu lato as separate subgenera. The
677 taxonomic framework ideally should be optimized for utility, reflecting monophyly of taxa and
678 their differences in sets of biologically significant characters, as well as stability, reducing the
679 need for additional taxonomic changes in future (*Vences et al., 2013; Gorin et al., 2021*).
680 Although, the present evidence indicates that we can be confident in the respective monophyly of
681 *Pareas* sensu lato and of *Asthenodipsas* sensu lato, it should be noted that the basal radiations

682 within the both genera are very old: the two clades of *Pareas* diverged in early Oligocene (ca.
683 31.3 mya), while the basal radiation within *Asthenodipsas* happened soon afterwards (ca. 30.0
684 mya). These estimates are comparable with the split between *Pareas* sensu lato and *Aplopeltura*
685 (ca. 33.6 mya), and are of equal or greater age than many other Caenophidian genera (see *Zaher*
686 *et al.*, 2019). While taxon age is usually not taken into account in higher taxonomy, it is however
687 desirable for taxa of equal rank to be of generally comparable age (*Hennig, 1966; Vences et al.*,
688 2013; *Gorin et al.*, 2021). In addition to their substantial age, a number of important characters of
689 external morphology, scalation, and scale ultrastructure distinguish the major clades within
690 *Pareas* and *Asthenodipsas*, allowing their recognition both in collections and in the field
691 (summarized below in taxonomic accounts). Furthermore, there are pronounced differences in
692 the patterns of geographical distribution among the five clades of Pareinae: our hypothesis of the
693 biogeographic history of this subfamily demonstrated that while the whole group evolved in
694 Sundaland, *Pareas* clade A likely originated in Himalaya and Indo-Burma, and further dispersed
695 to East Asia and Indochina, while *Pareas* clade B likely originated in Western Indochina, from
696 where it colonized Sundaland and Eastern Indochina (Fig. 2). The cumulative evidence suggests
697 that the lack of taxonomic recognition for the major clades within the genera *Pareas* and
698 *Asthenodipsas* would conceal information on the ancient divergence between these lineages, as
699 well as the significant differences between them in a set of biologically relevant traits
700 (summarized in Supplementary Table S14).

701 We propose to recognize the clades A and B of *Pareas* and clades D and E of
702 *Asthenodipsas* as separate subgenera. This would enhance the diagnosability of the respective
703 taxa and make them more comparable units to other genera of Pareinae, and as a consequence
704 fully stabilize the taxonomy of the subfamily. This taxonomic action would therefore be in
705 accordance with all three primary Taxon Naming Criteria (TNCs): Monophyly, Clade Stability,
706 and Diagnosability, as well as the secondary TNCs: Time Banding and Biogeography (see
707 *Vences et al.*, 2013). The use of subgenera seems has been successfully applied in several recent
708 revisions of taxonomically challenging groups of reptiles (e.g., *Wallach, Wuester & Broadley,*
709 *2009; David et al.*, 2011; *Wood et al.*, 2020). *Wood et al. (2020)* argued that the defining
710 subgenera may aide taxonomists in species descriptions by allowing them to only diagnose
711 putatively new species from the most relevant members of the same subgenus. By creating
712 formally available supraspecific taxa, accompanied by character-based diagnoses and properly



713 assigned type species, the practice of recognizing subgenera also has the potential to restrain
714 taxonomic vandalism, a malpractice forming a long-standing problem in systematics (*Kaiser et*
715 *al.*, 2013; *Wood et al.*, 2020; *Wüster et al.*, 2021), and thus further enhance taxonomic stability.

716

717 **Species-level diversity in Pareinae**

718 Based on our updated phylogeny of Pareinae, we report on previously unrecognized
719 diversity within the subfamily, and also confirm several taxonomic conclusions made in earlier
720 studies. We document the high degree of uncorrected pairwise sequence divergence between the
721 two samples of *Aplopeltura boa* from Peninsular Malaysia and Sabah in Malaysian Borneo: with
722 *p*-distances of 13.0% in *cyt b* gene and 16.7% in *ND4* gene, the divergence between these
723 populations is estimated as 12.3 mya (Fig. 2; Supplementary Table S9). Further integrative
724 taxonomic studies are needed to clarify the taxonomic status of Malayan and Bornean
725 populations of *A. boa* that might lead to recognition of several species within the genus
726 *Aplopeltura*.

727 In the present study we re-define species groups within the genus *Pareas* recognizing two
728 species groups within the clade A (A1: *P. carinatus* group; and A2: *P. nuchalis* group), and four
729 species groups within the clade B (B1: *P. hamptoni* group; B2: *P. chinensis* group; B3: *P.*
730 *margaritophorus* group; and B4: *P. monticola* group) (Fig. 3). Within the clade B of *Pareas* our
731 results are largely concordant with a number of earlier studies. In *P. monticola* group our
732 analysis further confirms the species status of the recently described *P. victorianus* (*Vogel et al.*,
733 2021); the divergence between this species and its sister taxon *P. monticola* is estimated as 14.1
734 mya (Fig. 2). In *P. margaritophorus* group our results fully agree with the data of *Vogel et al.*
735 (2020) in recognizing *P. andersonii*, *P. modestus*, and *P. macularius* as species distinct from *P.*
736 *margaritophorus*. Moreover we report on a deep divergence between the two samples of *P.*
737 *macularius* from Myanmar and Laos with *p*-distances of 11.5% in *cyt b* gene and 10.4% in *ND4*
738 gene (Supplementary Tables S7–S8); the divergence between these populations is estimated as
739 ca. 8.2 mya (Fig. 2), what might be an indicative of an incomplete taxonomy of the group.
740 Within *P. hamptoni* species group we confirm the results of *Ding et al.* (2020) and *Yang et al.*
741 (2021), suggesting that *P. kaduri* and *P. nigriceps* are sister taxa, while the phylogenetic position
742 of *P. vindumi* remains unresolved. Genetic divergence among the three members of the Taiwan –
743 Ryukyus clade of this group (*P. atayal*, *P. komaii*, and *P. iwasakii*) is comparatively low (6.9% <



744 $p < 9.0\%$ in *cyt b* gene; see Supplementary Table S7), and the basal radiation of this clade is
745 estimated to happen only ca. 5.7 mya (Fig. 2). However a number of recent integrative studies,
746 combining molecular, morphological, behavioral, and ecological data provide strong evidence
747 that these taxa represent distinct species (You, Poyarkov & Lin, 2015; Chang et al., 2021). Our
748 data support the conclusions of Liu & Rao (2021) that *P. mengziensis*, recently described by
749 Wang et al. (2020) is conspecific to *P. niger*, a taxon which has been for a long time placed into a
750 synonymy of *P. hamptoni*. Genetic divergence between *P. niger* and *P. mengziensis* is minimal
751 (0.3% in *cyt b* gene; see Supplementary Table S7), and given the morphological data reported by
752 Liu & Rao (2021) there is little doubt that the latter taxon represents a junior synonym of the
753 former. We further confirm the earlier results of Ding et al. (2020) in assigning the majority of
754 populations of *P. hamptoni* complex from Vietnam, including the specimen identified as “*P.*
755 *tonkinensis*”, to *P. formosensis* (Fig. 3). Our results also agree with that of Ding et al. (2020) in
756 recognizing *P. geminatus* as a species distinct from *P. hamptoni*, but its relationships with the
757 recently described *P. xuelinensis* (Liu & Rao, 2021; our data) are less clear. In our analysis, *P.*
758 *geminatus* consists of two major lineages (*P. geminatus* 1 from northern Thailand and *P.*
759 *geminatus* 2 from southern Yunnan of China and northern Laos), and is paraphyletic with respect
760 to *P. xuelinensis*, which is grouped with *P. geminatus* 1 with strong support (Fig. 3). Two
761 taxonomic solutions are possible to keep the monophyly of the recognized taxa: (1) to split *P.*
762 *geminatus* sensu lato and assign the Thai population to *P. xuelinensis*; or (2) to consider *P.*
763 *xuelinensis* a junior synonym of *P. geminatus*. Genetic divergence among *P. geminatus* 1 + *P.*
764 *xuelinensis* and *P. geminatus* 2 is low (4.1% in *cyt b* gene; see Supplementary Table S7), the
765 divergence between these clades is estimated as only ca. 2.0 mya (Fig. 2), while the
766 morphological characters distinguishing *P. xuelinensis* from *P. geminatus* are vague (Liu & Rao,
767 2021). For the time being, we refrain from a taxonomic decision on *P. geminatus* – *P. xuelinensis*
768 clade pending further integrative studies to address this problem, which should include additional
769 materials from China and northern Indochina.

770 Our study reports on a previously unrecognized diversity within the clade A of the genus
771 *Pareas*: altogether we reveal nine well-supported and highly-divergent clades within this group,
772 five of which were previously unknown. Phylogenetic relationships among these lineages are
773 generally well-resolved (Fig. 3) and genetic divergence between them varies from $p = 4.8\%$ to
774 22.1% in *cyt b* gene, and from $p = 5.2\%$ to 20.1% in *ND4* gene (Supplementary Tables S7–S8).

775 Recently *Wang et al. (2020)* revised the *P. carinatus* complex and described a new species from
776 southern Yunnan of China. In their analyses *Wang et al. (2020)* only included samples from
777 Peninsular Malaysia (*P. carinatus* sensu stricto) and from Yunnan, and based on genetic
778 divergence and concordant morphological differences between these two populations, concluded
779 that the Yunnan population should be regarded as a new distinct species – *P. menglaensis*.
780 However this taxonomic decision had several flaws:

- 781 1) *Wang et al. (2020)* only included in their analyses two populations of *P. carinatus*
782 complex (from Yunnan and Peninsular Malaysia), but omitted any samples or
783 sequences of *P. carinatus* complex from the major part of its range in Indochina and
784 Sundaland, including the sequences available in GenBank.
- 785 2) *Wang et al. (2020)* overlooked two available species-level names presently coined as
786 junior synonyms of *P. carinatus*: *Pareas berdmorei* Theobald, 1868, and
787 *Amblycephalus carinatus unicolor* Bourret, 1934 (see Table 1).
- 788 3) Finally, in their revision *Wang et al. (2020)* did not examine any type specimens of the
789 *P. carinatus* complex members.

790 Our updated tree indicates that *P. carinatus* sensu lato is paraphyletic with respect to both
791 *P. menglaensis* and *P. nuchalis* + *P. temporalis*, and that taxonomy of the complex needs to be
792 reconsidered. The preponderance of data suggests that the pronounced phylogeographic structure
793 within *P. carinatus* – *P. nuchalis* group that bear deep genetic divergences, generally wide
794 morphospacial separation among the sampled populations, and statistically different character
795 state means is indicative of a species complex and as such we consider each population to be
796 recognized as a distinct taxon, which we formally describe below:

- 797 1) The lineage of *P. cf. carinatus* from mountains of central Vietnam (lineage 7) and *P.*
798 *temporalis* from southern Vietnam (lineage 8) form a well-supported clade with sister
799 relationships to *P. nuchalis* (though with moderate node support) (Fig. 3). Genetic
800 distance between these lineages is high (12.7% in *cyt b* gene, 9.6% in *ND4* gene; see
801 Supplementary Tables S7–S8); the divergence between them is estimated as ca. 9.3 mya
802 (Fig. 2); they differ in a number of taxonomically significant characters from each other
803 and other congeners (see below; summarized in Supplementary Table S12), and are
804 widely separated in PCA analysis (Fig. 4). We recognize lineage 7 as a separate new
805 species and together with *P. nuchalis* and *P. temporalis* assign them to the *P. nuchalis*

806 species group (subclade A2, Fig. 3), while all other members of clade A we assign to
807 the *P. carinatus* species group (subclade A1, Fig. 3).

808 2) The population from Peninsular Malaysia (lineage 5), which morphologically and
809 biogeographically corresponds to *P. carinatus* sensu stricto, forms a clade with lineage
810 6 from Tenasserim Mountains in western Thailand and adjacent Myanmar. Lineages 5
811 and 6 are separated by the Isthmus of Kra and likely diverged ca. 5.0 mya (Fig. 2); they
812 are characterized by a moderate level of divergence in mtDNA gene sequences ($p =$
813 7.7% in *cyt b* gene, 5.7% in *ND4* gene; see Supplementary Tables S7–S8), well-
814 separated in PCA analysis (Fig. 4), and are diagnosed by stable differences in a number
815 of morphological characters (see below). We propose to recognize the Tenasserim
816 lineage 6 as a new subspecies within *P. carinatus*.

817 3) All samples of *P. carinatus* complex from the mainland Southeast Asia form a clade
818 sister to the clade inhabiting Thai-Malay Peninsula and Sundaland. Within the mainland
819 clade a single specimen from Phu Yen Province of Vietnam (lineage 4) is highly
820 divergent ($p = 11.9\%–12.7\%$ *cyt b* gene, 13.8%–14.2% in *ND4* gene; see
821 Supplementary Tables S7–S8), forming a sister lineage with respect to all remaining
822 populations (Fig. 3). Though no geographic barrier is known to separate the Phu Yen
823 population from other mainland lineages of *P. carinatus* complex, the divergence
824 between them is estimated as ca. 11.3 mya (Fig. 2). Moreover, the Phu Yen specimen is
825 different from all other congeners in a number of diagnostic morphological features (see
826 below) and is widely separated from them in the PCA morphospace (Fig. 4). Below we
827 describe the Phu Yen lineage 4 as a new species.

828 4) Finally, all mainland populations of *P. carinatus* complex except the Phu Yen lineage 4
829 form a clade with three well-supported subclades (see Fig. 3): (1) the basal subclade
830 (lineage 3) encompasses populations from northern Tenasserim to Thailand and
831 Yunnan, and includes the topotypic population of *P. berdmorei* from Mon State,
832 Myanmar (Fig. 1, loc. 16) and *P. menglaensis* (Fig. 1, loc. 22); (2) populations from
833 southern Vietnam (lineage 1), including the type of *Amblycephalus carinatus unicolor*
834 in Kampong Speu, Cambodia (Fig. 1, loc. 29); and (3) populations from Northern
835 Annamites in Vietnam and Laos (lineage 2). These three lineages are separated from
836 each other by moderate genetic distances ($p = 4.8\%–7.4\%$ in *cyt b* gene, 5.2%–6.8% in

837 *ND4* gene; see Supplementary Tables S7–S8) with estimated divergence times of 5.9–
838 4.0 mya. They are only partially separated in PCA analysis, with a wide overlap in the
839 morphospace for lineages 1 and 3, and moderate separation of lineage 2 (Fig. 4), but are
840 readily distinguished from each other in a number of chromatic and certain
841 morphological differences (see below). We thus suggest that *P. menglaensis* Wang et
842 al., 2020 represents a subjective junior synonym of *P. berdmorei* Theobald, 1868, and
843 propose to recognize *P. berdmorei* as a full species with three subspecies: *berdmorei*
844 (for lineage 3), *unicolor* (for lineage 1), and a new subspecies for lineage 2 described
845 below.

846 In the updated taxonomy for *P. carinatus* – *P. nuchalis* complex we propose to recognize
847 two new species and two new subspecies (see above). Though there has been a certain skepticism
848 regarding the usage of subspecies in herpetological taxonomy in the past (e.g., *Wilson & Brown,*
849 *1953; Frost & Hillis, 1990; Frost, Kluge & Hillis, 1992*), recently the category of subspecies is
850 getting more popular in scope of wide application of phylogenomic data allowing to reveal new
851 cases of mito-nuclear discordance due to ongoing or ancient hybridization (e.g., *Kindler & Fritz,*
852 *2018; De Queiroz, 2020; Hillis, 2021; Marshall et al., 2021*). *Marshall et al. (2021)* define the
853 subspecies as a geographically circumscribed lineage that may have been temporarily isolated in
854 the past, but which has since merged over broad zones of intergradation that show no evidence of
855 reproductive isolation. We tend to tentatively recognize the lineages 1–3 within *P. berdmorei*,
856 and the lineages 5–6 within *P. carinatus* as subspecies but not as full species due to the following
857 reasons: (1) *Amblycephalus carinatus unicolor* was traditionally recognized as a subspecies of *P.*
858 *carinatus* (*Nguyen, Ho & Nguyen, 2009*), thus keeping this taxon along with its sister lineages 2
859 and 3 in the rank of subspecies would support the taxonomic stability; (2) genetic distances
860 among the lineages 1–3 within *P. berdmorei*, and the lineages 5–6 within *P. carinatus* are
861 notably lower than between the ‘good’ species within the *P. carinatus* group (see above); (3)
862 though lineages 5–6 within *P. carinatus* are well separated in the PCA analysis, lineages 1–3
863 within *P. berdmorei* are poorly separated in the PCA analysis (see Fig. 4) and are differentiated
864 from each other primarily by chromatic traits; (4) the estimated time of divergence between the
865 lineages 1–3 (ca. 5.9–4.0 mya), and the lineages 5–6 (ca. 5.0 mya) within *P. carinatus* is notably
866 younger than the age of divergence of ‘good’ species within the *P. carinatus* group (ca. 17.2–9.3
867 mya) and is comparable with the age of basal divergence of other wide-ranged species of *Pareas*,

868 e.g. *P. margaritophorus* (ca. 5.2 mya), *P. formosensis* (ca. 3.6 mya), and *P. monticola* (ca. 3.4
869 mya) (see Fig. 2); (5) lineages 2 and 6 are represented in our analyses by a limited sampling of
870 two specimens for each lineage; this material may be not sufficient to fully assess the variation of
871 diagnostic morphological characters. Further studies including examination of additional
872 materials and localities are needed to test whether the lineages within *P. carinatus* and *P.*
873 *berdmorei* have zones of intergradation or are reproductively isolated from each other.

874

875 Taxonomic accounts

876

877

Family Pareidae Romer, 1956

878

Subfamily Pareinae Romer, 1956

879 **Type genus:** *Pareas* Wagler, 1830.

880 **Phylogenetic definition:** Pareinae is a maximum crown-clade name referring to the clade
881 originating with the most recent common ancestor of *Asthenodipsas malaccanus* and *Pareas*
882 *carinatus*, and includes all extant species that share a more recent common ancestor with these
883 taxa than with *Xylophis captaini*.

884 **Updated diagnosis:** Body strongly laterally compressed with long tail; a short skull, head
885 strongly distinct from neck; large eyes with vertical pupil; vertebrals sharp, weakly enlarged or
886 not enlarged; 13–15 rows dorsal scale rows (DSR) throughout the body; no mental groove;
887 ventrals preceded by a strongly enlarged preventral larger than the first ventral scale. Pareinae are
888 nocturnal, generally arboreal, oviparous snakes, mainly inhabiting of moist tropical and
889 subtropical forests, all members are specialized feeders on snails and slugs.

890 **Distribution:** Widely distributed through the Oriental zoogeographic region from Eastern
891 Himalaya and Northeastern India, central, southern and eastern China including the islands of
892 Hainan and Taiwan, the Yaeyama group of the Ryukyus across the Indochina and the Thai-
893 Malay Peninsula to the Greater Sunda Islands.

894 **Content:** includes all members of the three genera: *Pareas* Wagler, 1830, *Aplopeltura*
895 Duméril, 1853, and *Asthenodipsas* Peters, 1864 (see below).

896 **English name:** Slug-eating snakes.

897 **Remark:** Diagnostic morphological features for the genera and subgenera of the subfamily
898 Pareinae recognized herein are summarized in Supplementary Table S14.

899

900

Genus *Asthenodipsas* Peters, 1864901 **Type species:** *Asthenodipsas malaccana* Peters, 1864. 902 **Synonyms:** *Internatus* Yang & Rao in Rao & Yang, 1992 (type species – *Amblycephalus*
903 *laevis* Boie, 1827).904 **Phylogenetic definition:** *Asthenodipsas* sensu lato is a maximum crown-clade name
905 referring to the clade originating with the most recent common ancestor of *Asthenodipsas*
906 *malaccanus* and *Asthenodipsas vertebralis*, and includes all extant species that share a more
907 recent common ancestor with these taxa than with any of the type species of other Pareinae
908 genera recognized herein.909 **Updated diagnosis:** Dorsal scales smooth, in 15 rows throughout the body; vertebrals
910 enlarged, hexagonal; sharp vertebral keel developed; head distinct from neck, snout blunt; one or
911 two loreals; preocular and subocular scales absent; supraoculars may be fused to the postoculars;
912 nasal undivided; prefrontal, loreal and at least one supralabial in contact with the eye;
913 supraoculars may be fused to the postocular; frontal subhexagonal with the lateral sides
914 converging posteriorly; two anterior temporals; the anterior single inframaxillary shield present
915 (Fig. 5C–F); inframaxillaries wider than long in two or three pairs; the first or third pair of
916 inframaxillaries in contact with each other (Fig. 5C–F); cloacal plate entire; subcaudals divided
917 (*Peters, 1864; Grossmann & Tillack, 2003; Quah et al., 2019, 2020; our data; see Supplementary*
918 *Table S14*).919 **Distribution:** Sundaic region, including the southern Peninsular Thailand, Peninsular
920 Malaysia, and the Greater Sunda Islands (Sumatra, Java and Borneo).921 **Content:** Nine species, including *A. borneensis* Quah, Grismer, Lim, Anuar & Chan; *A.*
922 *ingeri* Quah, Lim & Grismer, 2021; *A. jambilinai* Quah, Grismer, Lim, Anuar & Imbun; *A.*
923 *laevis* (Boie); *A. malaccanus* Peters; *A. lasgalenensis* Lored, Wood, Quah, Anuar, Greer,
924 Ahmad & Grismer; *A. tropidonotus* (Lidth de Jeude); *A. stuebingi* Quah, Grismer, Lim, Anuar &
925 Imbun; and *A. vertebralis* (Boulenger).926 **Etymology:** The genus name is derived from the Greek word “*asthenos*” (ασθενός) for
927 “weak”, “lacking strength”, and the generic name “*Dipsas*”, which is believed to come from the
928 Greek word “*dipsa*” (διψά), meaning “thirst” (and probably refers to the fact that the bite of
929 *Dipsas* snakes was believed to cause intense thirst). 

930 **Recommended English name:** Sundaic slug-eating snakes.

931 **Material examined (n= 38):** For the detailed information (specimen IDs, locality, sex, and
932 the main morphological characteristics) of *Asthenodipsas borneensis* (n=1), *A. laevis* (n=15), *A.*
933 *lasgalensis* (n=5), *A. malaccanus* (n=10), *A. stuebingi* (n=1), *A. tropidonotus* (n=5), and *A.*
934 *vertebralis* (n=1); see Supplementary Table S15 and Appendix II.

935 **Remark:** We recognize the following two subgenera within the genus *Asthenodipsas* for
936 the *A. laevis* and *A. vertebralis* species groups based on stable morphological differences
937 between their members concordant with the ancient phylogenetic divergence between these
938 groups (see above). We propose the subgenus level for the taxa recognized below based on (1)
939 strong support for the monophyly of the genus *Asthenodipsas* sensu lato (see above); (2)
940 biogeographic similarity between these two groups, which are both distributed in the Sundaland
941 region.

942

943 **Subgenus *Asthenodipsas* Peters, 1864**

944 **Type species:** *Asthenodipsas malaccana* Peters, 1864.

945 **Synonyms:** *Internatus* Yang & Rao in Rao & Yang, 1992 (type species – *Amblycephalus*
946 *laevis* Boie, 1827).

947 **Phylogenetic definition:** *Asthenodipsas* sensu stricto is a maximum crown-clade name
948 referring to the clade originating with the most recent common ancestor of *Asthenodipsas*
949 *malaccanus* and *A. laevis*, and includes all extant species that share a more recent common
950 ancestor with these taxa than with *A. vertebralis*.

951 **Diagnosis:** The subgenus *Asthenodipsas* differs from the subgenus *Spondylodipsas*
952 **subgen. nov.** (described below) by the following morphological **characteristics:** two pairs of chin
953 shields (vs. three pairs); 5–7 supralabials; 4–7 infralabials; the third pair of infralabials in contact
954 with each other behind the single anterior inframaxillary shield (vs. the first pair) (Fig. 5C–D; see
955 Supplementary Table S14 for details).

956 **Distribution:** Southern Peninsular Thailand, **Peninsular** Malaysia, Borneo, Sumatra, Java,
957 Bangka, **Mentawai**, and Natuna Archipelagos.

958 **Content:** Six species, including *A. borneensis* Quah, Grismer, Lim, Anuar & Chan; *A.*
959 *ingeri* Quah, Lim & Grismer; *A. jambilinasi* Quah, Grismer, Lim, Anuar & Imbun; *A. laevis*
960 (Boie); *A. malaccanus* Peters; and *A. stuebingi* Quah, Grismer, Lim, Anuar & Imbun.

961 **Recommended English name and Etymology:** as for the genus *Asthenodipsas*. 

962

963 **Subgenus *Spondylodipsas* Poyarkov, Nguyen TV & Vogel subgen. nov.**

964 [urn:lsid:zoobank.org:act:3FE7563C-2BFE-4BA4-A084-1A66E3D9B706]

965 **Type species:** *Amblycephalus vertebralis* Boulenger, 1900. 

966 **Phylogenetic definition:** *Spondylodipsas* **subgen. nov.** is a maximum crown-clade name
967 referring to the clade originating with the most recent common ancestor of *Asthenodipsas*
968 *vertebralis* and *A. lasgalenensis*, and includes all extant species that share a more recent common
969 ancestor with these taxa than with *A. malaccanus*. 

970 **Diagnosis:** The subgenus *Spondylodipsas* **subgen. nov.** differs from *Asthenodipsas* sensu
971 stricto by the following characteristics: three pairs of chin shields (vs. two pairs); 6–8
972 supralabials; 6–8 infralabials; the first pair of infralabials in contact with each other behind the
973 mental (vs. the third pair) (Fig. 5E–F; see Supplementary Table S14 for details).

974 **Distribution:** Mountain areas of Sumatra and Peninsular Malaysia, and Pulau Tioman.

975 **Content:** Three species, including *A. lasgalenensis* Loredó, Wood, Quah, Anuar, Greer,
976 Ahmad & Grismer, *A. tropidonotus* (Lidth de Jeude), and *A. vertebralis* (Boulenger).

977 **Etymology:** The genus name is a Latinized noun in **masculine** gender and is derived from 
978 the Greek word “*spondylon*” (σπονδύλων) for “vertebra”, and the generic name “*Dipsas*” (for
979 etymology of this name see above). The name is given in reference to the well-developed
980 vertebral keel in the members of the subgenus.

981 **Recommended English name:** **Vertebral** slug-eating snakes. 

982

983 **Genus *Aplopeltura* Duméril, 1853** 

984 **Type species:** *Amblycephalus boa* Boie, 1828.

985 **Phylogenetic definition:** *Aplopeltura* is a maximum crown-clade name referring to
986 *Aplopeltura boa* originating as the sister lineage to *Pareas* sensu lato.

987 **Updated diagnosis:** Dorsal scales smooth, in 13 rows throughout the body; vertebral keel
988 weakly developed; two or three loreals; preocular and subocular scales present; supralabials not
989 in contact with the eye; three anterior temporals; the anterior single inframaxillary shield absent
990 (Fig. 5G); generally four (rarely three) pairs of chin shields, anterior pair of chin shields broader
991 than long; at least the first and second pairs of chin shields in contact; subcaudals undivided

992 (*Duméril, 1853; Taylor, 1965*; our data; see Supplementary Table S14 for details).

993 **Distribution:** Sundaic region, including: southern Peninsular Thailand, Peninsular
994 Malaysia, Borneo, Sumatra, Java, Nias, Bangka, and Natuna Islands, and the Philippines (reliably
995 recorded from the Balabac, Basilan, Mindanao, Palawan, and Luzon islands). The published
996 record from southern Peninsular Myanmar by *Dowling & Jenner (1998)* requires further
997 verification.

998 **Content:** A monotypic genus including the single species, *A. boa* Boie.

999 **Etymology:** The genus name is likely derived from the Greek words “*aplos*” (*απλώς*) for
1000 “simple”, and “*pelte*” (*πέλτη*), for “scale”, originally a name of a type of a small shield used in
1001 Ancient Greece.

1002 **Recommended English name:** Blunt-headed slug-eating snakes.

1003 **Material examined (n= 2):** For detailed information (specimen IDs, locality, sex, and
1004 main morphological characteristics) of *Aplopeltura boa* (n=2) see Supplementary Table S15 and
1005 Appendix II.

1006 **Remark:** Our study reports on the significant genetic divergence between the samples of
1007 *A. boa* from Borneo (Sabah) and Peninsular Malaysia, corresponding to the species level in
1008 Pareinae (see above). Further integrative taxonomic studies are required to clarify the status of
1009 the lineages within this species.

1010

1011

Genus *Pareas* Wagler, 1830

1012 **Type species:** *Pareas carinata* Wagler 1830.

1013 **Phylogenetic definition:** *Pareas* sensu lato is a maximum crown-clade name referring to
1014 the clade originating with the most recent common ancestor of *Pareas carinatus* and *P.*
1015 *formosensis*, and includes all extant species that share a more recent common ancestor with these
1016 taxa than with any of the type species of other Pareinae genera recognized herein.

1017 **Updated diagnosis:** Dorsal scales smooth or keeled, in 15 rows throughout the body;
1018 vertebrals slightly larger than other dorsal scales or not enlarged; one (rarely two) loreals;
1019 preocular and subocular scales present; supralabials generally not contacting the eye (except for
1020 *P. monticola* and *P. stanleyi*); three anterior temporals; the anterior single inframaxillary shield
1021 absent (Fig. 5H–G); three pairs of inframaxillaries, all in contact with each other; subcaudals
1022 divided (*Wagler, 1830; Smith, 1943; Taylor, 1965; Vogel et al., 2020*; our data; see

1023 Supplementary Table S14 for details).

1024 **Distribution:** Widely distributed throughout the Oriental zoogeographic region from
1025 Northeastern India and Himalaya to Eastern China and the Greater Sunda Islands.

1026 **Content:** 26 species, including *P. andersonii* Boulenger; *P. atayal* You, Poyarkov & Lin;
1027 *P. berdmorei* Theobald; *P. boulengeri* (Angel); *P. carinatus* Wagler; *P. chinensis* (Barbour); *P.*
1028 *formosensis* (van Denburgh); *P. geminatus* Ding, Chen, Suwannapoom, Nguyen, Poyarkov &
1029 Vogel; *P. hamptoni* (Boulenger); *P. iwasakii* (Maki); *P. kaduri* Bhosale, Phansalkar, Sawant,
1030 Gowande, Patel & Mirza; *P. komaii* (Maki); *P. macularius* Theobald; *P. margaritophorus* (Jan);
1031 *P. modestus* Theobald; *P. monticola* (Cantor); *P. niger* (Pope); *P. nigriceps* Guo & Deng; *P.*
1032 *nuchalis* (Boulenger); *P. stanleyi* (Boulenger); *P. temporalis* Le, Tran, Hoang & Stuart, 2021; *P.*
1033 *victorianus* Vogel, Nguyen & Poyarkov; *P. vindumi* Vogel; and *P. xuelinensis* Liu & Rao; and
1034 the two new species described herein below: *P. abros* Poyarkov, Nguyen & Vogel **sp. nov.**; and
1035 *P. kuznetsovorum* Poyarkov, Yushchenko & Nguyen **sp. nov.**

1036 **Etymology:** The genus name is linked to the Greek word “*pareas*” (*παρείας*), a name of a
1037 mythological snake dedicated to Asclepius, and which was believed to be non-venomous and
1038 create a furrow anytime it moves.

1039 **Recommended English name:** Oriental slug-eating snakes.

1040 **Material examined (n= 257):** Detailed information (specimen IDs, locality, sex, and main
1041 morphological characteristics) for *P. abros* (n=3), *P. berdmorei* (n=19), *P. carinatus* (n=26), *P.*
1042 *kuznetsovorum* (n=1), *P. nuchalis* (n=9), and *P. temporalis* (n=6) is presented in Supplementary
1043 Tables S11–S13 and Appendix II; for *P. vindumi* (n=1) see Vogel (2015); for *P. andersonii*
1044 (n=13), *P. macularius* (n=15), *P. margaritophorus* (n=51), and *P. modestus* (n=8) see Vogel et
1045 al. (2020); for *P. geminatus* (n=9) and *P. hamptoni* (n=5) see Ding et al. (2020); for *P.*
1046 *formosensis* (n=29), *P. kaduri* (n=1), *P. monticola* (n=24), and *P. victorianus* (n=1) see Vogel et
1047 al. (2021); for the abovementioned species and *P. atayal* (n=6), *P. boulengeri* (n=10), *P.*
1048 *chinensis* (n=7), *P. komaii* (n=9), and *P. stanleyi* (n=4) the information is summarized in
1049 Supplementary Tables S13 and S16 and Appendix II.

1050 **Remark:** The taxonomic status of *Amblycephalus yunnanensis* Vogt (1922) currently
1051 considered a junior synonym of *Pareas chinensis* is unclear due to the high morphological
1052 similarity within the group and the geographic proximity of the type localities of two taxa (both
1053 described from Yunnan Province in China). Ding et al. (2020) discussed this issue and suggested

1054 that the integrative taxonomic analysis including detailed comparisons of the type specimens is
1055 required to clarify the relations of these taxa. Several recent studies on phylogenetic relationships
1056 within *Pareas* have revealed a deep divergence within the group, suggesting that its taxonomy
1057 still may be incomplete (Guo et al., 2011; You, Poyarkov & Lin, 2015; Wang et al., 2020;
1058 Bhosale et al. 2020; Ding et al., 2020; Vogel et al., 2020, 2021).

1059

1060

Subgenus *Pareas* Wagler, 1830

1061

Type species: *Pareas carinata* Wagler 1830.



1062

1063

1064

1065

Phylogenetic definition: *Pareas* sensu stricto is a maximum crown-clade name referring to the clade originating with the most recent common ancestor of *Pareas carinatus* and *Pareas nuchalis*, and includes all extant species that share a more recent common ancestor with these taxa than with *Pareas formosensis*.

1066

1067

1068

1069

1070

1071

Diagnosis: The members of the subgenus *Pareas* differ from the members of the subgenus *Eberhardtia* (designated below) by the following morphological characteristics: frontal hexagonal with the lateral sides parallel to each other (Fig. 5B); anterior pair of chin shields broader than long (Fig. 5H); two or three distinct narrow suboculars; and the ravine-like ultrastructure of dorsal scales (Wagler, 1830; Smith, 1943; Taylor, 1965; Vogel et al., 2020; He, 2009; Guo et al., 2020; our data; see Supplementary Table S14 for details).

1072

1073

1074

Distribution: Distributed in the south-eastern part of the Oriental zoogeographic region from the southernmost China throughout the Indochina Peninsula to Peninsular Malaysia, Sumatra, Java, and Borneo (see Fig. 1).

1075

1076

1077

1078

1079

1080

Content: Six species, including *P. berdmorei* Theobald (with three subspecies: *P. b. berdmorei* **stat. nov.**, *P. b. unicolor* **comb. nov.**, and *P. b. annamiticus* **ssp. nov.**); *P. carinatus* Wagler (with two subspecies: *P. c. carinatus*, and *P. c. tenasserimicus* **ssp. nov.**); *P. nuchalis* (Boulenger); *P. temporalis* Le, Tran, Hoang & Stuart, 2021; and the two new species described herein below: *P. abros* Poyarkov, Nguyen & Vogel **sp. nov.**; and *P. kuznetsovorum* Poyarkov, Yushchenko & Nguyen **sp. nov.**

1081

1082

1083

1084

Recommended English name and Etymology: as for the genus *Pareas*.

Pareas carinatus species group

The monophyly of the *carinatus* group is well-supported in both analyses (A1, Fig. 3); the



1085 members of this species group are widely distributed across the Indochina from southern Yunnan
1086 Province of China to the Thai-Malay Peninsula southwards to Sumatra, Java, Borneo and smaller
1087 adjacent islands (Fig. 1). Our phylogeny indicated that the group is composed of three species-
1088 level lineages, which were further supported by morphological analysis. The first lineage inhabits
1089 Sundaland and the Thai-Malay Peninsula and corresponds to *P. carinatus* sensu stricto. It
1090 includes two subgroups divided by the Isthmus of Kra, an important biogeographic boundary (*De*
1091 *Bruyn et al., 2005*). The populations from Sundaland and the Thai-Malay Peninsula south of Kra
1092 correspond to *P. c. carinatus* (lineage 5, Fig. 3), while the populations northwards of Kra
1093 inhabiting the southern part of Tenasserim Range in western Thailand and adjacent Myanmar, we
1094 assign to a new subspecies *P. c. tenasserimcus* **ssp. nov.** described below (lineage 6, Fig. 3). The
1095 second lineage which we identify as *P. bermorei* inhabits the mainland Indochina and includes
1096 three subgroups which we treat as subspecies. The first subgroup (lineage 3, Fig. 3) is widely
1097 distributed from southern Myanmar, western and northern Thailand, to Yunnan Province, China,
1098 and corresponds to *P. b. bermorei* **stat. nov.**). The second subgroup (lineage 1, Fig. 3) is
1099 restricted to southern Vietnam and southeastern Cambodia and represents the subspecies *P. b.*
1100 *unicolor* **comb. nov.** The third subgroup recorded from the northern part of the Annamite Range
1101 we assign to a new subspecies *P. b. annamiticus* **ssp. nov.** described below (lineage 2, Fig. 3).
1102 Finally, the third species-level lineage of this group was recorded from the north-western
1103 foothills of the Langbian (Da Lat) Plateau in southern Vietnam (lineage 4, Fig. 3); we below
1104 describe it as a new species *P. kuznetsovorum* **sp. nov.** Morphological data on the *P. carinatus*
1105 group members is summarized in Table 2 and Supplementary Tables S11 and S12. All members
1106 of the *carinatus* group lack the characteristic large black ring-shaped blotch on the nape and
1107 lateral sides of the neck; in *P. kuznetsovorum* **sp. nov.** the black blotch on the nape is present, but
1108 it is not ring-shaped.

1109

1110 *Pareas carinatus* Wagler, 1830

1111 Figures 6A–B, 7–9; Table 2; Supplementary Tables S11–S12.

1112 **Chresonymy:**1113 *Amblycephalus carinatus* H. Boie in *Schlegel, 1826: 1035 (nomen nudum).*1114 *Amblycephalus carinatus* Boie, 1828: 251 (*nomen nudum*).1115 *Pareas carinata* Wagler, 1830: 181; *Duméril, Bibron & Duméril, 1854: 439.*

1116 *Dipsas carinata* — Schlegel, 1837: 285; Nguyen & Ho, 1996: 61.

1117 *Leptognathus carinatus* — Jan, 1863.

1118 *Amblycephalus carinatus* — De Rooij, 1917: 277; Smedley, 1931: 53; Kopstein, 1936;
1119 Deuve, 1961: 30.

1120 *Pareas carinatus* — Cochran, 1930; Smith, 1943: 121; Manthey & Grossmann, 1997: 376;
1121 Cox et al., 1998: 78; Schmidt & Kunz, 2005: 41; Wallach, Williams & Boundi, 2014: 535.

1122 **Lectotype** (designated herein) (Fig. 6A; Fig. 7): RMNH 954C, adult male, collected by C.
1123 G. C. Reinwardt from Java Island, Indonesia. We designate the RMNH 954C as the lectotype,
1124 since it is the best preserved specimen of the type series.

1125 **Paralectotypes:** Two specimens, RMNH 954A and RMNH 954B, both adult males, with
1126 the same collection data as the lectotype.

1127 **Updated diagnosis:** *Pareas carinatus* differs from all other members of the genus *Pareas*
1128 by the following combination of morphological characters: body slender, **body size** medium (TL
1129 337–702 mm); frontal scale hexagonal with lateral sides parallel to the body axis; anterior pair of
1130 chin shields longer than broad; loreal and prefrontal not contacting the eye; 1–3 suboculars;
1131 usually one postocular; temporals 3+4 or 3+3; three median vertebral rows slightly enlarged; 7–9
1132 infralabials; 15 dorsal scale rows, at midbody the **first** 5 DSR might be slightly keeled; 158–194
1133 ventrals; 54–96 subcaudals, all divided; dorsum yellow-brown with dark vertebral blotches and
1134 dark mottling, transverse dark bands on the body present or absent; upper postorbital stripes
1135 continue to nape forming one or two longitudinal black spots; iris bronze laterally, beige dorsally
1136 (*Wagler, 1830*; our data).

1137 **Material examined:** We directly examined 26 specimens of *P. carinatus* sensu stricto
1138 from Malaysia, Indonesia and Thailand (Table 1).

1139 **Description of the lectotype** (RMNH 954C) (Fig. 6A, Fig. 7): Adult male, body slender
1140 and notably flattened laterally; head comparatively large, narrowly elongated, clearly distinct
1141 from thin neck, snout blunt; eyes large, pupil vertical.

1142 **Body size.** SVL 373 mm; TaL 101 mm; TL 474 mm; TaL/TL: 0.213

1143 **Body scalation.** Dorsal scales in 15–15–15 rows, slightly keeled at midbody, and without
1144 apical pits; three vertebral scale rows slightly enlarged; outermost dorsal scale row not enlarged;
1145 ventrals 170 (+ 1 preventral), without lateral keels; subcaudals 67; cloacal plate single.

1146 **Head scalation.** Rostral not visible from above; one nasal; two internasals, much wider
1147 than long, narrowing and slightly curving back laterally (in dorsal view), anteriorly in contact
1148 with rostral, laterally in contact with nasal and loreal, posteriorly in contact with prefrontal, not
1149 contacting preocular; two large irregular pentagonal prefrontals, much larger than internasals and
1150 with a slightly diagonal suture between them, not contacting the eye; frontal scale hexagonal with
1151 the lateral sides parallel to the body axis, longer than wide, smaller than parietals; one preocular;
1152 two suboculars; one postocular, not fused with subocular; one loreal in contact with prefrontal,
1153 not touching the eye; 7/7 supralabials, 3rd and 5th SL touching the subocular, none of them
1154 reaching the eye, 7th by far the largest, elongated; temporals 3+4; 9/9 infralabials, the anterior
1155 most in contact with the opposite along the midline, bordering mental, anterior 5 pairs of
1156 infralabials bordering anterior chin shields; 3 pairs of chin shields interlaced, no mental groove
1157 under chin and throat; anterior chin shields relatively large, generally wider than long, followed
1158 by two pairs of chin shields much wider than long.

1159 **Coloration.** After over 200 years in preservative, the dorsal and ventral surfaces of the
1160 head, brownish with some dark-brown dusted spots (Fig. 7). Head with two lateral dark-brown
1161 postorbital stripes: the lower one is an interrupted dark line starting from the posterior edge of the
1162 eye, going diagonally down onto the anterior part of the last supralabial; the upper postorbital
1163 stripe is a dark-brown line running from the postocular backwards to the dorsal scales on the
1164 neck, where it meets the similar line on the opposite side of the body forming a narrow X-shaped
1165 dark-brown marking on the nuchal area (Fig. 7A). Upper labials marked with some fine irregular
1166 brown speckling (Fig. 7C–D). Dorsal surface is nearly uniformly light brown with slightly visible
1167 dark cross bands; ventral surfaces yellowish with sparse brownish mottling forming the
1168 interrupted line along the midline, descending backwards. Coloration in life unknown.

1169 **Comparisons:** *Pareas carinatus* differs from *Pareas berdmorei* (revalidated below) by the
1170 generally smaller body size (494.25 ± 73.29 mm vs. 554.15 ± 76.52 mm); generally lower number
1171 of ventrals (171.35 ± 9.29 vs. 177.26 ± 5.77); by slightly lower number keeled dorsal scale rows
1172 (6.05 ± 3.30 vs. 8.96 ± 2.81); and by generally thicker upper postorbital stripe and more
1173 pronounced dark markings on the nape (vs. thinner postorbital stripe and less pronounced dark
1174 markings on the nape); *P. carinatus* differs from *P. nuchalis* by prefrontal not contacting the eye
1175 (vs. in contact); by the absence of the large ring-shaped black blotch on the nape (vs. present); by
1176 lower number of ventrals (171.35 ± 9.29 vs. 209.89 ± 5.25); lower number of subcaudals

1177 (73.22±7.64 vs. 111.11±6.05); and by having keeled dorsal scales (vs. dorsal scales totally
1178 smooth) (see Supplementary Tables S11–S13). Morphological comparisons between all species
1179 of the subgenus *Pareas* are detailed in Supplementary Table S13. This species can be
1180 distinguished from other species of *Pareas* belonging to subgenus *Eberhardtia* **stat. nov.** by
1181 having two or three distinct narrow suboculars (vs. one thin and elongated) and by having a
1182 hexagonal frontal with its lateral sides parallel to the body axis (vs. subhexagonal) (Table 2).

1183 **Distribution:** Based on molecular and morphological data, we suggest that this species is
1184 restricted to the Greater Sunda Islands (Java, Borneo and Sumatra), Peninsular Malaysia and
1185 Thailand, including the Tenasserim Mountains in western Thailand and south-eastern Myanmar
1186 (Fig. 1).

1187 **Etymology:** The species name “*carinatus*” is a Latin adjective in nominative singular,
1188 masculine gender, derived from “*carina*” for a “keel of a ship”, and is given in reference to the
1189 keeled dorsal scales in this species.

1190 **Recommended English name:** Keeled slug-eating snake.

1191 **Remark:** Based on the concordant results of morphological and molecular analyses, we
1192 recognize two subspecies within *P. carinatus*: the populations southwards of the Isthmus of Kra
1193 correspond to the nominative subspecies *P. c. carinatus*, while the populations from the
1194 Tenasserim Mountains northwards from Kra we describe below as *P. c. tenasserimcus* **ssp. nov.**
1195 Although the morphological variation among the sampled specimens of *P. c. carinatus* is
1196 significant (Fig. 4; Table 2), in molecular analyses this subspecies is only represented by
1197 specimens from Peninsular Malaysia. Further phylogenetic analyses of *P. carinatus* populations
1198 from Java, Sumatra and Borneo are required and might reveal new presently unknown lineages
1199 within this species.

1200

1201 *Pareas carinatus carinatus* Wagler, 1830

1202 Figures 6A, 7, 9A–C; Table 2; Supplementary Tables S11–S12.

1203 **Chresonymy:**

1204 *Pareas carinata* Wagler, 1830: 181.

1205 *Amblycephalus carinatus carinatus* — (in part) Mertens, 1930.

1206 *Pareas carinatus carinatus* — (in part) Haas, 1950; Chan-ard et al., 1999: 177; Nguyen,
1207 Ho & Nguyen, 2009: 374.

1208 **Diagnosis:** *Pareas carinatus carinatus* differs from *Pareas carinatus tenasserimicus* ssp.
1209 nov. described below by the following combination of morphological characters: body size
1210 medium (TL 337–608 mm); anterior pair of chin shields wider than long; one postocular;
1211 temporals generally 3+4 (rarely 3+3, 2+3); 15 dorsal scale rows slightly keeled in 3–11 scale
1212 rows at midbody; 158–190 ventrals; 54–84 subcaudals; dorsum light brown with distinct dark
1213 vertebral spots and generally 44–73 transverse dark brownish or blackish bands (Fig. 9A–C);
1214 upper postorbital stripes generally contacting each other on the nuchal area forming a narrow X-
1215 shaped dark marking; ventral scales yellowish with sparse brownish mottling forming the
1216 interrupted line along the midline.

1217 **Variation:** Measurements and scalation features of the subspecies *P. c. carinatus* are
1218 presented in Table 2. There is a certain variation among the sexes observed in the body size and
1219 the number of ventral scales. Males are generally smaller (TL 337.0–571.0 mm, average
1220 471.47±59.47 mm, n=15) than females (TL 446.0–608.0 mm, average 511.0±56.69 mm, n=8);
1221 males also have a generally lower number of ventrals than females (158–183, average
1222 167.27±6.23, n=15 in males vs. 162–190 average 175.20±8.83, n=10 in females). In five
1223 specimens from from Java (ZMH R11546 and R11542), Sumatra (SMF 37825–37826) and
1224 Borneo (NMW 28131:1) keels on dorsal scales are hardly visible; it is unclear if this feature
1225 reflects the geographic variation, or it might arise from the poor preservation of the specimens.
1226 Other morphological features showed no significant variation among the specimens of the series
1227 examined. In our phylogenetic analysis, *P. c. carinatus* was represented only by specimens from
1228 Peninsular Malaysia; further integrative molecular and morphological studies are needed to
1229 assess the geographic variation among the populations of *P. c. carinatus* from Java, Sumatra,
1230 Borneo, and Peninsular Malaysia.

1231 **Distribution:** Peninsular Thailand south of the Isthmus of Kra, Peninsular Malaysia,
1232 Borneo (Sarawak, Sabah, Brunei, and Kalimantan), Sumatra, Java, Lombok, and Bali Islands
1233 (Fig. 1).

1234 **Recommended English name and Etymology:** as for *Pareas carinatus*.

1235

1236 *Pareas carinatus tenasserimicus* Poyarkov, Nguyen TV, Vogel, Pawangkhanant,
1237 Yushchenko & Suwannapoom ssp. nov.

1238 [urn:lsid:zoobank.org:act:11F7F6BA-4733-41FB-8E2D-405DCA5743E5]

1239 Figures 6B, 8, 9D–E; Table 2; Supplementary Tables S11–S12.

1240 **Chresonymy:**

1241 *Pareas carinatus* — (in part) *Mulcahy et al., 2018: 98.*

1242 **Holotype** (Fig. 6B, Fig. 8): ZMMU R-16800 (field number NAP-10160), adult male,
1243 collected by P. V. Yushchenko from mountain forest in Joot Chomwil area, Suan Phueng
1244 District, Ratchaburi Province, western Thailand (N 13.56346, E 99.19465, elevation 800 m asl.)
1245 on 16 July 2019.

1246 **Diagnosis:** *Pareas carinatus tenasserimicus* **spp. nov.** differs from the nominative
1247 subspecies by the following combination of morphological characteristics: body size medium
1248 (TL 702 mm); anterior pair of chin shields as long as broad; two postoculars; temporals 3+3; 15
1249 dorsal scale rows slightly keeled in 7 scale rows at midbody; 194 ventrals; 96 subcaudals;
1250 dorsum light brown to beige, 73 weak dark vertebral spots; transverse dark bands on the body
1251 absent (Fig. 9D–E); upper postorbital stripes not contacting each other on the nuchal area
1252 forming a weak)(shaped dark marking; ventral scales beige with dense brownish mottling not
1253 forming the interrupted midventral line.

1254 **Description of the holotype:** Adult male, specimen in a good state of preservation (Fig. 8),
1255 body slender and notably flattened laterally; head comparatively large, narrowly elongated,
1256 clearly distinct from the thin neck, snout blunt; eye rather large, pupil vertical and slightly
1257 elliptical.

1258 **Body size.** SVL 524 mm; TaL 178 mm; TL 702 mm; TaL/TL: 0.254.

1259 **Body scalation.** Dorsal scales in 15–15–15 rows, slightly keeled in 7 scale rows at
1260 midbody, without apical pits; vertebral scales (three median rows) slightly enlarged; outermost
1261 dorsal scale row not enlarged; ventrals 194 (+ 1 preventral), lacking lateral keels; subcaudals 96,
1262 paired; cloacal plate single.

1263 **Head scalation.** Rostral not visible from above; nasal single; two internasals, much wider
1264 than long, narrowing and slightly curving back laterally (in dorsal view), anteriorly in contact
1265 with rostral, laterally in contact with nasal and loreal, posteriorly in contact with prefrontal, not
1266 contacting preocular; two large irregular pentagonal prefrontals, much larger than internasals and
1267 with a slightly diagonal suture between them, not contacting the eye; frontal scale hexagonal with
1268 the lateral sides parallel to the body axis, longer than wide, of the same size as the parietals; two
1269 preoculars; two suboculars; two postoculars, not fused with suboculars; one loreal in contact with

1270 prefrontal, not touching the eye; 7/7 supralabials, 3rd and 5th SL touching suboculars, none of
1271 them reaching the eye, 7th subocular the largest, elongate; temporals 3+3; 9/9 infralabials, the
1272 anterior most in contact with the opposite along the midline, bordering mental, anterior five pairs
1273 of infralabials bordering anterior chin shields, 3rd pair of infralabials in contact with each other
1274 (Fig. 8F); unpaired inframaxillary shield absent; two pairs of chin interlaced shields contacting
1275 each other, no mental groove under chin and throat; anterior chin shields relatively large, as long
1276 as broad, the second pair of chin shields much broader than long.

1277 **Coloration.** In life, the dorsal and ventral surfaces of the head are uniform light brown
1278 dorsally, yellowish-beige ventrally (Fig. 9E). Head with two lateral postorbital stripes: the lower
1279 one is a thin dark-brown line starting from the lower posterior edge of the eye onto the anterior
1280 part of the last supralabial; the upper one is a strong dark-brown line running from postocular
1281 backwards to the medial dorsal scale rows on the neck; upper postorbital stripes not contacting
1282 each other on the nuchal area forming a weak -shaped dark marking. Upper labials marked with
1283 numerous irregular dark-brown speckling continuing and getting denser on lateral and dorsal
1284 surfaces of the head; 5th supralabial with a larger black spot. Dorsal surfaces with ca. 73 faint
1285 dark blotches along the vertebral keel; transverse dark bands on the body absent; ventral surfaces
1286 of body and tail yellowish cream with very sparse small black spots concentrating laterally, dark
1287 spots and speckles getting denser on the posterior portion of the belly. Iris yellowish-orange
1288 laterally and ventrally, light beige dorsally; pupil black. **In preservative:** After two years of
1289 storage in ethanol (Fig. 8) the general coloration pattern has not changed; light brown of the
1290 coloration of dorsum, head and eye has faded becoming grayish-brown; other features of
1291 coloration remain unchanged.

1292 **Variation:** A single male specimen observed in Kaeng Krachan N.P., Phetchaburi
1293 Province, Thailand (specimen not collected) is overall similar to the holotype of the new
1294 subspecies, but demonstrates certain differences in color pattern, including more pronounced
1295 dark vertebral spots and a series of dark spots along the lower row of dorsal scales (Fig. 9D),
1296 while the holotype has a more uniform coloration lacking dark markings on dorsum and body
1297 sides (Fig. 9E). Given the geographic proximity of the Kaeng Krachan N.P. to the type locality
1298 of the new subspecies, and morphological similarity, we tentatively identify the Kaeng Krachan
1299 population as *P. c. cf. tenasserimicus* **ssp. nov.**; its taxonomic status requires further verification
1300 using morphological examination and molecular data.

1301 **Comparisons:** *Pareas carinatus tenasserimicus* **ssp. nov.** differs from *P. c. carinatus* by
1302 its generally larger size (702 mm vs. 337–608 [485.22±59.74] mm); a slightly higher number of
1303 ventrals (194 vs. 158–190 [170.44±8.22]); a higher number of subcaudals (96 vs. 54–84
1304 [68.13±7.19]); by two postoculars (vs. single postocular); by the 3rd pair of infralabials in
1305 contact with each other (vs. not in contact); by a uniform light brown coloration of dorsum
1306 lacking transverse dark bands (vs. transverse dark bands present); and by upper postorbital
1307 stripes not contacting each other on the nuchal area forming a weak)(-shaped dark marking (vs.
1308 usually contacting each other forming a dark X-shaped marking). For the detailed comparison of
1309 the two subspecies of *P. carinatus* see Supplementary Table S12.

1310 **Distribution:** To date the new subspecies is reliably known from only **threelocalities** in the
1311 southern portion of Tenasserim Range: the type locality in Suan Phueng District, Ratchaburi
1312 Province and Kaeng Krachan N.P., Phetchaburi Province of Thailand (locality 14, Fig. 1), and
1313 from Yaephyu area in Tanintharyi **Division** of Myanmar (locality 15, Fig. 1).

1314 **Etymology:** The new subspecies name “*tenasserimicus*” is a Latin **toponymic** adjective in
1315 nominative singular, masculine gender, and is given in reference to the Tenasserim Mountain
1316 Range in western Thailand and southeastern Myanmar, where the new subspecies occurs.

1317 **Recommended English name:** **Tenasserim** slug-eating snake.

1318 **Ecology notes:** The new subspecies inhabits montane evergreen forests of the Tenasserim
1319 Range on elevations above 800 asl. This is a nocturnal snake, **all** specimens were recorded at
1320 night while perching or crawling on the tree branches and bushes ca. 1–2 m above the ground.
1321 The diet of the new **subspecies** is not known in detail, though it likely consists of land snails or
1322 slugs. In Suan Phueng area (locality 14, Fig. 1), the new subspecies occurs in sympatry with *P. b.*
1323 *berdmorei*, but was not recorded in the same habitats: the new subspecies inhabits montane
1324 forests at ca. 800–1000 m asl., while the specimens of *P. b. bermorei* were recorded in lowland
1325 bamboo forest at 300 m asl. Other co-occurring species of *Pareas* include *P. margaritophorus*.

1326

1327 *Pareas bermorei* **Theobald, 1868**

1328 Figures 6C–F, 10–13; Table 2; Supplementary Tables S11–S12.

1329 **Chresonymy:**

1330 *Pareas bermorei* **Theobald, 1868**; *Das et al., 1998*.

1331 *Amblycephalus carinatus unicolor* **Bourret, 1934**.

1332 *Pareas carinatus* — (in part) Smith, 1943; Taylor, 1965; Yang & Rao, 2008; Nguyen, Ho &
1333 Nguyen, 2009; Teynié & David, 2010; Le et al., 2014; Wallach, Williams & Boundi, 2014; Chan-
1334 ard et al., 2015; Pham & Nguyen, 2019.

1335 *Pareas carinatus unicolor* — (in part) Nguyen, Ho & Nguyen, 2009.

1336 *Pareas menglaensis* Wang, Che, Liu, Ki, Jin, Jiang, Shi & Guo, 2020.

1337 **Lectotype** (designated herein) (Fig. 6C; Fig. 10): ZSI 8022, adult male collected by T. M.  
1338 Berdmore from “Tenasserim”, corresponding to Mon Region in southeastern Myanmar according
1339 to Das et al. (1998) (locality 16, Fig. 1).

1340 **Paralectotypes**: Two specimens, ZSI 8021 and ZSI 8023, adult males, with the same 
1341 collection information as the lectotype.

1342 **Remark**: Theobald (1868) described *Pareas berdmorei* based on a series of two adults and 
1343 three smaller specimens, which he considered to be juveniles; all specimens were collected from
1344 “Tenasserim” by Major T. M. Berdmore. Theobald (1868) has himself noted that the smaller
1345 specimens correspond to *P. macularius* Blyth, and proposed the new name for the larger 
1346 specimens “to prevent confusion of synonyms” (Theobald, 1868: 63). According to Das et al.
1347 (1998), the type series of *P. macularius* includes ZSI 8024–26, while the syntypes of *P.*
1348 *berdmorei* are catalogued under the numbers ZSI 8021–23. We designate the ZSI 8022 as the 
1349 lectotype of *P. berdmorei*, since it is the best preserved specimen of the type series; ZSI 8021 and 
1350 ZSI 8023 represent the paralectotypes.

1351 **Updated diagnosis**: *Pareas berdmorei* differs from other members of the genus *Pareas* by 
1352 the following combination of morphological characters: body size medium (TL 421–770 mm);
1353 frontal scale hexagonal with its lateral sides parallel to the body axis; the anterior pair of chin
1354 shields broader than long; loreal and prefrontal not contacting the eye; generally 1 or 2
1355 preoculars; regularly 2 (rarely 1 or 3) suboculars; generally single postocular (rarely 0 or 2);
1356 temporals 3+4 or 3+3; one to three median vertebral dorsal scale rows slightly enlarged;
1357 generally 8 (7–9) infralabials; 15 dorsal scale rows, of them 3–13 scale rows at midbody feebly
1358 keeled; 162–187 ventrals; 57–89 subcaudals, all divided; dorsum yellow-brown to orange, dark
1359 markings on dorsum variable; thin upper postorbital stripes continue to nape often forming
1360 elongated dark markings; iris uniform, color varies from beige to bright reddish-orange
1361 (Theobald, 1868; Bourret, 1934; Taylor, 1965; Yang & Rao, 2008; Le et al., 2014; Pham &
1362 Nguyen, 2019; Wang et al., 2020; our data).

1363 **Material examined:** In this study we used morphological data from 34 specimens of *P.*
1364 *berdmorei*, including the 19 specimens examined directly (among them the lectotype of *Pareas*
1365 *berdmorei* Theobald and the holotype of *Amblycephalus carinatus unicolor* Bourret) and the
1366 published data for 15 specimens formerly listed as “*P. carinatus*” (Taylor, 1965; Yang & Rao,
1367 2008; Le et al., 2014; and Pham & Nguyen, 2019), and “*P. menglaensis*” (Wang et al., 2020)
1368 (Table 2).

1369 **Description of the lectotype** (ZSI 8022): Adult male, a well-preserved specimen, with
1370 coloration significantly faded due to the long time of preservation in ethanol (Fig. 10), body
1371 slender and notably flattened laterally; head comparatively large, narrowly elongated, slightly
1372 distinct from neck, snout blunt; eyes large.

1373 **Body size.** SVL 490 mm; TaL 120 mm; TL 610 mm; TaL/TL: 0.197.

1374 **Body scalation.** Dorsal scales in 15–15–15 rows, slightly keeled in 9 scale rows at
1375 midbody, lacking apical pits; vertebral scales in three median rows slightly enlarged; the
1376 outermost dorsal scale row not enlarged; ventrals 174 (+ 1 preventral), lacking lateral keels;
1377 subcaudals 64; cloacal plate single.

1378 **Head scalation.** Rostral not visible from above; single nasal; two internasals, much wider
1379 than long, narrowing and slightly curving back laterally (in dorsal view), anteriorly in contact
1380 with rostral, laterally in contact with nasal and loreal, posteriorly in contact with prefrontal, not
1381 contacting preocular; two large irregular pentagonal prefrontals, much larger than internasals and
1382 with a slightly diagonal suture between them, not in contact with eye; the frontal scale hexagonal
1383 with the lateral sides parallel to the body axis, longer than wide, smaller than parietals; two
1384 preoculars; one subocular; one postocular, not fused with subocular; one loreal in contact with
1385 prefrontal, not touching the eye; 7/7 supralabials, 3rd and 5th SL touching the subocular, none of
1386 them reaching the eye, 7th SL the largest, elongate; temporals 3+4; 8/8 infralabials, 3 pairs of
1387 chin shields interlaced, all notably broader than long, no mental groove under chin and throat;
1388 anterior chin shields relatively large.

1389 **Coloration.** Due to preservation in ethanol for over 150 years, the colors of the holotype
1390 have significantly faded, the specimen is uniform light brownish-yellow (Fig. 10A); the present
1391 body pattern of the lectotype no longer retains the original characteristics, though the thin dark
1392 postorbital stripes are still discernable and faded to orange-brown (Fig. 10B). In the original
1393 description, Theobald (1868: 63) gives the following information on the type coloration: “color is

1394 uniform ochraceous, with obsolete traces of vertical bands down the body; two dark lines
1395 converge on the nape; <...> belly white”, indicating that the specimen has already significantly
1396 faded at the moment of the original description.

1397 **Comparisons:** *Pareas berdmorei* is distinguishable from *P. carinatus* by the generally
1398 larger body size (554.15±76.52 mm vs. 494.25±73.29 mm); by slightly higher number of ventrals
1399 (177.26±5.77 vs. 171.35±9.29); slightly higher number of keeled dorsal rows (8.96±2.81 vs.
1400 6.05±3.30); by generally less pronounced dark markings in the nuchal area, thinner postorbital
1401 stripes and a more uniform coloration of the iris; from *P. nuchalis* by prefrontal not contacting
1402 the eye (vs. in contact); by the absence of the ring-shaped black blotch on the nape (vs. present);
1403 by lower number of ventrals (177.26±5.77 vs. 209.89±5.25); lower number of subcaudals
1404 (71.17±7.45 vs. 111.11±6.05); and by the presence of keeled dorsal scale rows (vs. dorsals totally
1405 smooth) (see Supplementary Tables S11–S13). Morphological comparisons between all species
1406 of the subgenus *Pareas* are detailed in Supplementary Table S13. This species can be
1407 distinguished from other species of *Pareas* belonging to subgenus *Eberhardtia* **stat. nov.** by
1408 having two or three distinct narrow suboculars (vs. one thin and elongated) and by having a
1409 hexagonal frontal with its lateral sides parallel to the body axis (vs. subhexagonal) (Table 2).

1410 **Distribution:** The distribution of *P. berdmorei* is restricted to the mainland Indochina
1411 north from the Kra Isthmus (Fig. 1), it is reliably known from western, northern and eastern
1412 Thailand, southeastern Myanmar, Laos, Cambodia, Vietnam and southernmost Yunnan Province
1413 of China.

1414 **Etymology:** *Theobald* (1868) named his new species in honor of British naturalist Captain
1415 Thomas Matthew Berdmore (1811–1859), who was the collector of the type specimens.

1416 **Recommended English name:** Berdmore’s slug-eating snake.

1417 **Remark:** The cumulative evidence from molecular and morphological data strongly
1418 suggests that the populations of “*P. carinatus*” from the mainland Indochina are divergent and
1419 morphologically different from *P. carinatus* sensu stricto from Malayan Peninsula and the
1420 Greater Sunda Islands. Our results thus agree with the data of *Wang et al. (2020)*, who compared
1421 the samples of *P. carinatus* group from southern Yunnan of China and Peninsular Malaysia and
1422 based on the revealed differences described the Yunnan population as a new species *P.*
1423 *menglaensis*. *Wang et al. (2020)* postulated that *P. menglaensis* is endemic to China, but
1424 suggested that this species also may occur in the surrounding low mountainous areas of

1425 neighboring Laos and Myanmar. However, our analyses have demonstrated that the distribution
 1426 of this lineage is much wider and covers the entire territory of the mainland Indochina, including
 1427 the type localities of *Pareas berdmorei* Theobald, 1868 (Mon, southern Myanmar), and of
 1428 *Amblycephalus carinatus unicolor* Bourret, 1934 (Kampong Speu, eastern Cambodia), while the
 1429 Yunnan population of “*P. menglaensis*” is deeply nested within this radiation (Fig. 3). We thus
 1430 conclude that the name *Pareas berdmorei* Theobald, 1868, being the eldest available synonym,
 1431 has to be applied to the mainland populations of *P. carinatus* species group, while
 1432 *Amblycephalus carinatus unicolor* Bourret, 1934 and *Pareas menglaensis* Wang, Che, Liu, Ki,
 1433 Jin, Jiang, Shi & Guo, 2020 represent the subjective junior synonyms of this taxon.

1434 Altogether, based on the concordant results of morphological and molecular analyses we
 1435 report that three geographically restricted lineages exist within *P. berdmorei* (lineages 1–3, Fig.
 1436 3). Despite the significant morphological variation within *P. berdmorei*, these lineages can be
 1437 readily distinguished from each other by a number of chromatic and scalation characters. We
 1438 propose to recognize three subspecies within *P. berdmorei*: *P. b. berdmorei* **stat. nov.** from
 1439 Thailand, southern Myanmar and southern China (including *P. menglaensis* as a junior
 1440 subjective synonym), *P. b. unicolor* **comb. nov.** from southern Vietnam and Cambodia, and a
 1441 new subspecies *P. b. annamiticus* **ssp. nov.** for populations from the Northern Annamite
 1442 Mountains in Vietnam and Laos described below.

1444 ***Pareas berdmorei berdmorei* Theobald 1868 stat. nov.**

1445 Figures 6C–D, 10, 13A–D; Table 2; Supplementary Tables S11–S12.

1446 **Chresonymy:**

1447 *Pareas berdmorei* Theobald, 1868.

1448 *Pareas carinatus* — (in part) Smith, 1943; Taylor, 1965; Yang & Rao, 2008; Wallach,
 1449 Williams & Boundi, 2014; Chan-ard et al., 2015.

1450 *Pareas menglaensis* Wang, Che, Liu, Ki, Jin, Jiang, Shi & Guo, 2020.

1451 **Updated diagnosis:** *Pareas berdmorei berdmorei* differs from other subspecies *P.*
 1452 *berdmorei* by the combination of the following morphological characters: body size large (TL
 1453 451–770 mm); anterior pair of chin shields wider than long; loreal and prefrontal not contacting
 1454 the eye; two suboculars; one postocular; temporals generally 3+4 (rarely 3+3, or 2+3); three
 1455 median vertebral scale rows slightly enlarged; 9 infralabial scales; 15 dorsal scale rows slightly

1456 keeled in 5–13 scale rows at midbody; 166–186 ventrals; 57–89 subcaudals, all divided; dorsum
1457 light brown to yellowish with distinct dark vertebral spots and 64–72 transverse dark brownish or
1458 blackish bands (Fig. 13A–D); upper postorbital stripes weak generally not contacting each other
1459 on the nuchal area forming a narrow)(–shaped dark marking; ventral scales yellowish, generally
1460 immaculate, iris uniform from golden-bronze to orange (Fig. 13A–D).

1461 **Variation:** Measurements and scalation features of the subspecies *P. b. berdmorei* are
1462 summarized in Table 2. There is a certain variation among sexes observed in TaL/TL ratio and
1463 the number of subcaudals scales: males have slightly longer tails (TaL/TL 0.18–0.27, average
1464 0.20 ± 0.03 , n=12) than females (TaL/TL 0.20–0.23, average 0.22 ± 0.01 , n=4); males have
1465 generally higher number of subcaudals than females (73–89, average 78.33 ± 6.67 , n=6, in males
1466 vs. 57–82 average 70.67 ± 7.09 , n=12 in females). In coloration, the specimens of *P. b. berdmorei*
1467 showed variation in iris color: golden-bronze iris in specimens from eastern Thailand (Fig. 13C);
1468 to orange iris in specimens from southern Yunnan and northern Thailand (Fig. 13A–B, D).
1469 Specimens also varied in the arrangement of dark markings in the nuchal area: thicker dark-
1470 brown to black markings in specimens from Thailand (Fig. 13A–C); less distinct dark markings
1471 in specimens from Laos and southern Yunnan (Fig. 13D). Other morphological features showed
1472 no significant variation among the specimens of the series examined.

1473 **Distribution:** Southeastern Myanmar, Northern peninsular Thailand north of the Isthmus
1474 of Kra, western, northern and eastern mainland Thailand, northern Laos, northern Vietnam,
1475 southernmost Yunnan Province of China (Fig. 1).

1476 **Recommended English name and Etymology:** as for *Pareas berdmorei*.

1477 **Ecology notes:** In Suan Phueng area (locality 14, Fig. 1), *P. b. berdmorei* occurs in
1478 sympatry with *P. c. tenasserimicus* **ssp. nov.**, though the two taxa are restricted to different
1479 habitats (see the account for *P. c. tenasserimicus* **ssp. nov.** for details). Across its range, *P. b.*
1480 *berdmorei* occurs in sympatry with various congeners, including *P. margaritophorus*, *P.*
1481 *macularius*, *P. geminatus*, and *P. xuelinensis*.

1482

1483 *Pareas berdmorei unicolor* (Bourret, 1934) **comb. nov.**

1484 Figures 6F, 11, 13E–F; Table 2; Supplementary Tables S11–S12.

1485 **Chresonymy:**

1486 *Amblycephalus carinatus unicolor* Bourret, 1934: 15.

1487 *Pareas carinatus unicolor* — Nguyen, Ho & Nguyen, 2009.

1488 **Holotype:** MNHN 1938.0149, adult female collected by R. Bourret from “Kompong Speu”
1489 (indicated as “Kompong Pseu” on the original label, now Kampong Spoe), Kampong Spoe Prov.,
1490 eastern Cambodia.

1491 **Updated diagnosis:** *Pareas berdmorei unicolor* **comb. nov.** differs from other subspecies
1492 *P. berdmorei* by the following combination of morphological characteristics: body size medium
1493 to small (TL 459–576 mm); anterior pair of chin shields slightly longer than broad; loreal and
1494 prefrontal not contacting the eye; two (rarely one) suboculars; two (rarely one) postoculars;
1495 temporals generally 3+3 (rarely 3+4); three median vertebral scale rows slightly enlarged; 9
1496 infralabial scales; 15 dorsal scale rows slightly keeled in 3–9 scale rows at midbody; 162–180
1497 ventrals; 57–75 subcaudals, all divided; dorsum uniform yellow-ochre to bright orange lacking
1498 distinct dark vertebral spots and transverse dark bands (Fig. 13E–F); upper postorbital stripes
1499 generally absent or weakly discernable not contacting each other on the nuchal area; ventral
1500 scales yellowish to orange, generally immaculate, iris uniform bright orange-red (Fig. 13E–F).

1501 **Description of the holotype** (MNHN 1938.0149): Adult female, specimen partially
1502 dehydrated due to preservation in ethanol for a long time (Fig. 11), body slender and notably
1503 flattened laterally; head comparatively large, narrowly elongated, clearly distinct from thin neck,
1504 snout blunt; eye rather large, pupil vertical and slightly elliptical.

1505 **Body size.** SVL 390 mm; TaL 96 mm; TL 486 mm; TaL/TL: 0.198.

1506 **Body scalation.** Dorsal scales in 15–15–15 rows, slightly keeled in seven scale rows at
1507 midbody, and without apical pits; three median vertebral scale rows slightly enlarged; the
1508 outermost dorsal scale row not enlarged; ventrals 164 (+ 2 preventrals), lacking lateral keels;
1509 subcaudals 64, all divided; cloacal plate single.

1510 **Head scalation.** Rostral not visible from above; nasal entire; two internasals, much wider
1511 than long, narrowing and slightly curving back laterally (in dorsal view), anteriorly in contact
1512 with rostral, laterally in contact with nasal and loreal, posteriorly in contact with prefrontal, not
1513 contacting preocular; two large pentagonal prefrontals, much larger than internasals and with a
1514 slightly diagonal suture between them, not contacting the eye; single hexagonal frontal scale with
1515 its lateral sides parallel to the body axis, frontal longer than wide, smaller than parietals; two
1516 preoculars; one subocular; one postocular, not fused with subocular; one loreal in contact with
1517 prefrontal, not touching the eye; 7/7 supralabials, 3rd to 5th SL touching the subocular, none of

1518 them reaching the eye, 7th by SL the largest, elongate; temporals 3+3; 8/8 infralabials, the
1519 anterior most in contact with the opposite along midline, bordering mental, anterior 5 pairs of
1520 infralabials bordering anterior chin shields; 3 pairs of chin shields interlaced, no mental groove
1521 under chin and throat; anterior chin shields relatively large, slightly longer than broad, followed
1522 by the two pairs of chin shields that are much broader than long.

1523 **Coloration.** Due to preservation in ethanol for almost a century, the color pattern has
1524 significantly faded; as the consequence the specimen no longer retains the original coloration
1525 characteristics. Presently the specimen is uniform dark reddish-brown with no pattern discernable
1526 on the ground color (Fig. 11). The original description contains the following information on the
1527 type specimen coloration: “the color is light reddish brown, absolutely uniform, without any
1528 spots on the body or head, yellower and lighter below” (Bourret, 1934: 15).

1529 **Variation:** Measurements and scalation features of the subspecies *Pareas berdmorei*
1530 *unicolor* **comb. nov.** are presented in Table 2. There is a certain sexual dimorphism observed in
1531 body size and the number of subcaudal scales: males (TL 505.0–576.0 mm, average 552.17±40.85
1532 mm, n=3) have slightly larger body size than females (TL 459.0–538.1 mm, average
1533 498.42±32.59 mm, n=6); males also have a generally higher number of subcaudals than females
1534 (73–75, average 73.67±1.15, n=3 in males vs. 58–75, average 66.33±5.65, n=6 in females).
1535 Coloration of the examined specimens varied in the ground color (from yellow-ochre to bright
1536 orange), and in the dark markings on the head and nuchal area (from upper postorbital stripes
1537 absent to weakly discernable). Other morphological features showed no significant variation
1538 among the examined specimens.

1539 **Comparisons:** *Pareas berdmorei unicolor* **comb. nov.** differs from *P. b. berdmorei* by
1540 slightly lower number of ventrals (162–180 [173.56±5.05] vs. 166–186 [178.10±5.19]), by
1541 generally lower number of keeled dorsal scale rows (3–9 [6.78±1.86] vs. 5–13 [9.60±2.20]), and
1542 by uniform orange to beige coloration lacking dark markings and transverse bands (vs. present)
1543 and brighter orange-red coloration of iris (vs. golden-bronze to orange). *Pareas berdmorei*
1544 *unicolor* **comb. nov.** differs from *P. b. annamiticus* **ssp. nov.** described below by slightly smaller
1545 **body** size (459–576 mm [516.33±42.46 mm] vs. 622–637 mm), by a lower number of ventrals
1546 (162–180 [173.56±5.05] vs. 187), by lower number of keeled dorsal scale rows (3–9 [6.78±1.86]
1547 vs. 13), and by uniform orange to beige coloration lacking dark markings and transverse bands
1548 (vs. dark markings present) and brighter orange-red coloration of iris (vs. off-white to golden).

1549 For the detailed comparisons of the three subspecies of *Pareas berdmorei* see Supplementary
1550 Table S12.

1551 **Distribution:** Based on our morphological and molecular data, *P. b. unicolor* **comb. nov.**
1552 inhabits the lowland and foothill tropical forests of southern Vietnam and eastern Cambodia (Fig.
1553 1), the region historically known as Cochinchina. The actual extend of the subspecies
1554 distribution in central Vietnam and central Cambodia is still unclear and requires further survey
1555 efforts.

1556 **Etymology:** The subspecies name “*unicolor*” is a Latin adjective in nominative singular
1557 meaning “monochrome” and was given in reference to the uniform coloration of this snake.

1558 **Recommended English name:** Cochinchinese slug-eating snake.

1559 **Ecology notes:** In Di Linh District, Lam Dong Province of southern Vietnam (locality 37,
1560 Fig. 1), *P. b. unicolor* **comb. nov.** occurs in sympatry with *P. temporalis* described below; these
1561 two taxa were recorded in the same habitat within the mid-elevation evergreen tropical forests of
1562 the Langbian Plateau (see the account for *P. temporalis* for details). Across its range, *P. b.*
1563 *unicolor* occurs in sympatry with other congeners, including *P. margaritophorus*, *P. macularius*,
1564 and *P. formosensis*.

1565

1566 ***Pareas berdmorei annamiticus* Poyarkov, Nguyen TV, Vogel, Brakels &**
1567 **Pawangkhanant ssp. nov.**

1568 [urn:lsid:zoobank.org:act:3E45EE5B-8DD5-4FB1-814A-76DC2B821E29]

1569 Figures 6E, 12, 13G–H; Table 2; Supplementary Tables S11–S12.

1570 **Chresonymy:**

1571 *Pareas carinatus* — (in part) Ziegler *et al.*, 2006; Nguyen, Ho & Nguyen, 2009; Teynié &
1572 David, 2010; Le *et al.*, 2014; Pham & Nguyen, 2019.

1573 **Holotype:** ZMMU R-16801 (field number NAP-09150), adult female collected by N. A.
1574 Poyarkov, P. Brakels, P. Pawangkhanant and T. V. Nguyen from limestone forest near the Tham
1575 Mangkon Cave, in Ban Nahin-Nai District, Khammouan Province, central Laos (N 18.22111, E
1576 104.81243; elevation 526 m asl.) on July 14, 2019.

1577 **Paratype:** ZMMU R-14796, adult male collected by N. A. Poyarkov and N. L. Orlov from
1578 limestone forest in environs of Kim Lich, Tuyen Hoa District, Quang Binh Province, central
1579 Vietnam (N 18.01206, E 105.92215; elevation 41 m asl.) on September 7, 2015.

1580 **Diagnosis:** *Pareas berdmorei annamiticus* **ssp. nov.** differs from other subspecies *P.*
1581 *berdmorei* by the combination of the following morphological characters: body size medium (TL
1582 622–637 mm); anterior pair of chin shields as long as broad; loreal and prefrontal not contacting
1583 the eye; one subocular; one postocular; temporals 3+4; three median vertebral scale rows slightly
1584 enlarged; 9 infralabial scales; 15 dorsal scale rows keeled in 13 scale rows at midbody; 187
1585 ventrals; 66–73 subcaudals, all divided; dorsum light brown with distinct dark-brown vertebral
1586 spots and 68–71 transverse dark bands, and with dense brownish-gray mottling covering dorsal,
1587 lateral and ventral surfaces of body and head (Fig. 13G–H); upper postorbital stripes discernable,
1588 contacting each other on the nuchal area forming a clear Y-shaped pattern; ventral scales
1589 yellowish-white with dense brownish mottling, iris uniform off-white to golden (Fig. 13G–H).

1590 **Description of the holotype** (ZMMU R-16801): Adult female, specimen in a good state of
1591 preservation (Fig. 12), body slender and notably flattened laterally; head large, narrowly
1592 elongated and flattened, clearly distinct from thin neck, snout blunt; eye large, pupil vertical and
1593 slightly elliptical.

1594 **Body size.** SVL 499 mm; TaL 123 mm; TL 622 mm; TaL/TL: 0.198.

1595 **Body scalation.** Dorsal scales in 15–15–15 rows, the medial 13 scale rows slightly keeled
1596 at midbody, all dorsal scales lacking apical pits; three median vertebral scale rows enlarged;
1597 outermost dorsal scale row not enlarged; ventrals 187 (+ 1 preventral), all lacking lateral keels;
1598 subcaudals 66; cloacal plate single.

1599 **Head scalation.** Rostral not visible from above; nasal single; internasals two, much wider
1600 than long, narrowing and slightly curving back laterally (in dorsal view), anteriorly in contact
1601 with rostral, laterally in contact with nasal and loreal, posteriorly in contact with prefrontal, not
1602 contacting preocular; two large irregular pentagonal prefrontals, much larger than internasals and
1603 with a slightly diagonal suture between them, not contacting the eye; the single frontal scale
1604 hexagonal with the lateral sides parallel to the body axis, longer than wide, smaller than parietals;
1605 one preocular; one subocular; one postocular, not fused with subocular; one loreal in contact with
1606 prefrontal, not touching the eye; 7/7 supralabials, 3rd to 5th SL touching the subocular, none of
1607 them reaching the eye, 7th SL the largest, elongate; temporals 3+4; 9/9 infralabials, the anterior
1608 most in contact with the opposite along the midline, bordering mental, anterior 5 pairs of
1609 infralabials bordering the anterior chin shields; 3 pairs of chin shields interlaced, no mental

1610 groove under chin and throat; anterior chin shields relatively large, as long as broad, followed by
1611 two pairs of chin shields that are much broader than long.

1612 **Coloration.** In life, dorsal surfaces of the head brownish with numerous marbled markings
1613 and dense brownish mottling (Fig. 13H). Head with two lateral postorbital stripes: the lower one
1614 is thick dark-brown line continuing from the middle of the eye onto the anterior part of the last
1615 supralabial; the upper one is a slightly thinner dark line running from postocular backwards to the
1616 dorsal scales on the neck (Fig. 12D). The upper postorbital stripes from the both sides of the
1617 body meet each other in the nape area forming a dark Y-shaped pattern (Fig. 13H). Lateral and
1618 ventral surfaces of the head marked with a dense brown dusting and larger dark spots (Fig. 12E–
1619 D). Dorsal surfaces light-brown with ca. 68 faint vertical dark brown bands. Ventral surfaces of
1620 the head, body and tail yellowish-cream with dense brown dusting. Iris uniform off-white, pupil
1621 black. **In preservative:** After two years of storage in ethanol the general coloration pattern has
1622 not changed (Fig. 12); yellowish tint in the coloration of dorsum, the head and eyes have faded
1623 becoming grayish-brown; other coloration features remain unchanged.

1624 **Variation:** Measurements and scalation features of the subspecies *Pareas berdmorei*
1625 *annamiticus* **ssp. nov.** are presented in Table 2. The paratype generally agrees with the holotype
1626 in all scalation features except the slightly higher number of subcaudals (SC 73 vs. 66).
1627 Coloration of the both specimens was very similar.

1628 **Comparisons:** *Pareas berdmorei annamiticus* **ssp. nov.** differs from *P. b. berdmorei* by
1629 slightly higher of number of ventrals (187 vs. 166–186 [178.10±5.19]), by higher number of
1630 keeled dorsal scale rows (13 vs. 5–13 [9.60±2.20]); by the dense brownish mottling and bigger
1631 brown spots on dorsal, lateral, and ventral surfaces of the head and body (vs. ventral surfaces
1632 immaculate, lateral and dorsal surfaces with sparse dusting); and by uniform off-white to golden
1633 color of iris (vs. golden-bronze to orange). The new subspecies differs from *P. b. unicolor* **comb.**
1634 **nov.** by slightly larger **body** size (622–637 mm vs. 459–576 mm [516.33±42.46 mm]), by a
1635 higher number of ventrals (187 vs. 162–180 [173.56±5.05]), by a higher of number keeled dorsal
1636 scale rows (13 vs. 3–9 [6.78±1.86]); by the presence of dark markings on dorsum and ventral
1637 surfaces, including the dark transverse bands and brownish mottling (vs. uniform orange to beige
1638 coloration lacking dark markings), and by off-white to golden coloration of iris (vs. bright
1639 orange-red color of iris). Detailed comparisons of the three subspecies of *Pareas berdmorei* are
1640 presented in Supplementary Table S12.

1641 **Distribution:** To date the new subspecies is known only from the northern portion of the
1642 Annamite (Truong Son) Mountain Range in central Vietnam and eastern Laos (localities 27–28,
1643 Fig. 1).

1644 **Etymology:** The new subspecies name “*annamiticus*” is a Latin **toponymic** adjective in
1645 nominative singular, **masculine gender**, and is given in reference to the Annamite (Truong Son)
1646 Mountain Range in Vietnam and Laos, where the new subspecies occurs.

1647 **Recommended English name:** Annamite slug-eating snake.

1648 **Ecology notes:** In Quang Binh Province of Vietnam, where the paratype of the new
1649 subspecies was collected, it was recorded in sympatry with *P. margaritophorus* and *P.*
1650 *formosensis*. This taxon seems to be associated with karst evergreen forests. As other members
1651 of the genus *Pareas*, *Pareas berdmorei annamiticus* **spp. nov.** is a nocturnal semi-arboreal snake,
1652 all specimens were recorded while crawling on branches of bushes ca. 1 m above the ground or
1653 on limestone rocks; the diet is unknown but it likely includes terrestrial mollusks.

1654

1655 ***Pareas kuznetsovorum* Poyarkov, Yushchenko & Nguyen TV sp. nov.**

1656 [urn:lsid:zoobank.org:act:1CD26CB3-F3E9-4370-B501-6F678851C9FB]

1657 Figures 6G, 14–15; Table 2; Supplementary Tables S11, S13.

1658 **Holotype:** ZMMU R-16802 (field number NAP-10333), adult male collected by N. A.
1659 Poyarkov from the lowland semideciduous monsoon forest in Song Hinh Protected Forest, Song
1660 Hinh District, Phu Yen Province, southern Vietnam (N 12.77522, E 109.04606; elevation 583 m
1661 asl.) on January 16, 2021.

1662 **Diagnosis:** *Pareas kuznetsovorum* **sp. nov.** differs from other members of the genus
1663 *Pareas* by the combination of the following morphological characteristics: **body** size large (TL
1664 639 mm); anterior pair of chin shields longer than broad; loreal and prefrontal not contacting the
1665 eye; two suboculars; one postocular; temporals 3+4; the single median vertebral scale row
1666 slightly enlarged; 7 supralabial scales; 7–8 infralabial scales; 15 dorsal scale rows, all smooth;
1667 167 ventrals; 87 subcaudals, all divided; dorsum tan to light brown with distinct dark-brown
1668 vertebral line, blackish vertebral spots and 70 transverse dark-brown bands (Fig. 14A–B); upper
1669 postorbital stripes thick, black, contacting each other on the nuchal area forming a dark black Ψ-
1670 shaped chevron (Fig. 14E); lower postorbital stripes thin, black, reaching the anterior part of
1671 SL7, not continuing to the lower jaw and chin; belly yellow with sparse dark-gray dusting and

1672 brown elongated spots forming three longitudinal lines on ventrals (Fig. 14A–B); iris uniform
1673 off-white with beige lateral parts (Fig. 14C–D).

1674 **Description of the holotype** (ZMMU R-16802): Adult male, specimen in a good state of
1675 preservation (Fig. 14); body slender and notably flattened laterally; head large, narrowly
1676 elongated, clearly distinct from thin neck (head more than two times wider than neck width near
1677 the head basis); snout blunt; eye rather large, pupil vertical and elliptical.

1678 **Body size.** SVL 478 mm; TaL 161 mm; TL 639 mm; TaL/TL: 0.252.

1679 **Body scalation.** Dorsal scales in 15–15–15 rows, all scales smooth and lacking apical pits;
1680 vertebral scales slightly enlarged; the outermost dorsal scale row not enlarged; ventrals 167 (+ 1
1681 preventral), lacking lateral keels; subcaudals 87, all divided; cloacal plate single.

1682 **Head scalation.** Rostral not visible from above; nasal single; two internasals, much wider
1683 than long, narrowing and slightly curving back laterally (in dorsal view), anteriorly in contact
1684 with rostral, laterally in contact with nasal and loreal, posteriorly in contact with prefrontal, not
1685 contacting preocular; two large pentagonal prefrontals, much larger than internasals and with a
1686 straight suture between them, not in contact with eye; one hexagonal frontal, longer than wide,
1687 with the lateral sides parallel to the body axis, roughly the same size as the parietals; single
1688 preocular; single postocular, **semicrescent** in shape, not fused with subocular; two suboculars;
1689 single loreal, in contact with preocular, prefrontal, internasal and nasal, not touching the eye; 7/7
1690 supralabials, 3rd to 5th SL touching the subocular, none of them reaching the eye, 7th by far the
1691 largest, elongated; 1/1 supraoculars; 3/3 anterior temporals and 3/4 posterior temporals; 8/7
1692 infralabials, the **anterior most** in contact with opposite along midline forming a straight suture,
1693 bordering mental, the anterior 5 pairs of infralabials bordering the anterior chin shields; 3 pairs of
1694 chin shields interlaced, no mental groove under chin and throat; anterior chin shields relatively
1695 large, notably longer than broad, followed by the two pairs of chin shields that are much broader
1696 than long.

1697 **Hemipenial morphology.** Fully everted hemipenis symmetrical, bilobed, forked (Fig. 15B–
1698 C); the surface from base to crotch smooth, with several (5–6) weakly discernable dermal ridges
1699 on the asulcal surface (Fig. 15C) and few (3–4) shallow folds on the sulcal surface (Fig. 15B).
1700 Sulcus spermaticus deep, with fleshy swollen edges, bifurcate into two separate canals towards or
1701 on the apical lobes. Apical lobes curved with well-developed ornamentation, covered with large

1702 fleshy transverse occasionally intertwining folds, separated with deep slits and forming a complex
1703 pattern resembling the bellows of an accordion (Fig. 15B–C).

1704 **Coloration.** In life, the dorsal surfaces of the head brownish with dense darker marbling
1705 (Fig. 15A). Head laterally off-white with dark-brown spots and blotches, ventrally yellowish-
1706 white with few small black spots. Head with two lateral postorbital stripes: the lower one is a thin
1707 black line starting from the posterior portion of subocular and running ventrally and posteriorly
1708 towards lower temporals to the posterior part of the 6th supralabial and further to the anterior part
1709 of 7th supralabial; the upper one is a well-defined thick black line starting from the upper part of
1710 postocular backwards to the dorsal scales of neck (Fig. 14C–D), where it joins a large rectangular
1711 black spot covering the nape, overall forming a dark black Ψ-shaped chevron pattern (Fig. 14E).
1712 Upper labials marked with a dense brown dusting. Dorsal surfaces of the body tan to light brown
1713 with a distinct dark-brown line running along the vertebral scale row, and with about 70 black
1714 vertebral spots and transverse dark-brown bands (Fig. 14A–B); ventral surfaces of the head, body
1715 and tail yellowish with sparse dark-gray dusting and brown elongated spots forming three
1716 longitudinal lines on ventrals (Fig. 14A–B). Iris uniform off-white with beige lateral parts; pupil
1717 black (Fig. 14C–D). **In preservative:** After six months of storage in ethanol the general
1718 coloration pattern has not changed; the tan coloration of dorsum slightly faded becoming light
1719 grayish-brown, light coloration on head and iris faded becoming brownish; other features of
1720 coloration remain unchanged.

1721 **Comparisons:** *Pareas kuznetsovorum* **sp. nov.** differs from *P. berdmorei* by all dorsal
1722 scales smooth (vs. 3–13 dorsal scale rows keeled), higher number of subcaudals (87 vs. 63–78
1723 [average 71.13±7.23]), by the presence of black chevron on the nuchal area (vs. absent); the new
1724 species further differs from *P. carinatus* by the presence of two postoculars (vs. single or
1725 absent); by a generally higher number of subcaudals (87 vs. 54–96 [average 69.24±8.98]), by all
1726 dorsal scale rows smooth (vs. 3–11 dorsal scale rows keeled [average 6.52±2.94]), by the
1727 presence of black nuchal chevron (vs. absent); and by a lower number of enlarged vertebral scale
1728 rows (1 vs. 3 [average 2.83±0.56]); it further differs from *P. nuchalis* (Boulenger) by prefrontal
1729 not contacting the eye (vs. in contact); by lower number of ventrals (167 vs. 201–220 [average
1730 209.89±5.25]); and by a lower number of subcaudals (87 vs. 102–120 [average 111.11±6.05]).
1731 Morphological comparisons between all species of the subgenus *Pareas* are detailed in
1732 Supplementary Table S13.

1764

1765

***Pareas nuchalis* (Boulenger, 1900)**

1766

Figures 6H, 16–17; Table 2; Supplementary Tables S11, S13.

Chresonymy:

1768

Amblycephalus nuchalis Boulenger, 1900: 185; De Rooij, 1917: 277. 

1769

Pareas nuchalis Malkmus & Sauer, 1996; Malkmus et al., 2002; Wallach, Williams & Boundi, 2014: 537.

1771

Pareas carinatus — (in part) David & Vogel, 1996.

1772

Holotype: NHMUK 1901.5.14.2, adult male from Saribas, Betong Division, West 

1773

Sarawak, Borneo, Malaysia (approximately N 1.410, E 111.527; elevation 15 m asl.), collected

1774

by A. H. Everett.

1775

Updated diagnosis: *Pareas nuchalis* differs from other members of the genus *Pareas* by

1776

the following combination of morphological characters: bony size medium (TL 345–678 mm); 

1777

anterior pair of chin shields longer than broad; loreal not contacting the eye; prefrontal in contact

1778

with the eye; 1–3 suboculars; 1–2 postoculars; temporals generally 3+4 or 3+3; one to three

1779

median vertebral scale rows slightly enlarged; 7–8 supralabial scales; generally 7 (rarely 6 or 8)

1780

infralabials; 15 dorsal scale rows at midbody, all totally smooth; 201–220 ventrals; 102–120

1781

subcaudals, all divided; dorsum tan to light brown with weak dark-brown vertebral spots and 61–

1782

78 distinct transverse dark-brown bands (Figs. 16–17); upper postorbital stripes thick, black,

1783

bifurcating posterior to the secondary temporals, forming a vertical black bar to the mouth angle;

1784

upper postorbital stripes contacting each other on the nuchal area forming a large black ring-

1785

shaped blotch (Fig. 17); lower postorbital stripes thick, black, reaching the anterior part of SL6,

1786

often continuing to the lower jaw and chin; belly yellowish immaculate or with sparse brown

1787

dusting (Figs. 16–17); iris in life whitish with brownish speckles and veins getting denser around

1788

the pupil (Fig. 17) (Boulenger, 1900; Stuebing et al., 2014; our data).

1789

Material examined: In this study we directly examined nine specimens of *Pareas nuchalis*

1790

from Borneo (Malaysia, Indonesia) and Sumatra, including the holotype of *Amblycephalus*

1791

nuchalis (see Table 2, Appendix II).

1792

Coloration. Due to preservation in ethanol for more than a century, the coloration and the

1793

pattern of the holotype has been changed, as the consequences the type specimen no longer

1794

retains the original coloration characteristics (Fig. 16). Dorsal surface of the head uniform dark

1795 brown, head with two postorbital stripes, the upper running laterally backwards to the dorsal
1796 scales on the neck, bifurcating posterior to the secondary temporal scales, forming a dark vertical
1797 bar reaching the mouth angle, upper postorbital stripes contacting each other on the nuchal area
1798 forming a large black ring-shaped blotch (Fig. 16); lower postorbital stripes partially faded,
1799 reaching the anterior part of SL6. Dorsal surface of the body light brown with 78 vertical faint
1800 dark-brown bands; ventral surface of the body and tail yellowish-cream with sparse brown
1801 dusting.

1802 **Variation:** Measurements and scalation features of the specimens examined is presented in
1803 Table 2. There is a certain sexual variation observed in the body size, numbers of ventral and
1804 subcaudal scales: males have slightly larger body size (TL 345.0–678.0 mm, average
1805 529.00 ± 110.19 mm, $n=6$) than females (TL 352.0–503.0 mm, average 422.33 ± 76.03 mm, $n=3$);
1806 males also have generally slightly higher number of ventral and subcaudal scales than females
1807 (VEN 207–220, average 212.17 ± 4.45 , $n=6$; SC 108–120, average 114.17 ± 4.71 , $n=6$ in males vs.
1808 VEN 201–208, average 205.33 ± 3.79 , $n=3$; SC 102–107, average 105.00 ± 2.65 , $n=3$ in females).
1809 Other morphological and coloration features showed no significant variation among the
1810 specimens of the examined series.

1811 **Distribution:** Until recently, this species was considered to be endemic to the island of
1812 Borneo (*Stuebing et al., 2014*), and was recorded both from Sarawak and Sabah of Malaysia,
1813 Brunei and from the Indonesian part of the island (Kalimantan). In this study we for the first time
1814 recorded *P. nuchalis* from central Sumatra the first time, where it was previously confused with
1815 *P. carinatus* (see *David & Vogel, 1996*).

1816 **Etymology:** The species name “*nuchalis*” is a Latin adjective in nominative singular
1817 meaning “nuchal” and was given in reference to the characteristic black ring-shaped spot in the
1818 nuchal area in this species.

1819 **Recommended English name:** Barred slug-eating snake.

1820

1821 *Pareas abros* Poyarkov, Nguyen TV, Vogel & Orlov sp. nov.

1822 [urn:lsid:zoobank.org:act:85CA3212-E8D4-48D1-8ED2-DC8CB183E7E9]

1823 Figures 6I, 18–19; Table 2; Supplementary Tables S11, S13.

1824 **Holotype:** ZMMU R-16393 (field number NAP-08867), adult male collected by N. A.
1825 Poyarkov from the montane evergreen tropical forest near the offsprings of the Paete River,

1826 within the Song Thanh N.P., Nam Giang District, La Dee Commune, Quang Nam Province,
1827 central Vietnam (N 15.53353, E 107.38434; elevation 1083 m asl.) on May 05, 2019.

1828 **Paratypes:** ZMMU R-16392 (field number NAP-06251), adult male, and ZMMU R-14788
1829 (field number NAP-06252), adult female, both collected by N. A. Poyarkov and N. L. Orlov from
1830 the montane evergreen tropical forest within the Sao La Nature Reserve, A Roang area, Thua
1831 Thien – Hue Province, central Vietnam (N 16.10334, E 107.444453; elevation 796 m asl.) on
1832 September 11–17, 2015.

1833 **Diagnosis:** *Pareas abros* **sp. nov.** differs from all other members of the genus *Pareas* by
1834 the combination of the following morphological characters: body size medium (TL 434–565
1835 mm); head notably flattened dorsoventrally; anterior pair of chin shields longer than broad; loreal
1836 and prefrontal not contacting the eye; three suboculars; two postoculars; temporals 3+3; the
1837 single median vertebral scale row slightly enlarged; 9 supralabial scales; generally 8 (rarely 9)
1838 infralabials scales; 15 dorsal scale rows at midbody, of them 9–11 median scale rows slightly
1839 keeled; 180–184 ventrals; 83–95 subcaudals, all divided; dorsum yellowish-brown with distinct
1840 dark-brown vertebral line, barely distinct blackish vertebral spots and 44–56 faint interrupted
1841 transverse dark-brown bands (Fig. 19A–C); upper postorbital stripes thick, slate-black,
1842 bifurcating posterior to the secondary temporals, forming a thick black line, continuing to the 7th
1843 SL and further on the neck; upper postorbital stripes contacting each other on the nuchal area
1844 forming a large ring-shaped blotch (Fig. 19A–C); two thick, black lower postorbital stripes
1845 reaching the 6th and 8th SL, and continuing to the lower jaw; belly beige with dense brownish-
1846 gray dusting and dark brown elongated spots forming two longitudinal lines on the lateral sides
1847 of ventrals (Fig. 18D); iris in life beige with ochraceous to orange speckles and veins getting
1848 denser around the pupil (Fig. 19).

1849 **Description of the holotype** (ZMMU R-16393): Adult male, specimen in a good state of
1850 preservation (Fig. 18); body slender and notably flattened laterally; head very large, notably
1851 flattened dorso-ventrally, clearly distinct from thin neck (head more than two times wider than
1852 neck width near the head basis), snout obtusely rounded in profile and in dorsal view; eye very
1853 large, pupil vertical and elliptical. Hemipenis not everted.

1854 **Body size.** SVL 314 mm; TaL 120 mm; TL 434 mm; TaL/TL: 0.276.

1855 **Body scalation.** Dorsal scales in 15–15–15 rows, slightly keeled in 11 scale rows at
1856 midbody (Fig. 18F), all lacking apical pits; the single median vertebral scale row slightly

1857 enlarged; the outermost dorsal scale row not enlarged; ventrals 184 (+ 1 preventral), lacking
1858 lateral keels; subcaudals 92; cloacal plate single.

1859 **Head scalation.** Rostral not visible from above; single nasal; two internasals, much wider
1860 than long, narrowing and slightly curving back laterally (in dorsal view), anteriorly in contact
1861 with rostral, laterally in contact with nasal and loreal, posteriorly in contact with prefrontal, not
1862 contacting preocular; two large irregularly pentagonal prefrontals, much larger than internasals
1863 and with a straight suture between them, not in contact with eye; the single frontal scale
1864 hexagonal with the lateral sides slightly concave, parallel to the body axis, longer than wide,
1865 smaller than parietals; single preocular; two postoculars, **semicrescent** in shape, not fused with
1866 subocular; single presubocular; three suboculars; two loreals, upper larger than lower, irregularly
1867 pentagonal, in contact with presubocular, prefrontal, internasal and nasal, not touching the eye;
1868 9/9 supralabials, 4th to 6th SL touching the subocular, none of them reaching the eye, 9th by far the
1869 largest, elongated; 1/1 supraoculars; 3/3 anterior temporals and 3/3 posterior temporals; 8/8
1870 infralabials, the **anterior most** in contact with the opposite along midline forming a diagonal
1871 suture between them, bordering mental, the anterior five pairs of infralabials bordering the
1872 anterior chin shields; 3 pairs of chin shields interlaced, no mental groove under chin and throat;
1873 the anterior chin shields relatively large, much longer than broad, followed by two pairs of chin
1874 shields that are much broader than long.

1875 **Coloration.** In life, dorsal and ventral surfaces of the head brownish with dense dark-brown
1876 mottling. Head with three lateral postorbital stripes: the upper postorbital stripes thick, slate-
1877 black lines running from postocular backwards towards the dorsal scales of neck, bifurcating
1878 posterior to the secondary temporals, forming a ventral branch – a thick black line, continuing to
1879 the 9th SL and further to the posterior corner of the jaw and on the neck; the dorsal branch
1880 extending to the top of the nape contacting each other on the nuchal area; both of the branches of
1881 the upper postorbital stripe join at the front of the neck to form a large black ring-shaped blotch
1882 that covers the entire nape area (Fig. 18C). Two lower postorbital stripes: the posterior one is a
1883 thick, black line starting from the lower portion of postorbital, running ventrally and posteriorly
1884 towards lower temporals to 8th and 9th supralabials, and further and continuing to the lower jaw;
1885 the anterior lower postorbital stripe is a short thick black vertical stripe starting from the middle
1886 subocular, reaching the 6th SL and continuing further to the 4th IL as a line of black spots (Fig.
1887 18C). Upper labials beige with dense brown dusting. Dorsal surfaces of body yellowish-brown

1888 with distinct dark-brown line running along the vertebral dorsal scale row, barely distinct
1889 blackish vertebral spots and ca. 56 faint interrupted transverse dark-brown bands (Fig. 18A–B).
1890 Ventral surfaces of the head, body and tail cream-beige with dense brownish-gray dusting and
1891 dark brown elongated spots forming two longitudinal lines on the lateral sides of ventrals (Fig.
1892 18D). Iris in life beige with orange speckles and veins getting denser around the pupil; pupil
1893 black (Fig. 18C). **In preservative:** After two years of storage in ethanol the general coloration
1894 pattern did not change; the tan tint of the dorsal coloration, and orange tints on the head and eye
1895 have faded becoming grayish-brown; other features of coloration remain unchanged.

1896 **Variation:** Measurements and scalation features of the type series is presented in Table 2.
1897 The holotype has two loreals while there is only one in the two paratypes. There is a certain
1898 variation observed in the number of ventral and dorsal scales: males have **generally** a higher
1899 number of subcaudals (92–95, n=2) than the single female (83, n=1); dorsal scales are keeled in
1900 11 scale rows at midbody in males vs. in 9 scale rows are keeled in the single female. Coloration
1901 features among the members of the type series were very similar.

1902 **Hemipenial morphology.** The hemipenis is partially everted in the adult male paratype
1903 ZMMU R-16392 (Fig. 19D). The partially everted organ **symmetrical**, bilobed, forked, the
1904 surface from base to crotch smooth, with numerous (7–11) shallow folds and on the sulcal
1905 surface and fewer 3–6 larger dermal ridges on the asulcal surface. Sulcus spermaticus deep, with
1906 fleshy swollen edges, bifurcating into two separate canals towards the apical lobes. Apical lobes
1907 with well-developed ornamentation, covered with large fleshy irregularly curved folds in 4–5
1908 rows and fleshy protuberances, separated with deep slits, forming a complex pattern resembling
1909 brain cortex.

1910 **Comparisons:** *Pareas abros* **sp. nov.** differs from *P. berdmorei* by the anterior pair of chin
1911 shields longer than broad (vs. broader than long), by slightly longer tail (TaL/TL 0.26–0.29
1912 [average 0.28±0.01] vs. 0.17–0.27 [average 0.21±0.02]), by slight higher number of ventrals (83–
1913 95 [**average 90.00±6.24**] vs. 57–89 [average 71.13±7.25]), by the presence of a large ring-shaped
1914 black blotch in the nuchal area (vs. absent); and by the presence of the dark vertebral line (vs.
1915 absent). The new species differs from *P. carinatus* by longer tail (TaL/TL 0.26–0.29 [average
1916 0.28±0.01] vs. 0.18–0.25 [average 0.22±0.02]), by a slightly higher number of subcaudals (83–95
1917 [average 90.00±6.24] vs. 54–96 [average 69.24±8.98]), by the presence of a large ring-shaped
1918 black blotch in the nuchal area (vs. absent); by the presence of the dark vertebral line (vs.

1919 absent); and by weakly-discernable faint transverse dark bands on body (vs. well-discernable
1920 dark bands). *Pareas abros* **sp. nov.** differs from *P. nuchalis* by prefrontal not in contact with the
1921 eye (vs. in contact); by keeled 9–11 dorsal scale rows (vs. all dorsal scales totally smooth); and
1922 by the black nuchal blotched forming a complete ring (vs. incomplete ring-shaped blotch). The
1923 new species differs from *P. kuznetsovorum* **sp. nov.** (described above) by a higher number of
1924 ventrals (180–184 [average 182.67±2.31] vs. 167); by keeled 9–11 dorsal scale rows (vs. all
1925 dorsal scales totally smooth); by smaller body size (TL 434–565 mm [average 506.67±66.67
1926 mm] vs. 639 mm). Morphological comparisons between all species of the subgenus *Pareas* are
1927 detailed in Supplementary Table S13.

1928 **Distribution:** The new species is to date known only from two localities in Quang Nam
1929 (locality 42, Fig. 1) and Thua Thien – Hue (locality 43, Fig. 1) provinces of central Vietnam,
1930 both of them are located within the Kon Tum – Gia Lai Plateau, the northern portion of the
1931 Central Highlands (Tay Nguyen) Region of Vietnam. The Kon Tum – Gia Lai Plateau is isolated
1932 from the adjacent mountain massifs by lowland areas and is characterized by a high level of
1933 herpetofaunal endemism (Bain & Hurley, 2011; Poyarkov et al., 2021); the new species is also
1934 likely an endemic of this mountain region. The holotype of the new species was collected in just
1935 2 km from the national border of Vietnam and Lao PDR (locality 42, Fig. 1), hence the
1936 occurrence of *Pareas abros* **sp. nov.** in Laos is highly anticipated.

1937 **Etymology:** The new species name “*abros*” is a Latinized adjective in nominative singular
1938 derived from the Ancient Greek word “*abros*” (αβρός), meaning “cute”, “handsome”, and
1939 “delicate”. The name is given in reference to the appealing and cute appearance of the new
1940 species, as well as other members of the genus *Pareas*.

1941 **Recommended English name:** Cute slug-eating snake.

1942 **Ecology notes:** *Pareas abros* **sp. nov.** inhabits montane evergreen tropical forests of Kon
1943 Tum – Gia Lai Plateau and was recorded on the elevations from 796 to 1083 m asl. In both
1944 localities, the new species was recorded in fragments of primary polydominant forest along the
1945 banks of montane streams. The new species was active at 21:00 – 00:00 h, the specimens were
1946 usually located while crawling on the branches of bushes and trees ca. 1–1.5 m above the
1947 ground; the holotype was spotted while crossing the small forest trail. Other sympatric members
1948 of Pareidae in both localities include *Pareas formosensis*. The diet of *Pareas abros* **sp. nov.** is
1949 unknown; it likely consists of terrestrial mollusks as in other congeners.

1950

1951

Pareas temporalis Le, Tran, Hoang & Stuart, 2021

1952

Figures 6J, 20–21; Table 2; Supplementary Tables S11, S13.

1953

1954 **Holotype:** UNS 09992 (field number LD25711), adult female, Doan Ket Commune, Da

1955 Huoai District, Lam Dong Province, Vietnam (11.340370°N, 107.620561°E, elevation of 496 m

1956 **Referred specimens** (n=6): ZMMU R-13656 (field number NAP-01610), adult male

1957 collected by N. A. Poyarkov from the low-elevation disturbed bamboo forest within the valley of

1958 the Sui Lan River in the environs of Ben Cau and Phuok Son ranger stations, Cat Loc sector of

1959 the Cat Tien National Park, Lam Dong Province, southern Vietnam (N 11.69444, E 107.30639;

1960 elevation 135 m asl.) on June 20, 2011; DTU 471, adult female, collected by L. H. Nguyen and

1961 H. M. Pham from the valley of Suoi Lanh Stream, Rung Ge Commune, Di Linh District, Lam

1962 Dong Province, southern Vietnam (N 11.46725, E 108.06915; elevation of ca. 1320 m asl.) on

1963 March 1, 2019; SIEZC 20214, adult female, collected by L. H. Nguyen in Gia Bac District, Lam

1964 Dong Province, southern Vietnam (N 14.220392, E 108.317133; elevation of ca. 1050 m asl.) on

1965 August 10, 2018; and SIEZC 20215, adult female, collected by V. B. Tran from Biduop – Nui Ba

1966 N.P., Lam Dong Province, southern Vietnam (N 12.23383, E 108.44866; elevation of ca. 790 m

1967 asl.) on May 30, 2017; DTU 486–487 (two adult females) collected by T. A. Pham and T. V.

1968 Nguyen in Rung Ge Commune, Di Linh District, Lam Dong Province, southern Vietnam (N

1969 11.46725, E 108.06915; elevation of ca. 1320 m asl.), on May 10, 2020.

1970 **Updated diagnosis:** *Pareas temporalis* differs from other members of the genus *Pareas* by

1971 the following combination of morphological characters: body size large (TL 555–665 mm); head

1972 distinctly flattened dorsoventrally; the anterior pair of chin shields notably longer than broad;

1973 loreal and prefrontal not contacting the eye; two suboculars; generally two (rarely one or absent)

1974 postoculars; temporals generally 3+3 (rarely 3+4); three median vertebral scale rows slightly

1975 enlarged; generally 8 (rarely 7) supralabial scales; generally 8 (rarely 7) infralabials scales; 15

1976 dorsal scale rows, all of them notably keeled; 187–198 ventrals; 86–92 subcaudals, all divided;

1977 dorsum bright yellowish-brown to light-orange with distinct blackish vertebral line edged with

1978 two light yellowish paravertebral lines; vertebral spots and transverse dark bands absent (Fig.

1979 21); dorsal scales with few scattered small black spots; two very clear thin black postorbital

1980 stripes beginning from the lower and upper edges of each postorbital scale; the lower postorbital

1981 stripe as two thin parallel black lines reaching the anterior part of 8th SL, not continuing to the
1982 lower jaw and chin; the left and right upper postorbital stripes contacting each other at the nuchal
1983 area forming a black ring-shaped blotch (Fig. 21A–C); belly yellowish-cream with sparse
1984 brownish dusting and irregular small spots; iris in life amber-colored to bright-orange (Fig. 21A–
1985 C).

1986 **Description of a male specimen** (ZMMU R-13656): Adult male, specimen in a good state
1987 of preservation, body dissected longitudinally along the ventral scales (Fig. 20); body slender and
1988 notably flattened laterally; head very large, distinctly flattened dorso-ventrally, clearly distinct
1989 from the thin neck (head more than three times wider than neck width near the head basis), snout
1990 blunt in dorsal and lateral views; eye very large, pupil vertical and elliptical. Hemipenis not
1991 everted.

1992 **Body size.** SVL 413 mm; TaL 142 mm; TL 555 mm; TaL/TL: 0.256.

1993 **Body scalation.** Dorsal scales in 15–15–15 rows, all scales notably keeled and lack apical
1994 pits; vertebral scale rows and the two adjacent rows of scales (3 medial dorsal scale rows)
1995 slightly enlarged; the outermost dorsal scale row not enlarged; ventrals 198 (+ 1 preventral),
1996 lacking lateral keels; subcaudals 98, all paired; cloacal plate single.

1997 **Head scalation.** Rostral not visible from above; single nasal; two internasals, much wider
1998 than long, narrowing and slightly curving back laterally (in dorsal view), anteriorly in contact
1999 with rostral, laterally in contact with nasal and loreal, posteriorly in contact with prefrontal, not
2000 contacting preocular; two large irregular pentagonal prefrontals, much larger than internasals and
2001 with a slightly diagonal suture between them, not in contact with the eye; one subhexagonal
2002 frontal, longer than wide, smaller than parietals, with the lateral sides almost parallel to each
2003 other, slightly converging posteriorly; single preocular; single postocular present on the left side,
2004 absent on the right side of the head, semicrescent in shape, not fused with subocular;
2005 presubocular absent; two suboculars; single loreal, in contact with presubocular, prefrontal,
2006 internasal and nasal, not touching the eye; 9/9 supralabials, 3rd to 5th or 3rd to 7th SL touching the
2007 subocular, none of them reaching the eye, 9th by far the largest, elongated; 1/1 supraocular; 3/3
2008 anterior temporals and 3/4 posterior temporals; 7/8 infralabials, the anterior most in contact with
2009 the opposite along the midline forming a diagonal suture between them, bordering mental, the
2010 anterior five pairs of infralabials bordering the anterior chin shields; three pairs of chin shields

2011 interlaced, no mental groove under chin and throat; the anterior chin shields relatively large,
2012 much longer than broad, followed by two pairs of chin shields that are much broader than long.

2013 **Coloration.** In life, dorsal surface of the head brownish with some blackish mottling and
2014 larger spots, getting denser on frontal and prefrontals. Head with two clear thin black lateral
2015 postorbital stripes: the upper one is a well-developed slate-black line starting from postocular and
2016 running backwards to dorsal scales of the neck, the left and right upper postorbital stripes
2017 contacting each other at the nuchal area forming a black X-shaped pattern in dorsal view (Fig.
2018 20E), and a large ring-shaped blotch in lateral view (Fig. 20C); the lower postorbital stripe is an
2019 interrupted black line starting from the lower portion of postorbital, and running ventrally and
2020 posteriorly towards lower temporals and to 8th and 7th supralabials and not continuing to the
2021 lower jaw and chin. Other markings on the lateral surfaces of the head include a large dark
2022 elongated spot on the 6th supralabial, and a thick slate-black line running from the posterior edge
2023 of the 9th supralabial backwards to the and further on the lateral surfaces of the neck, where it
2024 joins the ring-shaped nuchal blotch ventrally (Fig. 20C; Fig. 21A). Supralabials yellowish-white
2025 with rare tiny brown spots. Dorsal surfaces of the body bright yellowish-brown to light-orange
2026 with distinct blackish vertebral line edged with two light yellowish paravertebral lines; vertebral
2027 spots and transverse dark bands absent (Fig. 21); dorsal scales on the sides of the body with few
2028 irregularly scattered small dark spots; the ventral surfaces of the head, body and tail is yellowish-
2029 cream with sparse brownish dusting and irregular small spots; iris in life amber-colored to bright-
2030 orange; pupil black (Fig. 21A–C). **In preservative:** After ten years of storage in ethanol, the
2031 general coloration pattern has not changed; light brownish and yellowish tints in the coloration of
2032 dorsum, head and eyes faded becoming grayish-brown; other features of the coloration remain
2033 unchanged (Fig. 20).

2034 **Variation:** Measurements and scalation features of additional specimens of *P. temporalis*
2035 is presented in Table 2. All coloration features of the additional specimens are very similar to
2036 those described for the holotype (Le et al., 2021). The holotype UNS 09992 generally agrees with
2037 the series of specimens examined by us, it has slightly higher number of supralabials (9/8 vs. 7–
2038 8) and infralabials (8/9 vs. 7–8), higher number of anterior temporals (4/5 vs. 3/3), and generally
2039 slightly lower number of posterior temporals (3/3 vs. 3–4), it also has 2/3 postoculars, while in
2040 the specimens we examined generally had 2/2 postoculars and 1/0 postoculars in the single male
2041 specimen ZMMU R-13656. We observed a certain sexual dimorphism in *P. temporalis*: male

2042 ZMMU R-13656 has a higher number of ventrals (198 in a single male vs. 185–188 in five
2043 females), and subcaudals (92 in male vs. 86–89 in five females). Other morphological and
2044 chromatic features showed no significant variation among the examined specimens.

2045 **Updated comparisons:** *Pareas temporalis* differs from its sister species *Pareas abros* **sp.**
2046 **nov.** by a higher number of ventrals (185–198 vs. 180–184), by all dorsal scale rows strongly
2047 keeled (vs. weak keels present only on 9–11 dorsal scale rows), by a higher number of enlarged
2048 vertebral scales rows (3 vs. 1), and by the absence of dark cross-bands on the body (vs. 44–56
2049 faint dark transverse bands present). *Pareas temporalis* differs from *P. berdmorei* by a higher
2050 number of ventrals (185–198 vs. 164–186), by a higher number of subcaudals (86–92 vs. 63–78),
2051 by the presence of a black ring-shaped blotch on the collar (vs. absent), and by having all dorsal
2052 scale rows strongly keeled (vs. weak keels present only on 3–13 dorsal scale rows). *Pareas*
2053 *temporalis* differs from *P. carinatus* by having two postoculars (vs. single or absent); by
2054 generally slightly higher number of subcaudals (86–92 vs. 54–96), by having all dorsal scale
2055 rows strongly keeled (vs. weak keels present on 3–11 dorsal scale rows), and by the presence of
2056 a black ring-shaped blotch on the collar (vs. absent). *Pareas temporalis* differs from *P. nuchalis*
2057 by prefrontal not contacting the eye (vs. in contact), by a slightly lower number of ventrals (187–
2058 198 vs. 201–220), by a lower number of subcaudals (86–92 vs. 102–120), and by having all
2059 dorsal scale rows strongly keeled (vs. all dorsal scales smooth). Finally, *P. temporalis* differs
2060 from *Pareas kuznetsovorum* **sp. nov.** in having all dorsal scale rows strongly keeled (vs. all
2061 dorsal scales smooth), by a higher number of enlarged vertebral scales rows (3 vs. 1), and by a
2062 higher number of ventrals (185–198 vs. 167). Morphological comparisons between all species of
2063 the subgenus *Pareas* are detailed in Supplementary Table S13.

2064 **Updated distribution:** In addition to the type locality of this species, *P. temporalis* is also
2065 known from four localities, all in the Lam Dong Province of southern Vietnam (localities 37–40,
2066 Fig. 1). All these localities belong to the Langbian (Da Lat) Plateau – the southernmost part of
2067 the Annamite Range, well-known by its high level of endemism in herpetofauna (*Bain & Hurley,*
2068 *2011; Poyarkov et al., 2021*). We assume that *Pareas temporalis* is endemic to the Langbian
2069 Plateau; it is expected to occur on middle elevations in the adjacent provinces of southern
2070 Vietnam: Binh Phuoc, Dak Nong, Dak Lak, Ninh Thuan and Binh Thuan, and also likely might
2071 inhabit the southeasternmost part of the Mondulkiri Province of Cambodia.

2072 **Etymology:** The species name “*temporalis*” is a Latin adjective in nominative singular and
 2073 is given in reference to the high number of temporal scales in this species (*Le et al., 2021*).

2074 **Recommended English name:** Di Linh slug-eating snake.

2075 **Ecology notes:** *Pareas temporalis* is a nocturnal, elusive forest-dwelling snake inhabiting
 2076 mid-elevation montane evergreen tropical forests of the Langbian Plateau and its foothills; it was
 2077 recorded from elevations from 135 to 1320 m asl. All specimens were spotted after rain at night
 2078 between 21:00 and 01:00 h while crawling or perching on branches of bushes, bamboo and
 2079 *Calamus* sp. palm leaflets. The holotype was found at 21:00 h on a tree branch 1.5 m above the
 2080 ground in disturbed mixed broadleaf and bamboo forest, where it occurred in sympatry with *P.*
 2081 *margaritophorus* (*Le et al., 2021*). Diet of *P. temporalis* is unknown, but as in other congeners, it
 2082 likely consists of terrestrial mollusks. It is sympatric with a number of other *Pareas* species
 2083 across its range, and is commonly recorded in the same habitats with *P. b. unicolor* **comb. nov.**
 2084 In Di Linh District of Lam Dong Province, *P. temporalis* was recorded in sympatry with four
 2085 species of the genus *Pareas*, including *P. b. unicolor* **comb. nov.**, *P. margaritophorus*, *P.*
 2086 *macularius* and *P. formosensis*. With five species of *Pareas* co-occurring in the same habitat, the
 2087 area of Di Linh represents the center of the genus diversity in Vietnam.

2088

2089 **Key to the species of the subgenus *Pareas***

- 2090 1a. Prefrontal contacting the eye.....*P.*
 2091 *nuchalis*
- 2092 1b. Prefrontal not contacting the
 2093 eye.....2
- 2094 2a. Ratio $TaL/TL \geq 0.25$; large black blotch or a ring-shaped pattern on the nuchal
 2095 area.....
 2096 .3
- 2097 2b. Ratio $TaL/TL < 0.25$; large black blotch or a ring-shaped figure on the nuchal area
 2098 absent.....
 20995
- 2100 3a. All dorsal scales smooth, $VEN < 170$; black blotch on the nuchal area not forming a
 2101 ring-shaped pattern.....*P. kuznetsovorum*
 2102 **sp. nov.**

- 2103 3b. At least some dorsal scales strongly or slightly keeled, VEN>170; black blotch on the
 2104 nuchal area forming a ring-shaped
 2105 pattern.....4
- 2106 4a. All dorsal scale rows strongly keeled; VEN>185; no transverse dark bands on the
 2107 body..... *P. temporalis*
- 2108 4b. 9–11 rows of dorsal scales keeled at midbody; VEN<185; faint transverse dark bands
 2109 on the body.....*P. abros*
 2110 **sp. nov.**
- 2111 5a. Body size medium 337–702 mm; dorsal scales generally keeled in 3–11 rows at
 2112 midbody; upper postorbital stripes thick, contacting each other on the nape generally
 2113 forming a X- or)(shaped pattern; territories southwards from the Tenassenrim Range in
 2114 Thailand...*P. carinatus*
- 2115 5aa. VEN≤190; SC≤90; body with transverse dark bands; territories south of the
 2116 Isthmus of Kra.....*P.*
 2117 *c. carinatus*
- 2118 5ab. VEN>190; SC>90; uniform light brown coloration of dorsum lacking transverse
 2119 dark bands; Tenassenrim Range northwards from the Isthmus of
 2120 Kra.....*P. c. tenasserimicus* **ssp.**
 2121 **nov.**
- 2122 5b. Body size large 421–770 mm; dorsal scales keeled in 3–13 rows at midbody; upper
 2123 postorbital stripes thin, generally forming a Y-shaped pattern on the nape or absent;
 2124 mainland Indochina north from the Isthmus of
 2125 Kra.....*P. berdmorei*
- 2126 5ba. VEN 166–186; SC 57–89; dorsal scales keeled in 5–13 rows at midbody; ventral
 2127 surfaces immaculate, body with transverse dark bars; iris golden-bronze to orange;
 2128 restricted to northern Vietnam, northern Laos, northern Thailand, eastern Myanmar
 2129 (northern Tennasserin), and southern Yunnan.....*P. b. berdmorei* **stat.**
 2130 **nov.**
- 2131 5bb. VEN 162–180; SC 57–75; dorsal scales keeled in 3–9 rows at midbody; body
 2132 uniform orange to beige coloration lacking dark markings; iris bright orange-red;

2133 restricted to southern Vietnam and eastern Cambodia.....*P. b.*
 2134 *unicolor* **comb. nov.**
 2135 *5bc.* VEN 187; SC 66–73; dorsal scales keeled in 13 rows at midbody; dense brownish
 2136 mottling and spots on dorsal, lateral, and ventral surfaces of the head and body; iris
 2137 uniform off-white to golden; restricted to the northern Annamites (Truong Son)
 2138 Mountains in central Vietnam and Laos.....*P. b. annamiticus* **ssp.**
 2139 **nov.**

2141 Subgenus *Eberhardtia* Angel, 1920 stat. nov.

2142 Chresonymy:

2143 *Eberhardtia* Angel, 1920: 291.

2144 *Northpareas* Wang et al., 2020: Appendix S3 (*nomen nudum*).

2145 **Type species:** *Eberhardtia tonkinensis* Angel, 1920; this taxon is currently considered a
 2146 junior synonym of *Pareas formosensis* (Van Denburgh, 1909); see Ding et al. (2020) for
 2147 discussion.

2148 **Phylogenetic definition:** *Eberhardtia* is a maximum crown-clade name referring to the
 2149 clade originating with the most recent common ancestor of *Pareas formosensis* and *Pareas*
 2150 *monticola*, and includes all extant species that share a more recent common ancestor with these
 2151 taxa than with *Pareas carinatus*.

2152 **Diagnosis:** The members of the subgenus *Eberhardtia* differ from the members of the
 2153 subgenus *Pareas* by the following combination of morphological characteristics: frontal
 2154 subhexagonal to diamond-shaped with its lateral sides converging posteriorly (Fig. 5A); anterior
 2155 pair of chin shields longer than broad (Fig. 5I–J); a single thin elongated subocular; and the
 2156 ultrastructure of dorsal scales not ravine-like, having pore and arc structures, with arcs
 2157 connecting to each other forming characteristic lines (Wagler, 1830; Smith, 1943; Taylor, 1965;
 2158 Vogel et al., 2020; He, 2009; Guo et al., 2020; our data; see Supplementary Table S14 for
 2159 details).

2160 **Etymology:** Angel (1920) dedicated his new genus to the collector of the single specimen
 2161 of its type species, the French botanist Philippe Albert Eberhardt (1874–1942).

2162 **Distribution:** Distributed in the north-eastern part of the Oriental zoogeographic region
 2163 from the Eastern Himalaya to central and eastern China, islands of Hainan, Taiwan and the

2164 southern Ryukyus, southwards throughout the Indochina to the Peninsular Malaysia and
2165 Sumatra.

2166 **Content:** 20 species, including *P. andersonii* Boulenger; *P. atayal* You, Poyarkov & Lin;
2167 *P. boulengeri* (Angel); *P. chinensis* (Barbour); *P. formosensis* (van Denburgh); *P. geminatus*
2168 Ding, Chen, Suwannapoom, Nguyen, Poyarkov & Vogel; *P. hamptoni* (Boulenger); *P. iwasakii*
2169 (Maki); *P. kaduri* Bhosale, Phansalkar, Sawant, Gowande, Patel & Mirza; *P. komaii* (Maki); *P.*
2170 *macularius* Theobald; *P. margaritophorus* (Jan); *P. modestus* Theobald; *P. monticola* (Cantor);
2171 *P. niger* (Pope); *P. nigriceps* Guo & Deng; *P. stanleyi* (Boulenger); *P. victorianus* Vogel,
2172 Nguyen & Poyarkov; *P. vindumi* Vogel; and *P. xuelinensis* Liu & Rao.

2173 **Recommended English name:** Northern slug-eating snakes.

2174

2175 **Revised key to the genera and subgenera of the subfamily Pareinae**



2176 1a. Dorsal scales in 13 rows; subcaudals undivided.....genus

2177 *Aplopeltura*

2178 1b. Dorsal scales in 15 rows; all subcaudals

2179 divided.....2

2180 2a. Anterior single inframaxillary shield absent; vertebrals scales weakly or not enlarged;

2181 preocular and subocular scales present; supralabials usually not in contact with the

2182 eye.....genus

2183 *Pareas*

2184 2aa. Frontal hexagonal with its lateral sides parallel to the body axis; anterior pair of

2185 chin shields generally broader than long or slightly longer; two or three distinct narrow

2186 suboculars.....subgenus

2187 *Pareas*

2188 2ab. Frontal subhexagonal with the lateral sides converging posteriorly; anterior pair of

2189 chin shields much longer than broad; one thin elongated

2190 subocular.....subgenus *Eberhardtia* **stat.**

2191 **nov.**

2192 2b. Anterior single inframaxillary shield present; vertebral scales strongly enlarged;

2193 preocular and subocular scales absent; supralabials in contact with the eye.....genus

2194 *Asthenodipsas*

2195 *2ba.* Two pairs of chin shields; the third pair of infralabials in contact with each
 2196 other.....subgenus

2197 *Asthenodipsas*

2198 *2bb.* Three pairs of chin shields; the first pair of infralabials in contact with each
 2199 other.....subgenus *Spondylodipsas* **subgen.**

2200 **nov.**

2201

2202 DISCUSSION

2203

2204 *Phylogeny and classification of Pareinae*

2205 In this study we present an updated multilocus phylogeny for the ancient Asian subfamily
 2206 of slug-eating snakes, the Pareinae. We estimate the basal divergence within the Pareinae as the
 2207 late Eocene (ca. 39.3 mya) making this group one of the oldest radiations of Colubroidea snakes
 2208 (*Zaher et al., 2019; Li et al., 2020*). Our study includes representatives of all currently recognized
 2209 taxa within of the subfamily and is, to the best of our knowledge, the most comprehensive among
 2210 the published works both in terms of taxon and gene sampling. Our integrative analysis of the
 2211 molecular and morphological data resolves several longstanding systematic controversies
 2212 regarding the subfamily Pareinae. In particular, we confidently resolve the phylogenetic
 2213 relationships among the three genera of the Pareinae: *Aplopeltura* is strongly suggested as the
 2214 sister genus of *Pareas* sensu lato, while the genus *Asthenodipsas* is reconstructed as the most
 2215 basal taxon within the subfamily with sister relationships to the clade *Aplopeltura* + *Pareas*. This
 2216 topology contradicts several earlier studies on the taxonomy of the group (e. g., *Guo et al., 2011;*
 2217 *Wang et al., 2020*), but generally agrees with the recent multilocus phylogenetic study by *Deepak*
 2218 *et al. (2019)*, though in our phylogeny we got higher values of node support.

2219 We also provide strong evidence for the monophyly of all Pareinae genera; while
 2220 monophyly of the presently monotypic genus *Aplopeltura* was never questioned, a number of
 2221 studies suggested that the genera *Pareas* and *Asthenodipsas* might represent paraphyletic taxa
 2222 (*Guo et al., 2011; Pyron et al., 2011; Wang et al., 2020*), or were recovered as monophyletic
 2223 groups but without a significant support (e.g., *Deepak et al., 2019*). At the same time, we
 2224 demonstrate the deep differentiation within both *Pareas* and *Asthenodipsas*, each of these genera
 2225 comprises two reciprocally monophyletic groups, which diverged almost simultaneously during

2226 the early to middle Oligocene (ca. 30–31.3 mya). We also show that though the monophyly of
2227 *Pareas* and *Asthenodipsas* is not questioned anymore, the major clades within these genera
2228 demonstrate significant differences among each other in external morphology, scale
2229 microornamentation, and biogeographic affinities; similar results were also obtained by a number
2230 of earlier studies (*Grossmann & Tillack, 2003; He, 2009; Guo et al., 2011; Guo, Wang &*
2231 *Rao2020; Wang et al., 2020*). We argue that the groups within *Pareas* and *Asthenodipsas* should
2232 be taxonomically recognized, what would enhance the diagnosability and clade stability of these
2233 taxa, make them more comparable units to other snake genera, restrain taxonomic vandalism, and
2234 eventually fully stabilize the taxonomy of Pareinae. Therefore, we recognize two subgenera
2235 within the genus *Pareas* sensu lato (*Pareas* sensu stricto and *Eberhardtia* **stat. nov.**), and two
2236 subgenera within the genus *Asthenodipsas* sensu lato (*Asthenodipsas* sensu stricto and
2237 *Spondylodipsas* **subgen. nov.**). Earlier studies which addressed the genus-level taxonomy of
2238 *Pareas* have either wrongly identified the type species of the genus (*Guo et al., 2011*), or have
2239 overlooked the existence of an available genus-level name for one of the clades (*Eberhardtia*
2240 *Angel, 1920*), what resulted in the creation of a nomen nudum ('*Northpareas*', see *Wang et al.,*
2241 *2020*). We would like to emphasize the importance of a thorough analysis of the available
2242 literature and possible synonyms prior to making a taxonomic decision in order to prevent
2243 publication of unavailable names or junior synonyms. Within the genus *Pareas*, our phylogenetic
2244 results support the recognition of two species groups within the subgenus *Pareas* sensu stricto (*P.*
2245 *carinatus* and *P. nuchalis* groups), and four species groups within the subgenus *Eberhardtia* **stat.**
2246 **nov.** (*P. hamptoni*, *P. chinensis*, *P. margaritophorus*, and *P. monticola* groups) (see Fig. 3); this
2247 taxonomy is largely concordant with the results of the previous studies (*Guo et al., 2011; You,*
2248 *Poyarkov & Lin, 2015; Bhosale et al., 2020; Vogel et al., 2020, 2021; Wang et al., 2020; Ding et*
2249 *al., 2020*).

2250 Although our understanding of the phylogenetic relationships within the Pareinae is now
2251 improved, it is still far from complete. For example, our phylogeny included only five of nine
2252 currently recognized species of *Asthenodipsas*; five species of the genus were described within
2253 the last decade, of which four were described based solely on morphological evidence (*Quah et*
2254 *al., 2019, 2020, 2021*). We would like to further stress herein that in this age of molecular
2255 genetics and biodiversity crises, the application of molecular methods became crucial for
2256 taxonomic practice in studies of herpetofaunal diversity in Southeast Asia (*Smith et al., 2008;*

2257 *Murphy et al., 2013*). Not only the phylogenetic hypothesis is crucial for any comparative or
2258 biogeographic analyses, it now also became a keystone of biodiversity conservation (*Shaffer et*
2259 *al., 2015; Chomdej et al., 2020*). Phylogenetic studies on the remaining species of *Asthenodipsas*
2260 are required to fully resolve the taxonomy of the genus; furthermore, additional taxon and gene
2261 sampling will likely enhance the phylogenetic resolution on the level of the subfamily Pareinae
2262 and might lead to discovery of additional new lineages and species.

2263

2264 ***Underestimated species diversity of Pareas in Indochina***

2265 Though not being the most species-rich group of Asian snakes, the slug-eating snakes are
2266 widely distributed across the Southeast Asia and have a number of specialized morphological
2267 and ecological characteristics which are hypothesized to facilitate speciation. Being dietary
2268 specialists on terrestrial slugs and snails, the Pareinae occupy ecological niches inaccessible to
2269 other groups of Asian snakes, at the same time several species of the slug-eating snakes can
2270 successfully coexist with their congeners, likely due to niche partitioning and further
2271 specialization in preferred prey, dentition asymmetry, and feeding behavior (*Chang et al., 2021*).
2272 For example, up to three closely-related species of *Pareas* share same habitats in the areas of
2273 sympatry in Taiwan (*You, Poyarkov & Lin, 2015; Chang et al., 2021*); in our study we **for the**
2274 **first report** the sympatric co-occurrence of six *Pareas* species in the montane forests of Lam
2275 Dong Province of southern Vietnam (*P. temporalis, P. kuznetsovorum sp. nov., P. b. unicolor, P.*
2276 *macularius, P. margaritophorus, and P. formosensis*), of which five species were recorded
2277 sharing the same habitat in Di Linh District. On the other hand, the sympatric co-occurrence of
2278 several often closely related species of *Pareas*, often makes correct species identification
2279 difficult, and may also lead to some cryptic species being overlooked.

2280 Several recent taxonomic studies on *Pareas* have demonstrated that this genus has a high
2281 level of hidden and yet undescribed diversity (e.g. *You, Poyarkov & Lin, 2015; Bhosale et al.,*
2282 *2020; Vogel et al., 2020, 2021; Ding et al., 2020; Liu & Rao, 2021; Yang et al., 2021*). Out of 24
2283 currently recognized species of *Pareas* **ten species** were discovered within the last 12 years
2284 (*Uetz, Freed & Hošek, 2021*), **of them** nine species were described based on an integrative
2285 evidence from morphological and molecular data. At the same time, hasty taxonomic revisions
2286 may often lead to creation of unnecessary synonyms and taxonomic inflation (*Isaac, Mallet &*
2287 *Mace2004*). For example, recently *Wang et al. (2020)* revised the taxonomy of the genus *Pareas*

2288 and described two new species from China: *P. mengziensis* (member of the *P. hamptoni* group)
2289 and *P. menglaensis* (member of the *P. carinatus* group). Subsequent work by Liu & Rao (2021)
2290 noted that Wang et al. (2020) described their species without first resolving the historical
2291 taxonomic confusions of *P. yunnanensis* (Vogt) and *P. niger* (Pope), at that time considered as
2292 junior synonyms of *P. chinensis* (Wallach, Williams & Boundi, 2014). Liu & Rao (2021) further
2293 showed that *P. mengziensis* represents a subjective junior synonym of *P. niger*, and clarified
2294 distribution and the phylogenetic placement of this species, which was also confirmed by our
2295 analyses. Furthermore, as demonstrated in our study, in their description of *P. menglaensis*,
2296 Wang et al. (2020) did not provide any comments on the distribution and existing junior
2297 synonyms of *P. carinatus*, including *P. berdmorei*, originally described from Myanmar. Herein
2298 we also analyze the distribution of phylogenetic relationships within the *P. carinatus* species
2299 group and further demonstrate that *P. menglaensis* actually represents a subjective junior
2300 synonym of *P. berdmorei* (see Results). Therefore we would like to further emphasize herein the
2301 importance of careful treatment of the available synonyms and especially of the examination of
2302 the respective type specimens in taxonomic practice. It is thus recommended that scientists,
2303 before describing a new taxon would thoroughly evaluate the available old names, the existing
2304 type specimens and / or new materials from the respective type localities. This would prevent the
2305 taxonomy from becoming confusing and the available taxa from being overlooked. We would
2306 also like to further stress herein the importance of international collaboration in resolving
2307 taxonomically confusing species complexes distributed across the international borders.

2308 **In the present study, we applied the integrative taxonomic** approach to analyze the broad
2309 geographical sampling all over the range of the *P. carinatus-nuchalis* species complex, and also
2310 carefully examined all available names, species descriptions and the respective type specimens
2311 for the group. The combination of molecular and morphological data allowed this study to assess
2312 the diversity, clarify the actual geographical distribution as well as to evaluate the validity of the
2313 taxa included in this complex. As a result, our study revealed an unprecedented diversity within
2314 the *P. carinatus-nuchalis* complex, with six major lineages representing distinct species, each
2315 with significant genetic and morphological differences from the others (see Results). In our
2316 study, we consider *P. carinatus* sensu stricto distributed from the Tenasserim Range in the
2317 Peninsular Thailand and Myanmar southwards to Malayan Peninsula, Sumatra, Java, and Borneo
2318 Islands. We also revise the populations from the mainland Indochina and southern China

2319 previously referred to as *P. carinatus* or *P. menglanensis* (Wang *et al.*, 2020), and revalidate *P.*
2320 *berdmorei* as a distinct species; this taxon is widely distributed across the Indochina and the
2321 adjacent parts of Yunnan and eastern Myanmar, while *P. menglaensis* is considered as a
2322 subjective junior synonyms of this species. We also describe two new previously completely
2323 unknown species of *Pareas* from Vietnam, namely: *Pareas kuznetsovorum* **sp. nov.** (belongs to
2324 *P. carinatus* species group and represents a sister species of *P. berdmorei*); *Pareas abros* **sp.**
2325 **nov.**, and provide additional information on morphological variation and distribution of the
2326 recently described *P. temporalis*. The recent discovery of the latter two species is quite
2327 unexpected since they are morphologically profoundly different from all other mainland
2328 members of the subgenus *Pareas* and according to our phylogeny and morphological similarities
2329 belong to *P. nuchalis* species group, what is also indicated by an earlier study of Le *et al.* (2021).
2330 It also should be noted, that our study represents the first record of *P. nuchalis* on Sumatra
2331 Island; this species has been previously considered to be restricted to Borneo. Overall, the
2332 revalidation of *P. berdmorei* along with description of *Pareas abros* **sp. nov.** and *Pareas*
2333 *kuznetsovorum* **sp. nov.** brings the total number of species in *Pareas* to 26 and the number of
2334 Pareinae species to 36.

2335 In our study we also analyze geographic variation of morphological, chromatic and
2336 molecular characters within the wide-ranged species of the subgenus *Pareas*, namely *P.*
2337 *carinatus* and *P. berdmorei*. We report on a significant diversity within these species with two
2338 divergent, allopatric (to the best of our knowledge), and morphologically diagnosable groups
2339 revealed within *P. carinatus*, and three such groups within *P. berdmorei*. Should they be
2340 taxonomically recognized? The phylogenetic species concept (PSC, see Cracraft, 1983;
2341 reviewed by De Queiroz, 2007) suggests that the minimal monophyetic group on a tree should be
2342 considered a species. However, the recent progress in evolutionary phylogenomics allows
2343 revealing population genetic structure and estimate the geneflow among populations and even
2344 species in unparalleled detail (e.g., Benestan *et al.*, 2015). This, however, often makes an
2345 accurate characterization of species boundaries within an evolutionary framework quite
2346 challenging: distinguishing between population-level genetic structure and species divergence is
2347 often problematic (Chan *et al.*, 2020). A number of recent phylogenomic studies have
2348 demonstrated that a number of what was considered complexes of cryptic species actually
2349 represent highly admixed and structured metapopulation lineages, rather than true cryptic species

2350 (e.g., *Chan et al., 2020, 2021*). One of the adverse consequences of ignoring gene flow in species
2351 delimitation is the overestimation of species numbers by interpreting population structure as
2352 species divergence, thus enhancing taxonomic inflation (*Chan et al., 2020*). Therefore, in the
2353 present paper in order to to assess the revealed diversity within *P. carinatus* and *P. berdmorei* we
2354 apply the subspecies concept sensu *Hillis (2020)* and *Marshall et al. (2021)*, where subspecies
2355 are defined as geographically circumscribed lineages that may have been temporarily isolated in
2356 the past, but which may have since merged over broad zones of intergradation that not
2357 necessarily show the evidence of reproductive isolation between them. We recognize two
2358 subspecies within *P. carinatus*: *P. c. carinatus* (Sundaland and Malayan Peninsula south of Kra)
2359 and *P. c. tenasserimicus ssp. nov.* (Tenasserim Range north of Kra), and three subspecies within
2360 *P. berdmorei*: *P. b. berdmorei* (from eastern Myanmar across Thailand to northern Laos,
2361 northern Vietnam and southern China), *P. b. unicolor* (southern Vietnam and Cambodia), and *P.*
2362 *b. annamiticus ssp. nov.* (Northern Annamites in central Vietnam and Laos). Though with the
2363 data in hand we don't have any evidence of genetic admixture between these groups, it cannot be
2364 excluded that the future studies with a finer sampling might reveal a certain degree of gene flow
2365 among them. We herein prefer recognizing them as subspecies due to the overall morphological
2366 similarity of these lineages, which are mostly distinguished by coloration rather than scalation
2367 features, their presumably allopatric distribution pattern, their comparatively young evolutionary
2368 age (5.9–4.0 mya), and the historical precedent of use of the subspecies for describing diversity
2369 within these snakes (*P. b. unicolor* was originally described as a subspecies of *P. carinatus*) (see
2370 Results).

2371 Despite the recent significant progress (*Ding et al. 2020; Vogel et al., 2020, 2021; Le et al.,*
2372 *2021*), our understanding of *Pareas* diversity is still incomplete. Our study revealed a high
2373 morphological variation among the examined specimens of *P. berdmorei* and *P. carinatus*;
2374 however our genetic sampling is not fully comparable to the morphological sampling. For
2375 example, our phylogenetic analysis lacked specimens of *P. carinatus* from the Greater Sunda
2376 Islands and the adjacent smaller offshore islands; many areas in the central Indochina also
2377 remained unassessed. Further field survey and taxonomic efforts both in Indochina and
2378 Sundaland will likely reveal additional lineages within the widely-distributed and insufficiently
2379 sampled species of *Pareas*.

2380

2381 **Historical biogeography of Pareinae**

2382 The results of our biogeographic reconstruction suggest that the common ancestor of the
2383 Pareinae likely inhabited Sundaland (Fig. 2), while its sister group the Xylophiinae are restricted
2384 to peninsular India (Deepak et al., 2019). The split between Pareinae and Xylophiinae is dated to
2385 happen during the middle Eocene (ca. 42.2 mya in our analysis, estimated as ca. 44.9 mya in
2386 Deepak et al., 2019), and likely reflects the ancient faunal exchange between the Indian
2387 Subcontinent and the Sundaland via a land bridge which existed during the early and middle
2388 Eocene (Ali & Aitchison, 2008; Morley, 2018). Similar patterns were reported, for example, in
2389 Draconinae agamid lizards (Grismer et al., 2016), and Microhylinae narrow-mouth frogs (Garg
2390 & Biju, 2019; Gorin et al., 2020). In particular, the assumptive vicariance between Pareinae and
2391 Xylophiinae and the distribution patterns of the two subfamilies remarkably resembles the
2392 divergence pattern between microhylid genera *Micryletta* (widely distributed across the
2393 Southeast Asia) and *Mysticellus* (restricted to southern peninsular India), which was dated as
2394 39.7 – 40.6 mya (Garg & Biju, 2019). Our study thus provides further evidence for faunal
2395 exchange between the Indian Subcontinent and Sundaland during the middle Eocene.

2396 Our results accord with the “upstream” colonization hypothesis in Pareinae. The general
2397 pattern of colonization in Pareinae is from Sundaland to the mainland Asia, this dispersal and
2398 subsequent vicariance likely happened during the early Oligocene (ca. 33.6 mya; Fig. 2). It
2399 should be noted, that though now the Sundaland is mostly represented by a number of
2400 archipelagos, in Oligocene it was connected to the mainland Southeast Asia via the Sunda shelf,
2401 which remained subaerial during the most part of Cenozoic (Cao et al., 2017; Morley, 2018).
2402 Therefore, the general direction of diversification in Pareinae was likely from the tropical
2403 continental margins of Sundaland to a nontropical Asian landmass. Starting with at least middle
2404 Eocene Sundaland was covered with perhumid rainforests and became a major source of
2405 mainland Asian lineages for a vast number of taxa of plants and animals (see De Bruyn et al.,
2406 2014; Grismer et al., 2016, Grismer et al., in press; Morley, 2018, and references therein).
2407 Examples include the stream toad genus *Ansonia* (Grismer et al., 2017), the litter toads
2408 *Leptobrachella* (Chen et al., 2018), and the breadfruit genus *Artocarpus* (Williams et al., 2017).
2409 Our study is probably the first example of “upstream” colonization in Asian snakes. Further
2410 studies on the diversification patterns of other endemic Asian genera on a broad geographic scale

2411 might yield key insights into the drivers of speciation in Asia and result in a comprehensive
2412 picture of the regional source-sink dynamics between islands and continents.

2413 Our analyses suggest that the common ancestor of the genus *Pareas* likely inhabited parts
2414 of the Indochinese Peninsula, Indo-Burma, and the areas which now became the Himalayas (Fig.
2415 2). The basal split within *Pareas* is dated as early Oligocene (ca. 31.3 mya; Fig. 2), and
2416 temporally coincides with climatic shifts during this time. The period of late Eocene-early
2417 Oligocene transition was characterized by dramatically cool and dry climate in Southeast Asia
2418 (*Zachos et al., 2001*); during this time the perhumid forests contracted and fragmented (*Milne &*
2419 *Abbott, 2002; Bain & Hurley, 2011; Buerki et al., 2013; Morley, 2018*). These processes could
2420 potentially drive the initial diversification of *Pareas* through vicariance (Fig. 2). Moreover, the
2421 two major clades of *Pareas* (Fig. 2) are estimated to have begun diversification during the
2422 Miocene along with the significant growth of average temperature and humidity (ca. 23–12 mya;
2423 see *Bain & Hurley, 2011*). These climatic changes lead to expansion of perhumid tropical forests
2424 and likely promoted the expansion and further diversification of *Pareas*. A similar pattern was
2425 recently reported by *Chen et al. (2018)* for *Leptobranchella* toads.

2426 The territory of the Himalayas and Indo-Burma is suggested as the possible ancestral area
2427 for the subgenus *Eberhardtia stat. nov.*, the most species-rich group of *Pareas*. The further
2428 diversification of this clade into species groups took place during the early to middle Miocene
2429 and likely took place in Himalaya and the adjacent parts of western and southern China, with
2430 subsequent dispersals to Indochina and the East Asian islands (Fig. 2). The Himalaya are now
2431 recognized as an area of exceptional diversity and endemism largely due to the uplift-driven
2432 speciation, suggesting that orogeny created conditions favoring rapid in situ diversification of
2433 resident lineages, which accelerated during the Miocene (reviewed in *Xu et al., 2020*). Our data
2434 suggest that geomorphological factors are also likely responsible for shaping the diversification
2435 within the subgenus *Eberhardtia stat. nov.* The origin and diversification of the four species
2436 groups within *Eberhardtia stat. nov.* temporally coincide with the rapid increase of uplifting of
2437 the Qinghai–Tibet Plateau during the Miocene (15–7 mya, *An et al., 2001; Che et al., 2010*),
2438 which finally gave rise to the intensification of the modern South Asian monsoon climate. This
2439 process is considered to have accelerated the diversification of numerous Asian animal groups
2440 that share similar distributions with *Eberhardtia stat. nov.* (e.g., *Che et al., 2010; Blair et al.,*
2441 *2013; Gao et al., 2013; Chen et al., 2017, 2018; Xu et al., 2020*). It is noteworthy that following

2442 the dispersal of *Eberhardtia* **stat. nov.** across the mainland East Asia, its members at least twice
2443 have independently colonized the East Asian islands of Taiwan and the southern Ryukyus during
2444 the late Miocene to early Pliocene, giving rise to an in situ diversification of a number of
2445 endemic island species (You, Poyarkov & Lin, 2015; Chang et al., 2021). Similar patterns were
2446 reported in other groups of Asian herpetofauna (e.g., Yuan et al., 2016; Nguyen et al., 2020a;
2447 Yang & Poyarkov, 2021; Gorin et al., 2020).

2448 The origin of the subgenus *Pareas* likely took place in what is now the Western Indochina,
2449 from where during the early to middle Miocene it colonized the Eastern Indochina leading to
2450 formation of several endemic lineages and species (Fig. 2). The Annamite Range, including the
2451 mountains areas of the Kon Tum–Gia Lai and Langbian plateaus, are reknown as the center of
2452 floral and faunal endemism (e.g. Averyanov et al., 2003; Bain & Hurley, 2011; Monastyrskii &
2453 Holloway, 2013; Poyarkov et al., 2014, 2021). According to our analyses, Eastern Indochina
2454 appears as an evolutionary hotspot for *Pareas*, having the high species diversity and degree of
2455 endemism, with up to six species of the genus sympatrically distributed in the montane forests of
2456 the Langbian Plateau. Among the surprising results of our study is the independent
2457 “downstream” colonization of Sundaland from Indochina during the late Miocene, which
2458 happened twice by the members of the *P. carinatus* and *P. nuchalis* species groups (Fig. 2). The
2459 recent discovery of two new species of the *P. nuchalis* group in mountain areas of Eastern
2460 Indochina (*Pareas abros* **sp. nov.**, and *P. temporalis* by Le et al., 2021) is quite unexpected, and
2461 provides further evidence for faunal interchange between Eastern Indochina and Borneo.
2462 Throughout the late Cenozoic these territories were directly connected by a landbridge along the
2463 eastern edge of Sunda Shelf formed by the ancient delta joining the modern river systems of
2464 Mekong and Chao Phraya, and covered by lowland evergreen rain-forests (De Bruyn et al.,
2465 2014). However, similar biogeographic patterns are rarely reported for the herpetofauna (but see
2466 Wood et al., 2012; Geissler et al., 2015; Chen et al., 2017; Suwannapoom et al., 2018; Poyarkov
2467 et al., 2018a; Gorin et al., 2020; Grismer et al., in press), therefore additional sampling from
2468 other regions, including the different parts of the Sundaland, is needed to test this hypothesis.
2469 Overall, our study reinforces the idea that Indochina represents an indispensable hotspot for the
2470 evolution and maintenance of Southeast Asian biodiversity (De Bruyn et al., 2014).

2471

2472 *Conservation status of the newly described species and the importance of Indochina for*
2473 *herpetofaunal diversity and conservation*

2474 While *P. c. carinatus* and *P. b. berdmorei* are quite widely distributed taxa and their
2475 conservation status is of the least concern, the distribution of *P. c. tenasserimicus* **ssp. nov.**, *P. b.*
2476 *unicolor*, and *P. b. annamiticus* **ssp. nov.** is most likely restricted to comparatively narrow areas
2477 within the Indochina. At the same time, among the two newly described species *Pareas*
2478 *kuznetsovorum* **sp. nov.** is to date known only from a single specimen, while the ranges of
2479 *Pareas abros* **sp. nov.** and *P. temporalis* are restricted to isolated montane areas of Kon Tum –
2480 Gia Lai and Lam Dong plateaus, respectively. The estimated ranges of the two new *Pareas*
2481 species are likely relatively small, however the actual extent of their distribution and population
2482 trends remain unknown; urgent actions are needed for careful assessment of their conservation
2483 status. We herein tentatively suggest that at present *Pareas kuznetsovorum* **sp. nov.**, *Pareas*
2484 *abros* **sp. nov.**, and *P. temporalis* should be categorized as Data Deficient (DD) according to the
2485 *IUCN Red List criteria (2019)*. Further research is required to clarify the extent of their
2486 distribution population trends, and natural history, thereby facilitating elaboration of adequate
2487 conservation actions.

2488 Our work further highlights the importance of the Indochinese region, including the
2489 territories of Vietnam, Laos, Cambodia, and Thailand, as one of the key biodiversity hotspots
2490 with high levels of herpetofaunal diversity and endemism (*Bain & Hurley, 2011; Geissler et al.,*
2491 *2015; Duong et al., 2018; Nguyen et al., 2018, 2019, 2020b; Poyarkov et al., 2018b, 2019, 2021;*
2492 *Grismer et al., 2019, 2021a, 2021b; Chomdej et al., 2021; Uetz, Freed & Hošek, 2021*). This
2493 area is facing many pressures with major habitat loss by deforestation due to logging, the
2494 growing human population density and infrastructure development, agricultural extension, forest
2495 fires, and tourism development (*Lang, 2001; Meyfroidt & Lambin, 2009*). Therefore, further
2496 studies are urgently needed to assess and manage the biodiversity and elaborate the adequate
2497 conservation efforts before more undescribed species are **lost**.

2498

2499 CONCLUSIONS

2500

2501 In this work, we provide an updated phylogenetic hypothesis for the slug-eating snakes of
2502 the subfamily Pareinae. Herein we examined mtDNA and nuDNA markers for 29 of 33 currently



2503 recognized Pareinae species (88%), and also included data for six lineages that have not been
2504 examined phylogenetically before our work, including the previously unknown two new species
2505 and two new subspecies of *Pareas*. Thus our study provides the most comprehensive taxon
2506 sampling for Pareinae published to date. This, along with morphological examination of 269
2507 preserved specimens of Pareinae, including the available type specimens for the genus *Pareas*,
2508 allowed us to revise the phylogenetic relationships and taxonomy of the subfamily. Our work
2509 further highlights the importance of broad phylogenetic sampling, ground-level field surveys,
2510 and careful examination of type materials to achieve an accurate picture of phylogenetic
2511 relationships, global biodiversity, and evolutionary patterns in cryptic groups such as the
2512 Pareinae slug-eating snakes.

2513 We demonstrate that the subfamily Pareinae includes three strongly supported genera:
2514 *Asthenodipsas*, *Aplopeltura*, and *Pareas*, with the two latter taxa forming a clade. Our analyses
2515 reveal deep divergence within *Asthenodipsas* and *Pareas*; each of these genera is subdivided into
2516 two reciprocally monophyletic and morphologically diagnosable groups of presumably
2517 Oligocene origin. In to fully stabilize the taxonomy of Pareinae, we propose to regard these
2518 groups as subgenera, and recognize two subgenera within the genus *Asthenodipsas*
2519 (*Asthenodipsas* sensu stricto and the newly described *Spondylodipsas* **subgen. nov.**), and two
2520 subgenera within the genus *Pareas* (*Pareas* sensu stricto and the revalidated *Eberhardtia* **stat. nov.**). Overall, we recognize six species groups within *Pareas* sensu lato: *P. carinatus*, and *P.*
2522 *nuchalis* groups in the subgenus *Pareas*, and *P. hamptoni*, *P. margaritophorus*, *P. chinensis*, and
2523 *P. monticola* groups in the subgenus *Eberhardtia* **stat. nov.**

2524 The present work clearly indicates a vast underestimation of diversity in the subgenus
2525 *Pareas*, and that the present taxonomy of the group is incomplete. We herein restrict the
2526 distribution of *P. carinatus* to southern Southeast Asia, and recognize two subspecies within this
2527 species: the nominative subspecies *P. c. carinatus* inhabits Sundaland south of the Isthmus of
2528 Kra, while the newly described *P. c. tenasserimicus* **ssp. nov.** inhabits the Tenasserim Range in
2529 Thailand and Myanmar. We also revalidate *P. berdmorei* as a valid species, synonymize *P.*
2530 *menglaensis* with *P. berdmorei*, and recognize three subspecies within this taxon: the nominative
2531 subspecies *P. b. berdmorei*, distributed from eastern Myanmar across Thailand to northern Laos,
2532 Vietnam and southern China, *P. b. unicolor* from southern Vietnam and Cambodia, and the

2533 newly described subspecies *P. b. annamiticus* **ssp. nov.** Furthermore, we describe two new
2534 species of *Pareas* from montane areas of central and southern Vietnam: *P. kuznetsovorum* **sp.**
2535 **nov.** is to date known from only a single specimen from the northeastern foothills of the
2536 Langbian Plateau and belongs to the *P. carinatus* species group. We also describe a new species
2537 in the *P. nuchalis* group: *P. abros* **sp. nov.** from the Kon Tum – Gia Lai Plateau of central
2538 Vietnam, which together with the recently described *P. temporalis* restricted to the Langbian
2539 Plateau, represent the new record of *P. nuchalis* group members in the mainland Southeast Asia.
2540 This discovery is quite unexpected, since prior *Le et al. (2021)* and our study *P. nuchalis* was
2541 only known from Borneo. Further integrative studies combining morphological and genetic
2542 analyses are essential for a better understanding of evolutionary relationships within this cryptic
2543 and taxonomically challenging radiation of Asian snakes. Overall, our study further highlights
2544 the importance of comprehensive and accurate taxonomic revisions not only for the better
2545 understanding of biodiversity and its evolution, but also for the elaboration of adequate
2546 conservation actions.

2547 The Pareinae is an ancient group of Asian snakes. They originate during the middle
2548 Eocene and the basal radiation of the subfamily is dated to the late Eocene and likely took place
2549 in Sundaland. Our analyses support with the “upstream” colonization hypothesis in Pareinae,
2550 suggesting they dispersed from the perhumid tropical forests of Sundaland to the non-tropical
2551 mainland Asia during the early Oligocene. The genus *Pareas* likely originated in Indochina and
2552 Indo-Burma; the climatic shifts of the late Eocene – early Oligocene transition, characterized by
2553 cool and dry climate in Southeast Asia, could potentially drive the initial diversification in
2554 *Pareas* and *Asthenodipsas*. The following significant warming and wetting of climate during the
2555 Miocene likely promoted further diversification of *Pareas*, which lead to formation of the main
2556 species groups within the genus. The subsequent differentiation within *Pareas* was likely
2557 influenced by accelerated uplift of Himalaya and the Qinhai–Tibet Plateau during the Miocene,
2558 and the formation of firm land bridges between the Asian mainland and the islands of Southeast
2559 (Borneo, Sumatra, and Java) and East Asia (Hainan, Taiwan, and the Ryukyus) following the
2560 repeated marine transgressions. Overall, our study reinforces the idea of the global importance of
2561 Indochina as the principal evolutionary hotspot for the autochthonous herpetofaunal diversity, as
2562 well as a key area facilitating dispersals between East Asia, Indo-Burma and Sundaland. Further
2563 studies on phylogeny and the diversification patterns of different animal groups endemic to Asia

2564 on a broad geographic scale might provide key insights into the role of complex paleogeography
2565 and paleoclimate history as the drivers of speciation forming the extant Asian biodiversity.

2566

2567 **ACKNOWLEDGEMENTS**

2568

2569 The authors are grateful to Andrey N. Kuznetsov (JRVTTTC) and Thai Van Nguyen (SVW)
2570 for supporting our study. We thank Vladislav A. Gorin, Evgeniya N. Solovyeva, Roman A.
2571 Nazarov, Sabira S. Idiatullina, The Anh Nguyen, Hieu Minh Pham, Huy Xuan Ngoc Nguyen,
2572 Bang Van Tran, Eduard A. Galoyan, and Anna B. Vassilieva for their support during the
2573 fieldwork and assistance in the lab or with data analysis. We are also grateful to Liudmila B.
2574 Salamakha for preparation of drawings for this paper. We are deeply bgrateful to Leonid A.
2575 Neimark, Indraneil Das, Guek Hock Ping aka Kurt Orion, Huy X. N. Nguyen, **andn** Mali
2576 Naiduangchan for providing photos used in the present paper. We are grateful to Tasos Limnios
2577 for his advices on Ancient and Modern Greek grammar and lexicon. Furthermore, we thank the
2578 following collection curators, who gave access to specimens under their care and helped us while
2579 we visited their respective institutions: Jens Vindum and Alan Leviton (CAS); Yuezhao Wang,
2580 Xiaomao Zeng, Jiatang Li and Ermi Zhao (CIB); Ding Li (DL); Alan Resetar (FMNH); Nicolas
2581 Vidal and Annemarie Ohler (MNHN); Giuliano Doria (MNSG); Hmar Tlawmte Lalremsanga
2582 (MNZU); Colin McCarthy and Patrick Campbell (NHMUK); Silke Schweiger and Georg
2583 Gassner (NMW); Esther Dondorp, Pim Arntzen and Ronald de Rooter (RMNH); Gunther Köhler
2584 and Linda Acker (SMF); George Zug, Kenneth Tighe and Ronald Heyer (USNM); Dennis
2585 Rödder and Wolfgang Böhme (ZFMK); Oliver Rödel and Frank Tillack (ZMB); Jakob
2586 Hallermann (ZMH); Frank Glaw and Michael Franzen (ZSM); and Valentina F. Orlova and
2587 Roman A. Nazarov (ZMMU). Alan Leviton (CAS) is thanked for inviting GV to CAS. Ding Lee,
2588 Jiatang Li and Zening Chen are thanked for their support of the work of GV in China. The
2589 authors are grateful to Chris Joldnall for proofreading of the paper. The authors thank the two
2590 anonymous reviewers for their useful comments which improved the earlier draft of the
2591 manuscript.

2592

2593 **ADDITIONAL INFORMATION AND DECLARATIONS**

2594

2595 Funding

2596 This work was supported by the Russian Science Foundation to Nikolay A. Poyarkov (RSF
2597 grant No. 19-14-00050; specimen collection, molecular, phylogenetic and morphological
2598 analyses, data analysis); by the Unit of Excellence 2021 on Genetic diversity assessment of
2599 widely distributed aquatic animals and herpetofauna in Thailand, University of Phayao
2600 (UoE64003; specimen collection) to Chatmongkon Suwannapoom. The funders had no role in
2601 study design, data collection and analysis, decision to publish, or preparation of the manuscript.

2602

2603 Grant Disclosures

2604 The following grant information was disclosed by the authors:

2605 Russian Science Foundation: 19-14-00050.

2606 Thailand Research Fund: DBG6180001.

2607 Genetic diversity assessment of widely distributed aquatic animals and herpetofauna in
2608 Thailand, University of Phayao: UoE64003.

2609

2610 Competing Interests

2611 Nikolay A. Poyarkov serves as an Academic Editor for PeerJ. The other authors declare
2612 that no conflicts of interest exist.

2613

2614 Author Contributions

2615 Nikolay A. Poyarkov conceived and designed the experiments, performed the experiments,
2616 analyzed the data, prepared figures and tables, authored and reviewed drafts of the paper, and
2617 approved the final draft.

2618 Tan Van Nguyen conceived and designed the experiments, performed the experiments,
2619 analyzed the data, prepared tables, authored and reviewed drafts of the paper, and approved the
2620 final draft.

2621 Parinya Pawangkhanant analyzed the data, authored or reviewed drafts of the paper, and
2622 approved the final draft.

2623 Platon V. Yushchenko analyzed the data, authored or reviewed drafts of the paper, and
2624 approved the final draft.

2625 Peter Brakels analyzed the data, authored or reviewed drafts of the paper, and approved the

2626 final draft.

2627 Linh Hoang Nguyen analyzed the data, authored or reviewed drafts of the paper, and
2628 approved the final draft.

2629 Hung Ngoc Nguyen analyzed the data, authored or reviewed drafts of the paper, and
2630 approved the final draft.

2631 Chatmongkon Suwannapoom analyzed the data, authored or reviewed drafts of the paper,
2632 and approved the final draft.

2633 Nikolai L. Orlov conceived the experiments, performed the experiments, authored or
2634 reviewed drafts of the paper, and approved the final draft.

2635 Gernot Vogel conceived and designed the experiments, performed the experiments,
2636 analyzed the data, authored or reviewed drafts of the paper, and approved the final draft.

2637

2638 **Field Study Permissions**

2639 The following information was supplied relating to field study approvals (i.e., approving
2640 body and any reference numbers): No field studies were carried out specifically for this work;
2641 tissue samples and specimens stored in museum collections were used in this study. However,
2642 some specimens stored in the mentioned collections were collected by the coauthors of this
2643 manuscript or with their participation during numerous field trips in a time frame over 15 years.

2644 Specific permits from Thailand, Laos and Vietnam authorities are as follows:

2645 - The Institute of Animals for Scientific Purpose Development (IAD), Bangkok, Thailand
2646 granted permission for fieldwork under permit number U1-01205-2558, issued to Chatmongkon
2647 Suwannapoom (Thailand);

2648 - The Institute of Animals for Scientific Purpose Development (IAD), Bangkok, Thailand
2649 granted permission for fieldwork under permit number UP-AE59-01-04-0022, issued to
2650 Chatmongkon Suwannapoom (Thailand);

2651 - The Biotechnology and Ecology Institute Ministry of Science and Technology, Lao PDR
2652 (permit no. 299 of 1 August 2019) (Laos);

2653 - The Department of Forestry, Ministry of Agriculture and Rural Development of Vietnam
2654 granted permission for fieldwork under permit number #547/TCLN-BTTN (issued 21 April
2655 2016), #432/TCLN-BTTN (issued 30 March 2017), issued to JRVTRTC, Nikolay A. Poyarkov
2656 (Vietnam); #822/TCLN-BTTN (issued 01 June 2016), issued to JRVTRTC, Nikolay A.

2657 Poyarkov (Vietnam);

2658 - The Department of Forestry, Ministry of Agriculture and Rural Development of Vietnam
2659 approved additional fieldwork (permit numbers #142/SNgV-VP (Gia Lai Province, issued 4 May
2660 2016) to JRVTRTC; #1539/TCLN-DDPH (issued 19 September 2018) to JRVTRTC;
2661 #1700/UBND.VX (Nghe An Province, issued 22 March 2018) to JRVTRTC; #308/SNgV-LS
2662 (Quang Nam Province, issued 01 April 2019) to JRVTRTC; #05/UBND-KT (Phu Yen Province,
2663 issued 04 January 2021) to JRVTRTC; #1951/UBND-NV (Gia Lai Province, issued 04 May
2664 2016) to JRVTRTC; #2394/UBND-TH3 (Phu Tho Province , issued 16 June 2016) to
2665 JRVTRTC; #3532/UBND-THKH (Thanh Hoa Province, issued 27 March 2019) to JRVTRTC;
2666 - Forest Protection Departments of the Peoples' Committee of Gia Lai Province granted
2667 permission for fieldwork to Nikolay A. Poyarkov (permit number #530/UBND-NC, issued 20
2668 March 2018).

2669

2670 **Animal Ethics**

2671 The following information was supplied relating to ethical approvals (i.e., approving body
2672 and any reference numbers):

2673 Specimen collection protocols and animal operations followed the Institutional Ethical
2674 Committee of Animal Experimentation of the University of Phayao approved field collections
2675 under certificate number 610104022 issued to Chatmongkon Suwannapoom (Thailand).

2676

2677 **DNA Deposition**

2678 The following information was supplied regarding the deposition of DNA sequences:

2679 The sequences obtained in this study are available at GenBank: MZ712215–MZ712343.

2680

2681 **Data Availability**

2682 The following information was supplied regarding data availability:

2683 The raw morphological data are summarized in Supplemental Files. The raw data has been
2684 supplied as voucher specimens and tissue samples stored in the following herpetological
2685 collections:

- 2686 1) AUP: School of Agriculture and Natural Resources, University of Phayao, Phayao,
2687 Thailand;
- 2688 2) BNHS: Bombay Natural History Society, Mumbai, India;
- 2689 3) CAS: California Academy of Sciences Museum, California, USA;

- 2690 4) CHS: Song Huang's private collection, College of Life Sciences, Anhui Normal
 2691 University, Wuhu, Anhui, China;
- 2692 5) CIB: Chengdu Institute of Biology, Chengdu, China;
- 2693 6) DL: Ding Lee's private collection, Chengdu, China; 
- 2694 7) DTU: Duy Tan University, Da Nang, Vietnam;
- 2695 8) FMNH: Field Museum of Natural History, Chicago, USA;
- 2696 9) GP: Guo Peng's private collection, College of Life Science and Food Engineering, Yibin 
 2697 University, Yibin, China;
- 2698 10) KIZ: Kunming Institute of Zoology, Chinese Academy of Sciences, Kunming, Yunnan,
 2699 China; MNHN: Muséum National d'Histoire Naturelle, Paris, France; 
- 2700 11) LSUHC: La Sierra University Herpetological Collection, Riverside, California, USA;
- 2701 12) MSNG: Museo Civico di Storia Naturale "Giacomo Doria," Genova, Liguria, Italy;
- 2702 13) MZB: Museum Zoologicum Bogoriense, Juanda 3, Kebun Raya, Bogor, Java, Indonesia;
- 2703 14) MZMU: Departmental Museum of Zoology, Mizoram University, Mizoram, India;
- 2704 15) NHMUK (formerly BMNH): The Natural History Museum, London, UK;
- 2705 16) NMNS: National Museum of Natural Science, Taichung, Taiwan;
- 2706 17) NMW: Naturhistorisches Museum Wien, Vienna, Austria;
- 2707 18) QSMI: Queen Saovabha Memorial Institute, Thai Red Cross Society, Bangkok, Thailand;
- 2708 19) RMNH: Naturalis-Nationaal Natuurhistorisch Museum [formerly Rijksmuseum van
 2709 Natuurlijke Historie], Leiden, the Netherlands (includes MHNPB & ZMA);
- 2710 20) SIEZC: Southern Institute of Ecology, Ho Chi Minh City, Vietnam;
- 2711 21) SMF: Naturmuseum Senckenberg, Frankfurt am Main, Germany;
- 2712 22) UNS; University of Science, Ho Chi Minh City, Vietnam;
- 2713 23) USNM: National Museum of Natural History [formerly United States National Museum],
 2714 Smithsonian Institution, Washington, District of Columbia, USA;
- 2715 24) YPX: Field number for tissue samples stored in KIZ;
- 2716 25) ZFMK: Zoologisches Forschungsmuseum Alexander Koenig, Bonn, Germany;
- 2717 26) ZMB: Zoologisches Museum für Naturkunde der Humboldt-Universität zu Berlin, Berlin,
 2718 Germany;
- 2719 27) ZMH: Zoologisches Institut und Museum, Universität Hamburg, Hamburg, Germany;
- 2720 28) ZMMU: Zoological Museum of Moscow University, Moscow, Russia;
- 2721 29) ZSM: Zoologische Staatssammlung, München, Germany.

2722

2723 **New Species Registration**

2724 The following information was supplied regarding the registration of a newly described
 2725 species and subspecies:

2726 Subgenus name: *Spondylodipsas*

2727 urn:lsid:zoobank.org:act:3FE7563C-2BFE-4BA4-A084-1A66E3D9B706

2728 Subspecies name: *Pareas carinatus tenasserimicus*
2729 urn:lsid:zoobank.org:act:11F7F6BA-4733-41FB-8E2D-405DCA5743E5
2730 Subspecies name: *Pareas berdmorei annamiticus*
2731 urn:lsid:zoobank.org:act:3E45EE5B-8DD5-4FB1-814A-76DC2B821E29
2732 Species name: *Pareas kuznetsovorum*
2733 urn:lsid:zoobank.org:act:1CD26CB3-F3E9-4370-B501-6F678851C9FB
2734 Species name: *Pareas abros*
2735 urn:lsid:zoobank.org:act:85CA3212-E8D4-48D1-8ED2-DC8CB183E7E9
2736 Publication LSID:
2737 urn:lsid:zoobank.org:pub:192CDD83-E08C-40B1-92EB-3DB2C3E63CFA

2738

2739 Supplemental Information

2740 Supplemental information for this article can be found online at <http://dx.doi.org/XXXXXXXXXX>

2741

2742 REFERENCES

2743

2744 **Ali JR, Aitchison JC.** 2008. Gondwana to Asia: plate tectonics, paleogeography and the
2745 biological connectivity of the Indian subcontinent from the Middle Jurassic through latest Eocene
2746 (166-35 Ma). *Earth-Science Reviews* **88(3-4)**:145-166. DOI 10.1016/j.earscirev.2008.01.007.

2747 **An Z, Kutzbach JE, Prell WL, Porter SC.** 2001. Evolution of Asian monsoons and
2748 phased uplift of the Himalaya-Tibetan Plateau since late Miocene times. *Nature* **411(6833)**:62-
2749 66. DOI 10.1038/35075035.

2750 **Angel F.** 1920. Sur deux Ophidiens nouveaux de la collection du Muséum. *Bulletin du*
2751 *Muséum National d'Histoire Naturelle*, 26(4):291-294 (in France).

2752 **Averyanov LV, Loc PK, Hiep NT, Harder DK.** 2003. Phytogeographic review of
2753 Vietnam and adjacent areas of Eastern Indochina. *Komarovia* **3**:1-83.

2754 **Bain RH, Hurley MM.** 2011. A biogeographic synthesis of the amphibians and reptiles of
2755 Indochina. *Bulletin of the American Museum of Natural History* **360**:1-138.

2756 **Barraclough TG, Birky CW, Burt A.** 2003. Diversification in sexual and asexual
2757 organisms. *Evolution* **57**:2166-2172.



2758 **Benestan L, Gosselin T, Perrier C, Sainte-Marie B, Rochette R, Bernatchez L.** 2015.
2759 RAD genotyping reveals fine-scale genetic structuring and provides powerful population
2760 assignment in a widely distributed marine species, the American lobster (*Homarus americanus*).
2761 *Molecular Ecology* **24**(13):3299–3315. DOI 10.1111/mec.13245.

2762 **Bhosale H, Phansalkar P, Sawant M, Gowande G, Patel H, Mirza ZA.** 2020. A new
2763 species of snail-eating snakes of the genus *Pareas* Wagler, 1830 (Reptilia: Serpentes) from
2764 eastern Himalayas, India. *European Journal of Taxonomy* **729**:54–73. DOI
2765 10.5852/ejt.2020.729.1191.

2766 **Blair C, Davy CM, Ngo A, Orlov NL, Shi HT, Lu, SQ, Gao L, Rao DQ, Murphy RW.**
2767 2013. Genealogy and demographic history of a widespread amphibian throughout Indochina.
2768 *Journal of Heredity* **104**(1):72–85 DOI 10.1093/jhered/ess079.

2769 **Boie F.** 1828. Bemerkungen über die Abtheilungen im Natürlichen **systeme** und deren
2770 charakteristik. *Isis von Oken*, Leipzig **21**(4):351–363 (in German). 

2771 **Boulenger GA.** 1900. Description of new reptiles and batrachians from Borneo.
2772 *Proceedings of the Zoological Society of London*:182–187.

2773 **Bourret RL.** 1934. Notes herpétologiques sur l'Indochine **fran- çaise**. IV. Sur une  
2774 collection d'ophidiens de Cochinchine et du Cambodge. *Bulletin Général de l'Instruction*
2775 *Publique* **14**(1):5–17 (in French).

2776 **Buerki S, Forest F, Stadler T, Alvarez N.** 2013. The abrupt climate change at the
2777 Eocene-Oligocene boundary and the emergence of South-East Asia triggered the spread of
2778 sapindaceous lineages. *Annals of Botany* **112**:151–160. DOI 10.1093/aob/mct106.

2779 **Cao W, Zahirovic S, Flament N, Williams S, Golonka J, Müller RD.** 2017. Improving
2780 global paleogeography since the late Paleozoic using paleobiology. *Biogeosciences* **14**(23):5425–
2781 5439.

2782 **Chan KO, Hutter CR, Wood Jr PL, Grismer LL, Das I, Brown RM.** 2020. Gene flow
2783 creates a mirage of cryptic species in a Southeast Asian spotted stream frog complex. *Molecular*
2784 *Ecology* **29**(20):3970–3987. DOI 10.1111/mec.15603.

2785 **Chan KO, Hutter CR, Wood PL, Su YC, Brown RM (2021).** Gene flow increases
2786 phylogenetic structure and inflates cryptic species estimations: a case study on widespread
2787 Philippine puddle frogs (*Occidozyga laevis*). *Systematic Biology*, syab034. DOI
2788 10.1093/sysbio/syab034.

2789 **Chan-ard T, Grossmann W, Gumprecht A, Schulz KD.** 1999. Amphibians and reptiles
2790 of peninsular Malaysia and Thailand - an illustrated checklist [bilingual English and German].
2791 Bushmaster Publications, Würselen, Gemany, 240 pp.

2792 **Chan-ard T, Parr JWK, Nabhitabhata J.** 2015. *A field guide to the Reptiles of Thailand.*
2793 Oxford University Press, New York.

2794 **Chang KX, Huang BH, Luo MX, Huang CW, Wu SP, Nguyen HN, Lin SM.** 2021.
2795 Niche partitioning among three snail-eating snakes revealed by dentition asymmetry and prey
2796 specialisation. *Journal of Animal Ecology* **90**(4):967–977. DOI: 10.1111/1365-2656.13426.

2797 **Che J, Zhou W-W, Hu J-S, Yan F, Papenfuss TJ, Wake DB, Zhang Y-P.** 2010. Spiny
2798 frogs (*Paini*) illuminate the history of the Himalayan region and southeast Asia. *Proceedings of*
2799 *the National Academy of Sciences* **107**:13765–13770. DOI 10.1073/pnas.1008415107.

2800 **Chen J-M, Poyarkov NA, Suwannapoom C, Lathrop A, Wu Y-H, Zhou W-W, Yuan**
2801 **Z-Y, Jin J-Q, Chen H-M, Liu H-Q, Nguyen TQ, Nguyen SN, Duong TV, Eto K, Nishikawa**
2802 **K, Matsui M, Orlov NL, Stuart BL, Brown RM, Rowley JJJ, Murphy RW, Wang Y-Y,**
2803 **Che J.** 2018. Large-scale phylogenetic analyses provide insights into unrecognized diversity and
2804 historical biogeography of Asian leaf-litter frogs, genus *Leptolalax* (Anura: Megophryidae).
2805 *Molecular Phylogenetics and Evolution* **124**:162–171. DOI 10.1016/j.ympev.2018.02.020.

2806 **Chen J-M, Zhou W-W, Poyarkov NA, Stuart BL, Brown RM, Lathrop A, Wang Y-Y,**
2807 **Yuan Z-Y, Jiang K, Hou M, Chen H-M, Suwannapoom C, Nguyen SN, Duong TV,**
2808 **Papenfuss TJ, Murphy RW, Zhang Y-P, Che J.** 2017. A novel multilocus phylogenetic
2809 estimation reveals unrecognized diversity in Asian horned toads, genus *Megophrys* sensu lato
2810 (Anura: Megophryidae). *Molecular Phylogenetics and Evolution* **106**:28–43. DOI
2811 10.1016/j.ympev.2016.09.004.

2812 **Chiari Y, Vences M, Vieites DR, Rabemananjara F, Bora P, Ramilijaona**
2813 **Ravoahangimalala O, Meyer A.** 2004. New evidence for parallel evolution of colour patterns in
2814 Malagasy poison frogs (*Mantella*). *Molecular Ecology* **13**:3763–3774.

2815 **Chomdej S, Pradit W, Suwannapoom C, Pawangkhanant P, Nganvongpanit K,**
2816 **Poyarkov NA, Che J, Gao Y-C, Gong S-P.** 2021. Phylogenetic analyses of distantly related
2817 clades of bent-toed geckos (genus *Cyrtodactylus*) reveal an unprecedented amount of cryptic
2818 diversity in northern and western Thailand. *Scientific Reports* **11**:2328. DOI 10.1038/s41598-
2819 020-70640-8.

- 2820 **Chomdej S, Suwannapoom C, Pawangkhanant P, Pradit W, Nazarov RA, Grismer**
2821 **LL, Poyarkov NA.** 2020. A new species of *Cyrtodactylus* Gray (Squamata:Gekkonidae) from
2822 western Thailand and the phylogenetic placement of *C. inthanon* and *C. suthep*. *Zootaxa*
2823 **4838(2)**:179–209. DOI 10.11646/zootaxa.4838.2.2.
- 2824 **Cochran DM.** 1930. The herpetological collections made by Dr. Hugh M. Smith in Siam
2825 from 1923 to 1929. *Proceedings of the United States National Museum* **77(2834)**:1–39.
- 2826 **Cox MJ, Van Dijk PP, Nabhitabhata J, Kumthorn T.** 1998. *A photographic guide to*
2827 *snakes and other reptiles of Peninsular Malaysia, Singapore and Thailand*. Ralph Curtis
2828 Publishing, 144 pp.
- 2829 **Coyne JA, Allen OH.** 1998. The evolutionary genetics of speciation. *Philosophical*
2830 *Transactions of the Royal Society B* **353(1366)**:287–305. DOI 10.1098/rstb.1998.0210.
- 2831 **Cracraft J.** 1983. Species concepts and speciation analysis. In: Johnston R.F. (eds).
2832 *Current Ornithology*, vol 1. Springer, New York, NY. DOI 10.1007/978-1-4615-6781-3_6.
- 2833 **Cundall D, Greene H.W.** 2000. Feeding in snakes. **In:Feeding:Form**, Function and
2834 Evolution in Tetrapod Vertebrates (K. Schwenk, ed), pp. 293–333. Academic Press, San Diego.
- 2835 **Danaisawadi P, Asami T, Ota H, Sutcharit C, Pahan S.** 2016. A snail-eating snake
2836 recognizes prey handedness. *Scientific Reports* **6**:23832. DOI 10.1038/srep23832.
- 2837 **Danaisawadi P, Asami T, Ota H, Sutcharit C, Panha S.** 2015. Subtle asymmetries in the
2838 snail-eating snake **Pareas carinatus** (Reptilia: Pareatidae). *Journal of Ethology* **33**:243–246. DOI
2839 10.1007/s10164-015-0432-x.
- 2840 **Das I, Dattagupta B, Gayen NC.** 1998. History and catalogue of reptile types in the
2841 collection of the Zoological Survey of India. *Journal of South Asian Natural History* **3**:121–172.
- 2842 **Das I.** 2012. *A naturalist's guide to the snakes of South-East Asia:Malaysia, Singapore,*
2843 *Thailand, Myanmar, Borneo, Sumatra, Java and Bali*. John Beaufoy Publishing, Oxford, 176 pp.
- 2844 **Das I.** 2018. *A naturalist's guide to the snakes of Thailand and South-east Asia. 2nd*
2845 *edition*. John Beaufoy Publishing, Oxford, 176 pp.
- 2846 **David P, Vogel G, Dubois A.** 2011. On the need to follow rigorously the Rules of the
2847 Code for the subsequent designation of a nucleospecies (type species) for a nominal genus which
2848 lacked one:the case of the nominal genus *Trimeresurus* Lacépède, 1804 (Reptilia: Squamata:
2849 Viperidae). *Zootaxa* **2992**:1–51. DOI 10.11646/zootaxa.2992.1.1.

- 2850 **David P, Vogel G.** 1996. *The snakes of Sumatra, an annotated checklist and key with*
2851 *natural history notes.* A.S. Brahm, Ed. Chimaira, Frankfurt-am-Main, 260 pp. 
- 2852 **De Bruyn M, Nugroho E, Hossain MM, Wilson JC, Mather PB.** 2005. Phylogeographic
2853 evidence for the existence of an ancient biogeographic barrier: the Isthmus of Kra Seaway.
2854 *Heredity* **94**:370–378. DOI 10.1038/sj.hdy.6800613.
- 2855 **De Bruyn M, Stelbrink B, Morley RJ, Hall R, Carvalho GR, Cannon CH, Van den**
2856 **Bergh G, Meijaard E, Metcalfe I, Boitani L, Maiorano L, Shoup R, Von Rintelen T.** 2014.
2857 Borneo and Indochina are major evolutionary hotspots for Southeast Asian biodiversity.
2858 *Systematic Biology* **63(6)**:879–901. DOI 10.1093/sysbio/syu047.
- 2859 **De Queiroz A, Lawson R, Lemos-Espinal JA.** 2002. Phylogenetic relationships of North
2860 American garter snakes (*Thamnophis*) based on four mitochondrial genes: how much DNA is
2861 enough? *Molecular Phylogenetics & Evolution* **22**:315–329. DOI 10.1006/mpev.2001.1074.
- 2862 **De Queiroz K.** 2007. Species concepts and species delimitation. *Systematic biology.* 2007
2863 *Dec 1;56(6)*:879–86. DOI 10.1080/10635150701701083. 

- 2864 **De Queiroz K.** 2020. An updated concept of subspecies resolves a dispute about the
2865 taxonomy of incompletely separated lineages. *Herpetological Review* **51(3)**:459– 461.
- 2866 **De Rooij NDE.** 1917. The Reptiles of the Indo-Australian Archipelago. II. Ophidia. Leiden
2867 (E. J. Brill), 334 pp.
- 2868 **Deepak V, Narayanan S, Das S, Rajkumar KP, Easa PS, Sreejith KA, Gower DJ.**
2869 2020. Description of a new species of *Xylophis* Beddome, 1878 (Serpentes: Pareidae:
2870 Xylophiinae) from the western Ghats, India. *Zootaxa* **4755**:231–250. DOI
2871 10.11646/zootaxa.4755.2.2.
- 2872 **Deepak V, Ruane S, Gower DJ.** 2019. A new subfamily of fossorial colubroid snakes
2873 from the Western Ghats of peninsular India. *Journal of Natural History* **52**:2919–2934.
2874 DOI10.1080/00222933.2018.1557756.
- 2875 **Deuve J.** 1961. Liste *annotée* des Serpents du Laos. *Bulletin du Muséum National*
2876 *d'Histoire Naturelle* 1:5–32. 
- 2877 **Ding L, Chen Z, Suwannapoom C, Nguyen TV, Poyarkov NA, Vogel G.** 2020. A new
2878 species of the *Pareas hamptoni* complex (Squamata Serpentes:Pareidae) from the Golden
2879 Triangle. *Taprobanica* **9**:174–193.

- 2880 **Dowling HG, Jenner JV.** 1988. Snakes of Burma: checklist of reported species &
2881 bibliography. *Smithsonian Herpetological Information Service* **76**:1–19.
- 2882 **Dowling HG.** 1951. A proposed standard system of counting ventrals in snakes. *British*
2883 *Journal of Herpetology* **1**:97–99.
- 2884 **Drummond AJ, Suchard MA, Xie D, Rambaut A.** 2012. Bayesian phylogenetics with
2885 BEAUti and the BEAST 1.7. *Molecular Biology and Evolution* **29**:1969–1973. DOI
2886 10.1093/molbev/mss075.
- 2887 **Duméril A MC.** 1853. Prodrome de la classification des reptiles ophidiens. *Mémoires de*
2888 *l'Académie de Sciences de l'Institut de France*, Paris 23, 399–536 (in France). 
- 2889 **Duméril AMC, Bibron G, and Duméril A. H. A.** 1854. *Erpétologie générale, ou histoire*
2890 *naturelle complète des reptiles. Tomé septième, Première partie. Comprenant l'histoire des*
2891 *serpents non venimeux*, Librairie Encyclopédique de Roret, **Pari.** (In **France**).  
- 2892 **Duong TV, Do DT, Ngo CD, Nguyen TQ, Poyarkov NA.** 2018. A new species of the
2893 genus *Leptolalax* (Anura: Megophryidae) from southern Vietnam. *Zoological Research* **39**:185–
2894 201. DOI 10.24272/j.issn.2095-8137.2018.009.
- 2895 **Figuroa A, McKelvy AD, Grismer LL, Bell CD, Lailvaux SP.** 2016. A species-level
2896 phylogeny of extant snakes with description of a new colubrid subfamily and genus. *PLoS ONE*
2897 **11**:e0161070. DOI 10.1371/journal.pone.0161070.
- 2898 **Filardi C, Moyle R.** 2005. Single origin of a pan-Pacific bird group and upstream
2899 colonization of Australasia. *Nature* **438**:216–219 (2005). DOI 10.1038/nature04057.
- 2900 **Flot JF.** 2010. SeqPHASE: a web tool for interconverting PHASE input/output files and
2901 FASTA sequence alignments. *Molecular ecology resources* **10**(1):162–166.
- 2902 **Fontaneto D, Herniou EA, Boschetti C, Caprioli M, Melone G, Ricci C, Barraclough**
2903 **TG.** 2007. Independently evolving species in asexual bdelloid rotifers. *PLoS Biology* **5**(4):e87.
2904 DOI 10.1371/journal.pbio.0050087.
- 2905 **Frost DR, Hillis DM.** 1990. Species in concept and practice: Herpetological applications.
2906 *Herpetologica* **46**:87–104. 
- 2907 **Frost DR, Kluge AG, Hillis DM.** 1992. Species in contemporary herpetology: comments
2908 on phylogenetic inference and taxonomy. *Herpetological Review*, **23**:46–54. 
- 2909 **Gao YD, Harris AJ, Zhou SD, He XJ.** 2013. Evolutionary events in *Lilium* (including
2910 *Nomocharis*, Liliaceae) are temporally correlated with orogenies of the Q-T plateau and the

- 2911 Hengduan Mountains. *Molecular Phylogenetics and Evolution* **68(3)**:443–460. DOI
2912 10.1016/j.ympev.2013.04.026.
- 2913 **Garg S, Biju SD.** 2019. New microhylid frog genus from Peninsular India with Southeast
2914 Asian affinity suggests multiple Cenozoic biotic exchanges between India and Eurasia. *Scientific*
2915 *Reports* **9**:1906. DOI 10.1038/s41598-018-38133-x.
- 2916 **Geissler P, Hartmann T, Ihlow F, Rödder D, Poyarkov NA, Nguyen TQ, Ziegler T,**
2917 **Böhme W.** 2015. The lower Mekong: an insurmountable barrier to amphibians in southern
2918 Indochina? *Biological journal of the Linnean Society* 114:905–914.
- 2919 **Gorin VA, Scherz MD, Korost DV, Poyarkov NA.** 2021. Consequences of parallel
2920 miniaturisation in Microhylinae (Anura, Microhylidae), with the description of a new genus of
2921 diminutive South East Asian frogs. *Zoosystematics and Evolution* **97**:27–54. DOI:
2922 10.3897/zse.97.57968.
- 2923 **Gorin VA, Solovyeva EN, Hasan M, Okamiya H, Karunarathna DMSS,**
2924 **Pawangkhanant P, de Silva A, Juthong W, Milto KD, Nguyen LT, Suwannapoom C, Haas**
2925 **A, Bickford DP, Das I, Poyarkov NA.** 2020. A little frog leaps a long way: compounded
2926 colonizations of the Indian Subcontinent discovered in the tiny Oriental frog genus *Microhyla*
2927 (Amphibia: Microhylidae). *PeerJ* **8**:e9411. DOI 10.7717/peerj.9411.
- 2928 **Götz M.** 2002. The feeding behavior of the snail-eating snake *Pareas carinatus* Wagler
2929 1830 (Squamata: Colubridae). *Amphibia-Reptilia* **23(4)**:487–493. DOI
2930 10.1163/15685380260462383.
- 2931 **Grismer JL, Schulte JA, Alexander A, Wagner P, Travers SL, Buehler MD, Welton**
2932 **LJ, Brown RM.** 2016. The Eurasian invasion: phylogenomic data reveal multiple Southeast
2933 Asian origins for Indian Dragon Lizards. *BMC Evolutionary Biology* **16(1)**:43. DOI
2934 10.1186/s12862-016-0611-6.
- 2935 **Grismer L, Wood PL, Poyarkov NA, Le MD, Karunarathna S, Chomdej S,**
2936 **Suwannapoom C, Qi S, Liu S, Che J, Quah ESH, Kraus F, Oliver PM, Riyanto A, Pauwels**
2937 **OSG, Grismer JL.** 2021a. Karstic landscapes are foci of species diversity in the World's third-
2938 largest vertebrate genus *Cyrtodactylus* Gray, 1827 (Reptilia: Squamata: Gekkonidae). *Diversity*
2939 **13**:183. DOI 10.3390/d13050183.
- 2940 **Grismer LL, Wood PL, Aowphol A, Cota M, Grismer MS, Murdoch ML, Aguilar**
2941 **CA, Grismer JL.** 2017 “2016”. Out of Borneo, again and again: biogeography of the stream

2942 toad genus *Ansonia* Stoliczka (Anura:Bufonidae) and the discovery of the first limestone cave-
2943 dwelling species. *Biological Journal of the Linnean Society* **120**:371–395. DOI
2944 10.1111/bij.12886.

2945 **Grismer LL, Wood PL, Poyarkov NA, Le MD, Kraus F, Agarwal I, Oliver PM,**
2946 **Nguyen N Sang Ngoc, Nguyen TQ, Welton LJ, Stuart BL, Luu VQ, Bauer AM, Quah ESH,**
2947 **Chan KO, Ziegler T, Ngo HT, Aowphol A, Chomdej S, Suwannapoom C, Siler D, Anuar S,**
2948 **Ngo TV, Grismer JL.** 2021b. Phylogenetic partitioning of the third-largest vertebrate genus in
2949 the world, *Cyrtodactylus* Gray, 1827 (Reptilia; Squamata; Gekkonidae) and its relevance to
2950 taxonomy and conservation. *Vertebrate Zoology* **71**:101–154. DOI 10.3897/vz.71.e59307.

2951 **Grismer LL, Wood PL, Quah ESH, Anuar S, Poyarkov NA, Thy N, Orlov NL,**
2952 **Thammachoti P, Seiha H.** 2019. Integrative taxonomy of the Asian skinks *Sphenomorphus*
2953 *stellatus* (Boulenger, 1900) and *S. praesignis* (Boulenger, 1900), with the resurrection of *S.*
2954 *annamiticus* (Boettger, 1901) and the description of a new species from Cambodia. *Zootaxa*
2955 **4683**(3):381–411. DOI 10.11646/zootaxa.4683.3.4.

2956 **Grossmann W, Tillack F.** 2003. On the taxonomic status of *Asthenodipsas tropidonotus*
2957 (Van Lidth de Jeude, 1923) and *Pareas vertebralis* (Boulenger, 1900) (Serpentes: Colubridae:
2958 Pareatinae). *Russian Journal of Herpetology* **10**:175–190.

2959 **Groth JG, Barrowclough GF.** 1999. Basal divergences in birds and the phylogenetic
2960 utility of the nuclear RAG-1 gene. *Molecular Phylogenetics and Evolution* **12**:115–123.
2961 DOI10.1006/mpev.1998.0603.

2962 **Guo K, Deng X.** 2009. A new species of *Pareas* (Serpentes: Colubridae: Pareatinae) from
2963 the Gaoligong Mountains, southwestern China. *Zootaxa* **2008**:53–60.

2964 **Guo P, Zhao E-M.** 2004. *Pareas stanleyi* - A record new to Sichuan, China and a Key to
2965 the Chinese species. *Asiatic Herpetological Research* **10**:280–281.

2966 **Guo Y, Wang G, Rao D-Q.** 2020. Scale microornamentation of five species of *Pareas*
2967 (Serpentes, Pareidae) from China. *Zootaxa* **4742**(3):565-572. DOI 10.11646/zootaxa.4742.3.10.

2968 **Guo Y, Wu Y, He S, Zhao E.** 2011. Systematics and molecular phylogenetics of Asian
2969 snail-eating snakes (Pareatidae). *Zootaxa*, **3001**:57–64.

2970 **Haas, C.P.J, de.** 1950. Checklist of the snakes of the **IndoAustralian** Archipelago
2971 (Reptilia, Ophidia). *Treubia*, Bogor **20**(3):511–625.



- 2972 **Hall R.** 2012. Late Jurassic-Cenozoic reconstructions of the Indonesian region and the
2973 Indian Ocean. *Tectonophysics* **570**:1–41. DOI 10.1016/j.tecto.2012.04.021.
- 2974 **Hall TA.** 1999. BioEdit: a user-friendly biological sequence alignment editor and analysis
2975 program for Windows 95/98/NT. In: *Nucleic acids symposium series*. London: Information
2976 Retrieval Ltd c1979-c2000, 95–98.
- 2977 **Hauser S.** 2017. On the validity of *Pareas macularius* Theobald, 1868 (Squamata:
2978 Pareidae) as a species distinct from *Pareas margaritophorus* (Jan in Bocourt, 1866). *Tropical*
2979 *Natural History* **17**:147–174.
- 2980 **He M.** (2009) *Discussion on taxonomy of colurbid snakes based on scale micro-*
2981 *ornamentations*—Unpubl. Ph.D. thesis, Sichuan University (in Chinese).
- 2982 **Hennig W.** 1966. Phylogenetic systematics. University of Illinois Press, Urbana, Illinois
2983 USA.
- 2984 **Hillis DM.** 2020. The detection and naming of geographic variation within species.
2985 *Herpetological Review* **51**:52–56. DOI10.1016/S0022-3182(70)80093-0.
- 2986 **Hillis DM.** 2021. New and not-so-new conceptualizations of species and subspecies: A
2987 reply to the “It’s species all the way down” view. *Herpetological Review* **52**:49–50.
- 2988 **Hoang DT, Chernomor O, von Haeseler A, Minh BQ, Vinh LS.** 2018. UFBoot2:
2989 Improving the ultrafast bootstrap approximation. *Molecular Biology and Evolution* **35**:518–522.
2990 DOI 10.1093/molbev/msx281.
- 2991 **Hoso M, Asami T, Hori M.** 2007. Right-handed snakes: convergent evolution of
2992 asymmetry for functional specialization. *Biology Letters* **3**:169–172. DOI
2993 10.1098/rsbl.2006.0600.
- 2994 **Hoso M, Hori M.** 2006. Identification of molluscan prey from feces of Iwasaki’s slug
2995 snake, *Pareas iwasakii*. *Herpetological Review*, **37**:174–176.
- 2996 **Hoso M, Hori M.** 2008. Divergent shell shape as an antipredator adaptation in tropical
2997 land snails. *The American Naturalist* **172**:726–732. DOI 10.1086/591681.
- 2998 **Hoso M, Kameda Y, Wu S.P, Asami T, Kato M, Hori M.** 2010. A speciation gene for
2999 left–right reversal in snails results in anti-predator adaptation. *Nature Communications* **1**:133.
3000 DOI 10.1038/ncomms1133.



3001 **Hoso M.** 2007. Oviposition and hatchling diet of a snail-eating snake *Pareas iwasakii*
3002 (Colubridae: Pareatinae). *Current Herpetology* **26**:41–43. DOI 10.3105/1345-
3003 5834(2007)26[41:OAHDOA]2.0.CO;2.

3004 **Huelsenbeck JP, Ronquist F.** 2001. MrBayes: Bayesian inference of phylogenetic trees.
3005 *Bioinformatics* **17(8)**:754–755. DOI 10.1093/bioinformatics/17.8.754.

3006 **Isaac NJ, Mallet J, Mace GM.** 2004. Taxonomic inflation: its influence on macroecology
3007 and conservation. *Trends in ecology & evolution* **19(9)**:464–9.

3008 **Iskandar DT, Colijn E.** 2002“2001”. *A checklist of southeast asian and new guinean*
3009 *Reptiles. Part I. Serpentes*, Biodiversity Conservation Project, Jakarta.  

3010 **IUCN Standards and Petitions Committee** 2019. *Guidelines for Using the IUCN Red*
3011 *List Categories and Criteria. Ver. 14. Prepared by the Standards and Petitions Committee.*
3012 <http://www.iucnredlist.org/documents/RedListGuidelines.pdf> (accessed 2021-01-30).

3013 **Jan G.** 1863. *Elenco sistematico degli ofidi descritti e disegnati per l'iconografia generale*,
3014 A. Lombardi, Milano. 143 pp.

3015 **Jobb G.** 2011. TREEFINDER: March 2011 www.treefinder.de.

3016 **Jønsson KU, Fabre FH, Ricklefs RE, Fjeldså J.** 2011. Major global radiation of corvid
3017 birds originated in the proto-Papuan archipelago. *Proceedings of the National Academy of*
3018 *Sciences* **108(6)**:2328–33. DOI 10.1073/pnas.1018956108/

3019 **Kaiser H, Crother BI, Kelly CM, Luiselli L, O'Shea M, Ota H, Passos P, Schleich WD,**
3020 **Wüster W.** 2013. Best practices: in the 21st century, taxonomic decisions in herpetology are
3021 acceptable only when supported by a body of evidence and published via peer-review.
3022 *Herpetological Review* **44(1)**:8–23.

3023 **Katoh K, Misawa K, Kuma K, Miyata T.** 2002. MAFFT:a novel method for rapid
3024 multiple sequence alignment based on fast Fourier transform. *Nucleic Acids Research* **30**:3059–
3025 3066. DOI 10.1093/nar/gkf436.

3026 **Keogh JS.** 1999. Evolutionary implications of hemipenial morphology in the terrestrial
3027 Australian elapid snakes. *Zoological Journal of the Linnean Society* **125**:239–278. DOI
3028 10.1111/j.1096-3642.1999.tb00592.x.

3029 **Kindler C, Fritz U.** 2018. Phylogeography and taxonomy of the barred grass snake (*Natrix*
3030 *helvetica*), with a discussion of the subspecies category in zoology. *Vertebrate Zoology*
3031 **68(3)**:269–281.

- 3032 **Knowles LL, Carstens BC.** 2007. Delimiting species without monophyletic gene trees,
3033 *Systematic Biology* **56(6)**:887–895. DOI 10.1080/10635150701701091.
- 3034 **Kojima, Y, Fukuyama, I, Kurita, T. Hossman, Nishikawa K.** 2020. Mandibular sawing
3035 in a snail-eating snake. *Scientific Reports* **10**:12670. DOI 10.1038/s41598-020-69436-7.
- 3036 **Kopstein F.** 1936. Herpetologische Notizen. XIII. Ueber *Vipera russellii* von Java. *Treubia*
3037 **15(3)**:259–264.
- 3038 **Kumar S, Stecher G, Tamura K.** 2016. MEGA7: Molecular evolutionary genetics
3039 analysis Version 7.0 for Bigger Datasets. *Molecular Biology and Evolution* **33(7)**:1870–1874.
3040 DOI 10.1093/molbev/msw054.
- 3041 **Lanfear R, Calcott B, Ho SYW, Guindon S.** 2012. PartitionFinder: combined selection
3042 of partitioning schemes and substitution models for phylogenetic analyses. *Molecular Biology*
3043 *and Evolution* **29(6)**:1695–1701. DOI 10.1093/molbev/mss020.
- 3044 **Lang C.** 2001. Deforestation in Vietnam, Laos and Cambodia. Deforestation, environment,
3045 and sustainable development. *A comparative analysis* **2001**:111–37.
- 3046 **Le DT, Nguyen SHL, Pham CT, Nguyen TQ.** 2014. New records of snakes (Squamata:
3047 Serpentes) from Dien Bien Province. *Journal of Biology* **36**:460–470. DOI 10.15625/0866-
3048 7160/v36n4.6175.
- 3049 **Le DTT, Tran TG, Hoang HD, Stuart BL.** 2021. A new species of *Pareas* (Squamata,
3050 Pareidae) from southern Vietnam. *Vertebrate Zoology* **71**:439–451. DOI 10.3897/vz.71.e70438.
- 3051 **Li J-N, Liang D, Wang Y-Y, Guo P, Huang S, Zhang P.** 2020. A large-scale systematic
3052 framework of Chinese snakes based on a unified multilocus marker system. *Molecular*
3053 *Phylogenetics and Evolution* **148**:106807. DOI 10.1016/j.ympev.2020.106807.
- 3054 **Liu S, Rao D-Q.** 2021. A new species of the genus *Pareas* (Squamata, Pareidae) from
3055 Yunnan, China. *ZooKeys* **1011**:121–138. DOI 10.3897/zookeys.1011.59029.
- 3056 **Loredo AI, Wood PL, Quah ESH, Anuar S, Greer LF, Ahmad N, Grismer L.** 2013.
3057 Cryptic speciation within *Asthenodipsas vertebralis* (Boulenger, 1900) (Squamata: Paretidae),
3058 the description of a new species from Peninsular Malaysia, and the resurrection of *A.*
3059 *tropidonotus* (Lidth de Jude, 1923) from Sumatra: an integrative taxonomic analysis. *Zootaxa*
3060 **3664**:505–524. DOI 10.11646/zootaxa.3664.4.5.
- 3061 **Malkmus R, Manthey U, Vogel G. Hoffmann P. Kosuch J.** 2002. *Amphibians and*
3062 *reptiles of Mount Kinabalu (North Borneo)*. A.R.G. **Ganther** Verlag, Rugell, 404 pp.

3063 **Malkmus R, Sauer H.** 1996. Ruhestellung von *Pareas nuchalis* und Erstnachweis dieser
3064 Art im Nationalpark Mount Kinabalu/Malaysia. *Salamandra* **32(1)**:55–58.

3065 **Manthey U, Grossmann W.** (1997), *Amphibien and Reptilien Südostasiens*, Natur- und
3066 Tier Verlag, **Münster**.

3067 **Marshall TL, Chambers EA, Matz MV, Hillis DM.** 2021. How mitonuclear discordance
3068 and geographic variation have confounded species boundaries in a widely studied snake.
3069 *Molecular Phylogenetics and Evolution*, **162**:107194. DOI 10.1016/j.ympev.2021.107194.

3070 **Matzke NJ.** 2013. Probabilistic historical biogeography: new models for founder-event
3071 speciation, imperfect detection, and fossils allow improved accuracy and model-testing.
3072 *Frontiers of Biogeography* **5(4)**:242–248. DOI 10.21425/F5FBG19694.

3073 **Mertens, R.** 1930. Die Amphibien und Reptilien der Inseln Bali, Lombok, Sumbawa und
3074 Flores. Senck. Naturf. Gesell, Frankfurt am Main, **Abhandl.** 42(3):117–344.

3075 **Meyfroidt P, Lambin EF.** 2009. Forest transition in Vietnam and displacement of
3076 deforestation abroad. *Proceedings of the National Academy of Sciences* **106(38)**:16139–16144.

3077 **Milne RI, Abbot RJ.** 2002. The origin and evolution of Tertiary relict floras. **Advances in**
3078 *Botanical Research* **38**:281–314. DOI 10.1016/S0065-2296(02)38033-9.

3079 **Minh BQ, Nguyen MAT, von Haeseler A.** 2013. Ultrafast approximation for
3080 phylogenetic bootstrap. *Molecular Biology and Evolution* **30**:1188–1195. DOI
3081 10.1093/molbev/mst024.

3082 **Monastyrskii AL, Holloway JD.** 2013. The biogeography of the butterfly fauna of
3083 Vietnam with a focus on the endemic species (Lepidoptera). In: Silva-Opps M (Ed.). *Current*
3084 *Progress in Biological Research*. Rijeka, Croatia, InTech, pp. 95–123.

3085 **Morley RJ.** 2018. Assembly and division of the South and South-East Asian flora in
3086 relation to tectonics and climate change. *Journal of Tropical Ecology* **34(4)**:209–234 DOI
3087 10.1017/S0266467418000202.

3088 **Mulcahy DG, Lee JL, Miller AH, Chand M, Thura MK, Zug GR.** 2018. Filling the
3089 BINs of life: Report of an amphibian and reptile survey of the Tanintharyi (Tenasserim) Region
3090 of Myanmar, with DNA barcode data. *ZooKeys* **757**:85–152. DOI 10.3897/zookeys.757.24453.

3091 **Murphy RW, Crawford AJ, Bauer AM, Che J, Donnellan SC, Fritz U, Haddad CFB,**
3092 **Nagy ZT, Poyarkov NA, Vences M, Wang W-Z, Zhang Y.** 2013. Cold Code: the global

3093 initiative to DNA barcode amphibians and nonavian reptiles. *Molecular Ecology Resources*
3094 **13**:161–167. DOI 10.1111/1755-0998.12050.

3095 **Nguyen HN, Tran BV, Nguyen LH, Neang T, Yushchenko PV, Poyarkov NA.** 2020. A
3096 new species of *Oligodon* Fitzinger, 1826 from Langbian Plateau, southern Vietnam, with
3097 additional information on *Oligodon annamensis* Leviton, 1953 (Squamata: Colubridae). *PeerJ*,
3098 **8**:e8332. DOI 10.7717/peerj.8332.

3099 **Nguyen LT, Poyarkov NA, Le DV, Vo BD, Phan HT, Duong TV, Murphy RW,**
3100 **Nguyen SN.** 2018. A new species of *Leptotalax* (Anura: Megophryidae) from Son Tra Peninsula,
3101 central Vietnam. *Zootaxa* **4388**:1–21. DOI 10.11646/zootaxa.4388.1.1.

3102 **Nguyen LT, Poyarkov NA, Nguyen TT, Nguyen TA, Tran VH, Gorin VA, Murphy**
3103 **RW, Nguyen SN.** 2019. A new species of the genus *Microhyla* Tschudi, 1838 (Amphibia:
3104 Anura: Microhylidae) from Tay Nguyen Plateau, central Vietnam. *Zootaxa* **4543**:549–580. DOI
3105 10.11646/zootaxa.4543.4.4.

3106 **Nguyen LT, Schmidt HA, von Haeseler A, Minh BQ.** 2015. IQ-TREE: A fast and
3107 effective stochastic algorithm for estimating maximum likelihood phylogenies. *Molecular*
3108 *Biology and Evolution* **32**(1):268–274. DOI 10.1093/molbev/msu300.

3109 **Nguyen SV & Ho CT.** 1996. *A checklist of reptiles and amphibians in Vietnam*. Science
3110 and Technology Publishing House, Hanoi, 264 pp. (in Vietnamese).

3111 **Nguyen SV, Ho CT, Nguyen TQ.** 2009. *Herpetofauna of Vietnam*. Frankfurt: Edition
3112 Chimaira.

3113 **Nguyen TV, Brakels P, Maury N, Sudavanh S, Pawangkhanant P, Idiitullina S,**
3114 **Lorphengsy S, Inkhavilay K, Suwannapoom C, Poyarkov NA.** 2020b. New herpetofaunal
3115 observations from Laos based on photo records. *Amphibian & Reptile Conservation* **14**:218–249
3116 (e248).

3117 **Nguyen TV, Duong TV, Luu KT, Poyarkov NA.** 2020a. A new species of *Kurixalus*
3118 (Anura: Rhacophoridae) from northern Vietnam with comments on the biogeography of the
3119 genus. *Journal of Natural History* **54**:195–223. DOI 10.1080/00222933.2020.1728411.

3120 **Padial JM, Miralles A, De la Riva I, Vences M.** 2010. The integrative future of
3121 taxonomy. *Frontiers in Zoology* **7**:16(2010). DOI 10.1186/1742-9994-7-16.

- 3122 **Peters WCH.** 1864. Über neue Amphibien (*Typhloscincus*, *Typhlops*, *Asthenodipsas*,
3123 *Ogmodon*). *Monatsberichte der königlich Akademie der Wissenschaften zu Berlin* **1864(4)**:271–
3124 276.
- 3125 **Pham AV, Nguyen TQ.** 2019. New records of snakes (Reptilia: Squamata: Serpentes)
3126 from Lai Chau Province, Vietnam. *VNU Journal of Science: Natural Sciences and Technology*
3127 **35**:1–7. DOI 10.25073/2588-1140/vnunst.4854.
- 3128 **Pope CH.** 1935. *The reptiles of China. Turtles, Crocodilians, Snakes, Lizards. Natural*
3129 *History of Central Asia Vol. X.* The American Museum of Natural History, New York, 604 pp.
- 3130 **Poyarkov NA, Geissler P, Gorin VA, Dunayev EA, Hartmann T, Suwannapoom C.**
3131 2019. Counting stripes: revision of the *Lipinia vittigera* complex (Reptilia, Squamata, Scincidae)
3132 with description of two new species from Indochina. *Zoological Research* **40(5)**:358–393. DOI
3133 10.24272/j.issn.2095-8137.2019.052.
- 3134 **Poyarkov NA, Nguyen TV, Duong TV, Gorin VA, Yang J-H.** 2018a. A new limestone-
3135 dwelling species of *Micryletta* (Amphibia: Anura: Microhylidae) from northern Vietnam. *PeerJ*
3136 **6**:e5771. DOI 10.7717/peerj.5771.
- 3137 **Poyarkov NA, Nguyen TV, Popov ES, Geissler P, Paawangkhanant P, Neang T,**
3138 **Suwannapoom C, Orlov NL.** 2021. Recent progress in taxonomic studies, biogeographic
3139 analysis and revised checklist of Amphibians in Indochina. *Russian Journal of Herpetology*
3140 **28**:1–110. DOI 10.30906/1026-2296-2021-28-3A-1-110.
- 3141 **Poyarkov NA, Suwannapoom C, Pawangkhanant P, Aksornneam A, Duong TV,**
3142 **Korost DV, Che J.** 2018b. A new genus and three new species of miniaturized microhylid frogs
3143 from Indochina (Amphibia: Anura: Microhylidae: Asterophryinae). *Zoological Research* **39**:130–
3144 157. DOI 10.24272/j.issn.2095-8137.2018.019.
- 3145 **Poyarkov NA, Vassilieva AB, Orlov NL, Galoyan EA, Tran DTA, Le DTT, Kretova**
3146 **VD, Geissler P.** 2014. Taxonomy and distribution of narrow-mouth frogs of the genus *Microhyla*
3147 Tschudi, 1838 (Anura: Microhylidae) from Vietnam with descriptions of five new species.
3148 *Russian Journal of Herpetology* **21**:89–148.
- 3149 **Pyron RA, Burbrink FT, Colli GR, de Oca ANM, Vitt LJ, Kuczynski CA, Wiens JJ.**
3150 2011. The phylogeny of advanced snakes (Colubroidea), with discovery of a new subfamily and
3151 comparison of support methods for likelihood trees. *Molecular Phylogenetics and Evolution*
3152 **58**:329–342. DOI 10.1016/j.ympev.2010.11.006.

- 3153 **Pyron RA, Burbrink FT, Wiens JJ.** 2013. A phylogeny and revised classification of
3154 Squamata, including 4161 species of lizards and snakes. *BMC Evolutionary Biology* **13**:93. DOI
3155 10.1186/1471-2148-13-93.
- 3156 **Quah ESH, Grismer LL, Lim KKP, Anuar M. S. S, Chan KO.** 2020. A taxonomic
3157 revision of *Asthenodipsas malaccana* Peters, 1864 (Squamata: Pareidae) with a description of a
3158 new species from Borneo. *Zootaxa* **4729**:001–024. DOI 10.11646/zootaxa.4729.1.1.
- 3159 **Quah ESH, Grismer LL, Lim KKP, Anuar M. S. S, Imbun AY.** 2019. A taxonomic
3160 reappraisal of the Smooth slug snake *Asthenodipsas laevis* (Boie, 1827) (Squamata: Pareidae) in
3161 Borneo with the description of two new species. *Zootaxa* **4646**:501–526. DOI
3162 10.11646/zootaxa.4646.3.4.
- 3163 **Quah ESH, Lim KKP, Grismer LL.** 2021. On the taxonomic status of *Asthenodipsas*
3164 *vertebralis* (Boulenger, 1900) (Squamata: Pareidae) in Borneo with the description of a new
3165 species. *Zootaxa* **4949**:24–44. DOI 10.11646/zootaxa.4949.1.2.
- 3166 **Rambaut A, Drummond AJ.** 2007. Tracer. Version 1.5. Available at
3167 <http://beast.bio.ed.ac.uk/Tracer>.
- 3168 **Rao D-Q, Yang D-T.** 1992. Phylogenetic systematics of Pareatinae (Serpentes) of
3169 Southeastern Asia and adjacent islands with relationship between it and the geology changes.
3170 *Acta Zoologica Sinica* **38**:139–150 (in Chinese).
- 3171 **Ree RH, Moore BR, Webb CO, Donoghue MJ.** 2005. A likelihood framework for
3172 inferring the evolution of geographic range on phylogenetic trees. *Evolution* **59**(11):2299–2311.
3173 DOI 10.1111/j.0014-3820.2005.tb00940.x.
- 3174 **Ree RH, Smith SA.** 2008. Maximum likelihood inference of geographic range evolution
3175 by dispersal, local extinction, and cladogenesis. *Systematic Biology* **57**(1):4–14. DOI
3176 10.1080/10635150701883881.
- 3177 **Ronquist F, Huelsenbeck JP.** 2003. MrBayes 3: Bayesian phylogenetic inference under
3178 mixed models. *Bioinformatics* **19**(12):1572–1574. DOI 10.1093/bioinformatics/btg180.
- 3179 **Ronquist F.** 1997. Dispersal-vicariance analysis: a new approach to the quantification of
3180 historical biogeography. *Systematic Biology* **46**(1):195–203 DOI 10.1093/sysbio/46.1.195.
- 3181 **Russell DW, Sambrook J.** 2001. Molecular cloning: a laboratory manual. Cold Spring
3182 Harbor: Cold Spring Harbor Laboratory.

- 3183 **Salvi D, Harris DJ, Kaliontzopoulou A, Carretero MA, Pinho C.** 2013. Persistence
3184 across Pleistocene ice ages in Mediterranean and extra-Mediterranean refugia: Phylogeographic
3185 insights from the common wall lizard. *BMC Evolutionary Biology* 13:147. DOI 10.1186/1471-
3186 2148-13-147.
- 3187 **Schlegel H.** 1826. Notice sur l'Erpétologie de l'île de Java; par M. Böié (Ouvrage
3188 manuscrit). *Bulletin des Sciences Naturelles et de Géologie* 9(2):233–240.
- 3189 **Schlegel H.** 1837. *Essai sur la physionomie des serpents. I. Partie générale. II. Partie*
3190 *descriptive. Atlas, 21 planches et 3 cartes.* Arnz Arnz & Comp, Leiden, 606 pp.
- 3191 **Schmidt D, Kunz K.** 2005. *Ernährung von Schlangen.* Natur und Tier Verlag, Münster,
3192 159 pp (in German).
- 3193 **Shaffer, H.B, Gidis, M, McCartney-Melstad, E, Neal, K.M, Oyamaguchi, H.M, Tellez,**
3194 **M. & Toffelmeir, E.M.** 2015. Conservation genetics and genomics of amphibians and reptiles.
3195 *Annual Review of Animal Biosciences* 3:23.1–23.26. DOI 10.1146/annurev-animal-022114-
3196 110920.
- 3197 **Shimodaira H.** 2002. An approximately unbiased test of phylogenetic tree selection.
3198 *Systematic Biology* 51(3):492–508.
- 3199 **Slowinski JB, Lawson R.** 2002. Snake phylogeny: evidence from nuclear and
3200 mitochondrial genes. *Molecular Phylogenetics & Evolution* 24(2):194–202. DOI 10.1016/S1055-
3201 7903(02)00239-7.
- 3202 **Smedley N.** 1931. Amphibiens and Reptiles from the Cameron Highlands, Malay
3203 Peninsular. *The Raffles Bulletin of Zoology* 6:105–123.
- 3204 **Smith AM, Poyarkov NA, Hebert PDN.** 2008. CO1 DNA barcoding amphibians:take the
3205 chance, meet the challenge. *Molecular Ecology Notes* 8:235–246. DOI 10.1146/annurev-animal-
3206 022114-110920.
- 3207 **Smith MA.** 1943. *The fauna of British India Ceylon and Burma, including the whole of the*
3208 *Indo-Chinese Sub-region. Reptilia and Amphibia. Vol. III. Serpentes.* Taylor and Francis,
3209 London, 583 pp.
- 3210 **Stephens M, Smith NJ, Donnelly P.** 2001. A new statistical method for haplotype
3211 reconstruction from population data. *The American Journal of Human Genetics* 68(4):978–989.
3212 DOI 10.1086/319501.

- 3213 **Stuebing RB, Inger RF, Lardner B.** 2014. *A field guide to the snakes of Borneo* (2nd
3214 edition). Natural History Publications (Borneo), Kota Kinabalu, 310 pp.
- 3215 **Suntrarachun S, Chanhom L, Hauser S, Sumontha M, Kanya K.** 2020. Molecular
3216 phylogenetic support to the resurrection of *Pareas macularius* from the synonymy of *Pareas*
3217 *margaritophorus* (Squamata: Pareidae). *Tropical Natural History* **20**:182–190.
- 3218 **Suwannapoom C, Sumontha M, Tunprasert J, Ruangsawan T, Pawangkhanant P,**
3219 **Korost DV, Poyarkov NA.** 2018. A striking new genus and species of cave-dwelling frog
3220 (Amphibia: Anura: Microhylidae: Asterophryinae) from Thailand. *PeerJ* **6**:e4422. DOI
3221 10.7717/peerj.4422.
- 3222 **Taylor EH.** 1965. The serpents of Thailand and adjacent waters. *University of Kansas*
3223 *Science Bulletin* **45(9)**:609–1096.
- 3224 **Teynié A, David P.** 2010. *Voyages naturalistes au Laos. Les Reptiles.* Editions Revoir,
3225 Nohanent (France).
- 3226 **Theobald W.** 1868. Catalogue of Reptiles in the Museum of the Asiatic Society of Bengal.
3227 *Journal of the Asiatic Society of Bengal (Extra number)* 37: vi + 88 + iii pp, 4 pls.
- 3228 **Trifnopoulos J, Nguyen TL, von Haeseler A, Bui MQ.** 2016. W-IQTREE: a fast online
3229 phylogenetic tool for maximum likelihood analysis. *Nucleic Acids Research* **44(W1)**:W232–
3230 W235. DOI 10.1093/nar/gkw256.
- 3231 **Uetz P, Freed P, Hošek J.** 2021. *The Reptile Database*, <http://reptiledatabase.reptarium.cz>
3232 (accessed in March 2021).
- 3233 **Vences M, Guayasamin JM, Miralles A, de la Riva I.** 2013. To name or not to name:
3234 Criteria to promote economy of change in Linnaean classification schemes. *Zootaxa*
3235 **3636(2)**:201–244. DOI 10.11646/zootaxa.3636.2.1.
- 3236 **Vogel G, Nguyen TV, Lalremsanga HT, Biakzuala L, Hrima V, Poyarkov NA.** 2020.
3237 Taxonomic reassessment of the *Pareas margaritophorus-macularius* species complex
3238 (Squamata, Pareidae). *Vertebrate Zoology* **70**:547–569. DOI 10.26049/VZ70-4-2020-02.
- 3239 **Vogel G, Nguyen TV, Than Zaw, Poyarkov NA.** 2021. A new species of the *Pareas*
3240 *monticola* complex (Squamata, Serpentes, Pareidae) from Chin Mountains with additions to the
3241 *Pareas* fauna of Myanmar. *Journal of Natural History* **54(39-40)**:2577–2612. DOI
3242 10.1080/00222933.2020.1856953.

- 3243 **Vogel G.** 2015. New montane species of the genus *Pareas* Wagler, 1830 (Squamata:
3244 Pareatidae) from Northern Myanmar. *Taprobanica* **7(1)**:1–7.
- 3245 **Wagler JG.** 1830. *Natürliches System der Amphibien, mit vorangehender Classification*
3246 *der Säugetiere und Vögel. Ein Beitrag zur vergleichenden Zoologie.* 1.0. Cotta, München,
3247 Stuttgart, and Tübingen, 354 pp.
- 3248 **Wallach V, Wuester W, Broadley DG.** 2009. In praise of subgenera: taxonomic status of
3249 cobras of the genus *Naja* Laurenti (Serpentes: Elapidae). *Zootaxa*, **2236(1)**:26–36.
- 3250 **Wallach V, Williams KL, Boundy J.** 2014. *Snakes of the world: a catalogue of living and*
3251 *extinct species.* CRC press, Boca Raton:1237pp.
- 3252 **Wang P, Che J, Liu Q, Li K, Jin JQ, Jiang K, Shi L, Guo P.** 2020. A revised taxonomy
3253 of Asia snail-eating snakes *Pareas* (Squamata, Pareidae): evidence from morphological
3254 comparison and molecular phylogeny. *ZooKeys* **939**:45–64. DOI 10.3897/zookeys.939.49309.
- 3255 **Wilcox TP, Zwickl DJ, Heath TA, Hillis DM.** 2002. Phylogenetic relationships of the
3256 Dwarf Boas and a comparison of Bayesian and bootstrap measures of phylogenetic support.
3257 *Molecular Phylogenetics and Evolution* **25(2)**:361–371. DOI 10.1016/S1055-7903(02)00244-0.
- 3258 **Williams EW, Gardner EM, Harris R, Chaveerach A, Pereira JT, Zerega NJC.** 2017.
3259 Out of Borneo: biogeography, phylogeny and divergence date estimates of *Artocarpus*
3260 (Moraceae). *Annals of Botany* **119**:611–627. DOI 10.1093/aob/mcw249.
- 3261 **Wilson EO, Brown WL.** 1953. The subspecies concept and its taxonomic application.
3262 *Systematic Zoology* **2(3)**:967–111. DOI 10.2307/2411818.
- 3263 **Wood PL, Guo X-G, Travers SL, Su Y-C, Olson KV, Bauer AM, Grismer LL, Siler**
3264 **CD, Moyle RG, Andersen MJ, Brown RM.** 2020. Parachute geckos free fall into synonymy:
3265 *Gekko* phylogeny, and a new subgeneric classification, inferred from thousands of ultraconserved
3266 elements. *Molecular Biology and Evolution* **146**:106731. DOI 10.1016/j.ympbev.2020.106731.
- 3267 **Wood PL, Heinicke MP, Jackman TR, Bauer AM.** 2012. Phylogeny of bent-toed geckos
3268 (*Cyrtodactylus*) reveals a west to east pattern of diversification. *Molecular Phylogenetics and*
3269 *Evolution* **65(3)**:992–1003. DOI 10.1016/j.ympbev.2012.08.025.
- 3270 **Wüster W, Scott T, O'Shea M, Kaiser H.** 2021. Confronting taxonomic vandalism in
3271 biology: conscientious community self-organization can preserve nomenclatural stability.
3272 *Biological Journal of the Linnean Society* **133(3)**:645–670. DOI 10.1093/biolinnean/blab009.

3273 **Xu W, Dong WJ, Fu TT, Gao W, Lu CQ, Yan F, Wu YH, Jiang K, Jin JQ, Chen HM,**
3274 **Zhang YP.** 2020. Herpetological phylogeographic analyses support a Miocene focal point of
3275 Himalayan uplift and biological diversification. *National Science Review*: nwa263. DOI
3276 10.1093/nsr/nwa263/5934401.

3277 **Yang D-T, Rao D-Q.** 2008. *Amphibia and Reptilia of Yunnan*, Kunming, Yunnan
3278 Publishing Group Corporation, Yunnan Science (in Chinese).

3279 **Yang J-H, Poyarkov NA.** 2021. A new species of the genus *Micryletta* (Anura,
3280 Microhylidae) from Hainan Island, China. *Zoological Research* **42**:234–240. DOI
3281 10.24272/j.issn.2095-8137.2020.333.

3282 **Yang J-H, Yeung HY, Huang X-Y, Yang S-P.** 2021. First record of *Pareas Vindumi*
3283 Vogel, 2015 (Reptilia: Pareidae) from China with a revision to morphology. *Taprobanica* **10**:39–
3284 46. DOI 10.47605/tapro.v10i1.246.

3285 **Yang Z.** 2007. PAML 4: phylogenetic analysis by maximum likelihood. *Molecular*
3286 *Biology and Evolution* **24**(8):1586–1591. DOI10.1093/molbev/msm088.

3287 **You CW, Poyarkov NA, Lin SM.** 2015. Diversity of the snail-eating snakes *Pareas*
3288 (Serpentes, Pareatidae) from Taiwan. *Zoologica Scripta* **44**(4):349–361. DOI 10.1111/zsc.12111.

3289 **Yu Y, Harris AJ, Blair C, He X.** 2015. RASP (Reconstruct Ancestral State in
3290 Phylogenies): a tool for historical biogeography. *Molecular Phylogenetics and Evolution* **87**:46–
3291 49 DOI 10.1016/j.ympev.2015.03.008.

3292 **Yuan ZY, Zhou WW, Chen X, Poyarkov NA, Chen HM, Jang-Liaw NL, Chou WH,**
3293 **Matzke NJ, Iizuka K, Min MS, Kuzmin SL, Zhang YP, Cannatella DC, Hillis DM, Che J.**
3294 2016. Spatiotemporal diversification of the true frogs (genus *Rana*): an historical framework for
3295 a widely studied group of model organisms. *Systematic Biology* **65**(5):824–842;
3296 DOI10.1093/sysbio/syw055.

3297 **Zachos J, Pagani M, Sloan L, Thomas E, Billups K.** 2001. Trends, rhythms, and
3298 aberrations in global climate 65 Ma to present. *Science* **292**:686–693. DOI
3299 10.1126/science.1059412.

3300 **Zaher H, Murphy RW, Arredondo JC, Graboski R, Machado-Filho PR, Mahlow K,**
3301 **Montingelli GG, Quadros AB, Orlov NL, Wilkinson M, Zhang Y-P, Grazziotin FG.** 2019.
3302 Large-scale molecular phylogeny, morphology, divergence-time estimation, and the fossil record

3303 of advanced caenophidian snakes (Squamata: Serpentes). *PLoS ONE* 14:e0216148. DOI
3304 10.1371/journal.pone.0216148.

3305 **Ziegler T, Ohler A, Vu NT, Le KQ, Nguyen XT, Dinh HT, Bui NT.** 2006. Review of
3306 the amphibian and reptile diversity of Phong Nha – Ke Bang National Park and adjacent areas,
3307 central Truong Son, Vietnam. In: Vences M, Köhler J, Ziegler T, Böhme W (Eds.): *Herpetologia*
3308 *Bonnensis II*; Proceedings of the 13th Ordinary General Meeting of the Societas Europaea
3309 Herpetologica, Bonn: 247–262.

Table 1 (on next page)

Table 1. Species-level scientific names erected for the members of the subgenus *Pareas*.

1 **Table 1.** Species-level scientific names erected for the members of the subgenus *Pareas*.

No.	Authority	Original taxon name	Type locality	Present taxonomy	Proposed taxonomy
1	Wagler, 1830	<i>Pareas carinata</i>	Java, Indonesia	<i>Pareas carinatus</i>	<i>Pareas carinatus</i>
2	Theobald, 1868	<i>Pareas berdmorei</i>	Mon State, Myanmar	synonym of <i>Pareas carinatus</i>	<i>Pareas berdmorei</i>
3	Boulenger, 1900	<i>Amblycephalus nuchalis</i>	Matang, Kidi District, Sarawak, Malaysia	<i>Pareas nuchalis</i>	<i>Pareas nuchalis</i>
4	Bourret, 1934	<i>Amblycephalus carinatus unicolor</i>	Kampong Speu Province, Cambodia	synonym of <i>Pareas carinatus</i>	<i>Pareas berdmorei unicolor</i> comb. nov.
5	Wang et al., 2020	<i>Pareas menglaensis</i>	Mengla County, Yunnan Province, China	<i>Pareas menglaensis</i>	synonym of <i>Pareas berdmorei</i>
6	Le et al., 2021	<i>Pareas temporalis</i>	Doan Ket Commune, Da Huoai District, Lam Dong Province, Vietnam	<i>Pareas temporalis</i>	<i>Pareas temporalis</i>
7	this paper	<i>Pareas carinatus tenasserimicus</i>	Suan Phueng District, Ratchaburi Province, Thailand	-	<i>Pareas carinatus tenasserimicus</i> ssp. nov.
8	this paper	<i>Pareas berdmorei annamiticus</i>	Nahin District, Khammouan Province, Laos	-	<i>Pareas berdmorei annamiticus</i> ssp. nov.
9	this paper	<i>Pareas kuznetsovorum</i>	Song Hinh District, Phu Yen Province, Vietnam	-	<i>Pareas kuznetsovorum</i> sp. nov.
10	this paper	<i>Pareas abros</i>	Song Thanh N.P., Quang Nam Province, Vietnam	-	<i>Pareas abros</i> sp. nov.

2

Table 2 (on next page)

Table 2. Measurements and scale counts of members of the subgenus *Pareas*: *Pareas abros* sp. nov., *P. kuznetsovorum* sp. nov., *P. temporalis*, *P. carinatus* (including two subspecies: *P. c. carinatus* and *P. c. tenasserimicus*)

Abbreviations are listed in the Materials and methods. (? = not available).

1 **Table 2.** Measurements and scale counts of members of the subgenus *Pareas*: *Pareas abros* **sp. nov.**, *P. kuznetsovorum* **sp. nov.**, *P. temporalis*, *P. carinatus*
 2 (including two subspecies: *P. c. carinatus* and *P. c. tenasserimicus* **ssp. nov.**), *P. berdmorei* (including three subspecies: *P. berdmorei annamiticus* **ssp. nov.**, *P.*
 3 *berdmorei berdmorei*, and *P. berdmorei unicolor*), and *P. nuchalis*. Abbreviations are listed in the Materials and methods. (? = not available). (Continued on the
 4 next page)



#	Species	Type	Voucher number	Locality	Sex	SVL	TaL	VEN
1	<i>P. abros</i> sp. nov.	Holotype	ZMMU R-16393	Quang Nam, Vietnam	M	314	120	184
2	<i>P. abros</i> sp. nov.	Paratype	ZMMU R-16392	Thua Thien-Hue, Vietnam	M	403	162	180
3	<i>P. abros</i> sp. nov.	Paratype	ZMMU R-14788	Thua Thien-Hue, Vietnam	F	383	138	184
1	<i>P. kuznetsovorum</i> sp. nov.	Holotype	ZMMU R-16802	Song Hinh, Phu Yen, Vietnam	M	478.5	161	167
1	<i>P. temporalis</i>	Holotype	UNS 09992	Da Huoai, Lam Dong, Vietnam	F	426	152	191
2	<i>P. temporalis</i>	0	ZMMU R-13656	Cat Loc, Lam Dong, Vietnam	M	413	142	198
3	<i>P. temporalis</i>	0	DTU 471	Di Linh, Lam Dong, Vietnam	F	443.5	146.3	188
4	<i>P. temporalis</i>	0	DTU 487	Di Linh, Lam Dong, Vietnam	F	380	120	185
5	<i>P. temporalis</i>	0	DTU 488	Di Linh, Lam Dong, Vietnam	F	410	135	187
6	<i>P. temporalis</i>	0	SIEZC 20214	Gia Bac, Lam Dong, Vietnam	F	460	152	187
7	<i>P. temporalis</i>	0	SIEZC 20215	Bidoup, Lam Dong, Vietnam	F	508	157	187
1	<i>P. c. carinatus</i>	0	NMW 28131.1	Borneo, Malaysia	M	385	104	167
2	<i>P. c. carinatus</i>	0	NMW 28131.2	Borneo, Malaysia	M	311	82	167
3	<i>P. c. carinatus</i>	0	NMW 28134.3	Java, Indonesia	M	366	112	160
4	<i>P. c. carinatus</i>	0	NMW 28134.4	Java, Indonesia	M	395	112	168
5	<i>P. c. carinatus</i>	0	NMW 28134.8	Java, Indonesia	M	363	106	174
6	<i>P. c. carinatus</i>	0	NMW 39664.2	Fraser's Hill, Pahang, Malaysia	M	435	136	183
7	<i>P. c. carinatus</i>	Lectotype	RMNH 954 (C)	Java, Indonesia	M	262	75	164
8	<i>P. c. carinatus</i>	Paralectotype	RMNH 954 (A)	Java, Indonesia	M	373	101	170
9	<i>P. c. carinatus</i>	0	SMF 25995	Bogor, Java, Indonesia	M	343	97	164
10	<i>P. c. carinatus</i>	0	SMF 37825	Ranau, Sumatra	M	345	98	165
11	<i>P. c. carinatus</i>	0	SMF 37826	Ranau, Sumatra	M	351	97	166
12	<i>P. c. carinatus</i>	0	SMF 55295	Karimund, Java, Indonesia	M	401	133	161
13	<i>P. c. carinatus</i>	0	ZMH R11547	East Java, Indonesia	M	345	100	158
14	<i>P. c. carinatus</i>	0	ZMH R11548	East Java, Indonesia	M	407	118	169
15	<i>P. c. carinatus</i>	0	ZMH 4053	Kutai Kartanegara, Borneo, Indonesia	M	402	117	173
16	<i>P. c. carinatus</i>	0	NMW 28131.3	Muara Taweh, Borneo, Indonesia	F	?	?	176
17	<i>P. c. carinatus</i>	0	NMW 39664.9	West Malaysia	F	435	122	175
18	<i>P. c. carinatus</i>	0	NMW 39664.11	West Malaysia	F	438	121	178
19	<i>P. c. carinatus</i>	0	NMW 39664.15	Trengganu, Malaysia	F	476	132	188
20	<i>P. c. carinatus</i>	Paralectotype	RMNH 954 (B)	Java, Indonesia	F	365	81	165
21	<i>P. c. carinatus</i>	0	SMF 20797	Bogor, Java, Indonesia	F	405	91	173
22	<i>P. c. carinatus</i>	0	ZMH R05520-1	Java, Indonesia	F	381	?	175
23	<i>P. c. carinatus</i>	0	ZMH R11546	East Java, Indonesia	F	374	93	162

24	<i>P. c. carinatus</i>	0	ZMH R11542	West Java, Indonesia	F	381	101	170
25	<i>P. c. carinatus</i>	0	ZSM 154.1999	North Sumatra, Indonesia	F	371	102	190
26	<i>P. c. tenasserimicus</i> ssp. nov.	Holotype	ZMMU R-16800	Suan Phueng, Ratchaburi, Thailand	M	524	178	194
1	<i>P. b. annamiticus</i> ssp. nov.	Paratype	ZMMU R-14796	Tuyen Hoa, Quang Binh, Vietnam	M	499.0	123.0	187
2	<i>P. b. annamiticus</i> ssp. nov.	Holotype	ZMMU R-16801	Ban Nahin-Nai, Khammouan, Laos	M	502.0	135.0	187
3	<i>P. b. berdmorei</i>	Topotype	CAS 240362	Mon, Myanmar	M	522	154	185
4	<i>P. b. berdmorei</i>	0	CIB 725061	Xishuangbanna, Yunnan, China	M	488.0	122.0	183
5	<i>P. b. berdmorei</i>	0	CIB 736216	Pu'er, Yunnan, China	M	410.0	120.0	179
6	<i>P. b. berdmorei</i>	0	EHT-HMS 31796	Loei, Thailand	M	430.0	?	181
7	<i>P. b. berdmorei</i>	0	NHMUK 1912147	Lai Chau, Vietnam	M	465	?	183
8	<i>P. b. berdmorei</i>	Paratype of <i>P. menglangensis</i>	YBU 14141	Mengla, Yunnan, China	M	448	137	176
9	<i>P. b. berdmorei</i>	Paratype of <i>P. menglangensis</i>	YBU 14142	Mengla, Yunnan, China	M	353	98	176
10	<i>P. b. berdmorei</i>	Holotype	ZSI 8022	Mon, Myanmar	F	490	120	174
11	<i>P. b. berdmorei</i>	0	KIZ 7410023	Pu'er, Yunnan, China	M	?	?	172
12	<i>P. b. berdmorei</i>	0	KIZ 40	Pu'er, Yunnan, China	M	?	?	177
13	<i>P. b. berdmorei</i>	0	EHT-HMS 3626	Chiangmai, Thailand	F	488.0	108.0	174
14	<i>P. b. berdmorei</i>	0	EHT-HMS 31797	Loei, Thailand	F	522.0	111.0	178
15	<i>P. b. berdmorei</i>	0	HNUE MNR.15	Muong Nhe, Dien Bien, Vietnam	F	429	103	186
16	<i>P. b. berdmorei</i>	0	NMW 39664:3	Vinh Phuc, Vietnam	F	412	117	186
17	<i>P. b. berdmorei</i>	0	MNHN RA-1896.556	Luang Prabang, Laos	F	447	110	177
18	<i>P. b. berdmorei</i>	0	TBU LC.2018.11	Sin Ho, Lai Chau, Vietnam	F	595	175	185
19	<i>P. b. berdmorei</i>	Holotype of <i>P. menglangensis</i>	YBU 14124	Mengla, Yunnan, China	F	472	111	177
20	<i>P. b. berdmorei</i>	0	ZMMU R-16803	Suan Phueng, Ratchaburi, Thailand	F	404	101	166
21	<i>P. b. berdmorei</i>	0	KIZ 7911081	Pu'er, Yunnan, China	F	468.0	115.0	176
22	<i>P. b. berdmorei</i>	0	KIZ 741212	Pu'er, Yunnan, China	F	375.0	140.0	174
23	<i>P. b. berdmorei</i>	0	KIZ 79110081	Pu'er, Yunnan, China	F	500.0	120.0	175
24	<i>P. b. unicolor</i>	0	MNHN 1970.480	Cambodia	M	383	122	172
25	<i>P. b. unicolor</i>	0	ZMMU NAP-10584	Cat Tien, Dong Nai, Vietnam	M	468	108	172
26	<i>P. b. unicolor</i>	0	ZMMU NAP-10585	Cat Tien, Dong Nai, Vietnam	M	466	109.5	180
27	<i>P. b. unicolor</i>	0	DTU 472	Cat Tien, Dong Nai, Vietnam	F	412.8	114.5	176
28	<i>P. b. unicolor</i>	0	DTU 473	Cat Tien, Dong Nai, Vietnam	F	385.8	81.3	177
29	<i>P. b. unicolor</i>	0	DTU 474	Bay Nui, An Giang, Vietnam	F	426.9	111.2	174
30	<i>P. b. unicolor</i>	Holotype	MNHN 1938.0149	Kampong Speu, Cambodia	F	390	96	164
31	<i>P. b. unicolor</i>	0	MNHN RA-1937.27	Trang Bom, Dong Nai, Vietnam	F	366	93	173
32	<i>P. b. unicolor</i>	0	SIEZC 20216	Di Linh, Lam Dong, Vietnam	F	415	98	176
33	<i>P. berdmorei</i> ssp.	0	NHMUK 62.7.28.8	Laos	M	355	100	173
34	<i>P. berdmorei</i> ssp.	0	MNHN RA-1896.655	Northern Laos	F	482	125	175
35	<i>P. berdmorei</i> ssp.	0	MNHN RA-1896.656	Northern Laos	F	406	96	173
36	<i>P. berdmorei</i> ssp.	0	MNHN RA-1896.657	Laos	F	421	?	182
1	<i>P. nuchalis</i>	Holotype	NHMUK 1912247	Saribas, Sarawak, Malaysia	M	489	189	220

2	<i>P. nuchalis</i>	0	FMNH 131635	Niah, Sarawak, Malaysia	M	415	145	210
3	<i>P. nuchalis</i>	0	FMNH 239902	Tenom, Sabah, Malaysia	M	263	82	211
4	<i>P. nuchalis</i>	0	FMNH 239903	Tenom, Sabah, Malaysia	M	351	147	211
5	<i>P. nuchalis</i>	0	FMNH 269040	Bintulu, Sarawak, Malaysia	M	367	147	207
6	<i>P. nuchalis</i>	0	USNM 070863	Kepahiang, Sumatra, Indonesia	M	415	164	214
7	<i>P. nuchalis</i>	0	FMNH 131636	Niah, Sarawak, Malaysia	F	309	103	208
8	<i>P. nuchalis</i>	0	FMNH 269041	Bintulu, Sarawak, Malaysia	F	263	89	201
9	<i>P. nuchalis</i>	0	ZMH R3971	Indragiri, Sumatra, Indonesia	F	368	135	207

5 Table 2. Continued.

#	Species	Voucher number	KMD	VSE	SL	IL	At	Pt	SoO	PoO	Source
1	<i>P. abros</i> sp. nov.	ZMMU R-16393	11	1	9/9	8/8	3/3	3/3	3/3	2/2	this study
2	<i>P. abros</i> sp. nov.	ZMMU R-16392	11	1	9/9	8/9	3/3	3/3	3/3	2/2	this study
3	<i>P. abros</i> sp. nov.	ZMMU R-14788	9	1	9/9	8/8	3/3	3/3	3/3	2/2	this study
1	<i>P. kuznetsovorum</i> sp. nov.	ZMMU R-16802	0	1	7/7	8/7	3/3	4/4	2/2	1/1	this study
1	<i>P. temporalis</i>	UNS 09992	15	3	9/8	8/9	4/5	3/3	2/2	2/3	Le et al., 2020
2	<i>P. temporalis</i>	ZMMU R-13656	15	3	7/8	7/8	3/3	4/3	2/2	1/0	this study
3	<i>P. temporalis</i>	DTU 471	15	3	8/8	8/8	3/3	4/4	2/2	2/2	this study
4	<i>P. temporalis</i>	DTU 487	15	3	8/7	8/8	3/3	4/4	2/2	2/2	this study
5	<i>P. temporalis</i>	DTU 488	15	3	8/8	8/8	3/3	4/4	2/2	2/2	this study
6	<i>P. temporalis</i>	SIEZC 20214	15	3	8/8	8/8	3/3	4/4	2/2	2/2	this study
7	<i>P. temporalis</i>	SIEZC 20215	15	3	8/8	8/8	3/3	4/4	2/2	2/2	this study
1	<i>P. c. carinatus</i>	NMW 28131.1	1	3	7/7	8/8	3/3	4/4	2/2	1/1	this study
2	<i>P. c. carinatus</i>	NMW 28131.2	5	3	7/7	8/8	3/3	4/4	2/2	1/1	this study
3	<i>P. c. carinatus</i>	NMW 28134.3	3	3	7/7	8/7	3/3	3/3	2/2	0/1	this study
4	<i>P. c. carinatus</i>	NMW 28134.4	5	3	7/7	8/8	3/3	4/4	2/2	1/1	this study
5	<i>P. c. carinatus</i>	NMW 28134.8	9	3	7/7	7/8	3/3	4/4	2/2	1/1	this study
6	<i>P. c. carinatus</i>	NMW 39664.2	3	3	8/7	9/9	3/2	3/4	2/1	1/1	this study
7	<i>P. c. carinatus</i>	RMNH 954 (small)	?	3	7/7	8/?	3/3	3/3	1/1	1/1	this study
8	<i>P. c. carinatus</i>	RMNH 954 (big)	?	3	7/7	9/9	3/3	4/4	2/2	1/1	this study
9	<i>P. c. carinatus</i>	SMF 25995	5	3	6/7	7/7	4/3	4/4	2/2	1/1	this study
10	<i>P. c. carinatus</i>	SMF 37825	?	3	7/7	8/7	2/2	3/3	2/1	1/1	this study
11	<i>P. c. carinatus</i>	SMF 37826	?	3	7/7	7/7	3/2	3/3	1/2	1/1	this study
12	<i>P. c. carinatus</i>	SMF 55295	11	3	8/8	7/7	3/3	4/4	1/1	1/1	this study
13	<i>P. c. carinatus</i>	ZMH R11547	7	3	7/7	7/7	4/3	4/4	2/2	0/1	this study
14	<i>P. c. carinatus</i>	ZMH R11548	3	3	9/7	8/8	3/3	4/4	3/3	1/1	this study
15	<i>P. c. carinatus</i>	ZMH 4053	11	3	7/6	9/8	4/3	3/3	2/3	1/1	this study
16	<i>P. c. carinatus</i>	NMW 28131.3	9	3	7/7	7/8	3/3	4/4	2/1	1/1	this study
17	<i>P. c. carinatus</i>	NMW 39664.9	9	3	7/8	7/8	3/3	4/4	2/2	1/1	this study
18	<i>P. c. carinatus</i>	NMW 39664.11	7	3	8/8	7/8	3/3	5/4	2/1	1/1	this study

19	<i>P. c. carinatus</i>	NMW 39664.15	7	3	8/8	9/9	2/2	3/3	2/2	1/1	this study
20	<i>P. c. carinatus</i>	RMNH 954 (medium)	?	3	8/8	?/9	2/2	3/3	2/2	1/1	this study
21	<i>P. c. carinatus</i>	SMF 20797	5	3	7/7	7/7	3/3	4/4	2/3	1/1	this study
22	<i>P. c. carinatus</i>	ZMH R05520-1	3	3	8/7	8/8	2/2	3/3	3/3	1/1	this study
23	<i>P. c. carinatus</i>	ZMH R11546	0	3	7/7	8/8	3/3	3/3	2/2	1/1	this study
24	<i>P. c. carinatus</i>	ZMH R11542	?	3	7/7	9/9	3/3	2/4	2/1	1/1	this study
25	<i>P. c. carinatus</i>	ZSM 154.1999	11	3	8/8	7/7	3/2	4/5	2/3	1/1	this study
26	<i>P. c. tenasserimicus</i> ssp. nov.	ZMMU R-16800	7	3	7/7	9/9	3/3	3/3	2/2	2/2	this study
1	<i>P. b. annamiticus</i> ssp. nov.	ZMMU R-14796	13	3	7/7	9/9	3/3	4/4	1/1	1/1	this study
2	<i>P. b. annamiticus</i> ssp. nov.	ZMMU R-16801	13	3	7/7	9/10	3/3	4/4	1/1	1/1	this study
3	<i>P. b. berdmorei</i>	CAS 240362	6	3	7/7	10/10	3/3	4/4	3/3	1/1	this study
4	<i>P. b. berdmorei</i>	CIB 725061	11	3	?	?	3/3	3/3	?	?	Yang & Rao,
5	<i>P. b. berdmorei</i>	CIB 736216	11	3	?	?	3/3	4/4	?	?	Yang & Rao,
6	<i>P. b. berdmorei</i>	EHT-HMS 31796	?	3	7/7	8/9	?	?	?	?	Yang & Rao,
7	<i>P. b. berdmorei</i>	NHMUK 1912147	13	3	9/9	8/9	4/3	4/4	2/2	1/1	this study
8	<i>P. b. berdmorei</i>	YBU 14141	11	3	7/7	8/7	3/3	4/4	2/2	1/1	Wang et al.,
9	<i>P. b. berdmorei</i>	YBU 14142	11	3	7/7	7/8	3/3	4/4	2/2	1/1	Wang et al.,
10	<i>P. b. berdmorei</i>	ZSI 8022	9	3	7/7	8/8	3/3	4/4	2/2	1/1	this study
11	<i>P. b. berdmorei</i>	KIZ 7410023	9	3	?	?	3/3	4/4	?	?	Yang & Rao,
12	<i>P. b. berdmorei</i>	KIZ 40	11	3	?	?	3/3	3/4	?	?	Yang & Rao,
13	<i>P. b. berdmorei</i>	EHT-HMS 3626	?	3	8/7	9/8	?	?	?	?	Taylor, 19
14	<i>P. b. berdmorei</i>	EHT-HMS 31797	?	3	6/7	8/?	?	?	?	?	Taylor, 19
15	<i>P. b. berdmorei</i>	HNUE MNR.15	?	3	8/8	9/9	2/2	2/3	2/2	1/1	Le et al., 20
16	<i>P. b. berdmorei</i>	NMW 39664:3	?	3	7/7	8/8	3/4	4/5	2/2	1/1	this study
17	<i>P. b. berdmorei</i>	MNHN RA-1896.556	7	1	8/7	8/8	3/3	3/3	2/2	0/0	this study
18	<i>P. b. berdmorei</i>	TBU LC.2018.11	?	3	7/7	8/8	2/2	3/3	2/2	2/2	Pham & Nguyen
19	<i>P. b. berdmorei</i>	YBU 14124	11	3	7/7	8/7	3/3	4/4	2/2	1/1	Wang et al.,
20	<i>P. b. berdmorei</i>	ZMMU R-16803	5	3	7/7	8/?	2/2	2/2	2/2	1/1	this study
21	<i>P. b. berdmorei</i>	KIZ 7911081	9	3	?	?	3/3	3/3	?	?	Yang & Rao,
22	<i>P. b. berdmorei</i>	KIZ 741212	11	3	?	?	3/3	3/3	?	?	Yang & Rao,
23	<i>P. b. berdmorei</i>	KIZ 79110081	9	3	?	?	2/2	2/2	?	?	Yang & Rao,
24	<i>P. b. unicolor</i>	MNHN 1970.480	5	1	8/8	8/8	3/3	3/3	2/2	1/1	this study
25	<i>P. b. unicolor</i>	ZMMU NAP-10584	7	3	7/7	8/8	3/3	4/4	2/2	2/2	this study
26	<i>P. b. unicolor</i>	ZMMU NAP-10585	7	3	7/7	8/8	3/3	3/3	2/2	2/1	this study
27	<i>P. b. unicolor</i>	DTU 472	9	3	8/8	8/8	3/3	4/4	3/3	2/2	this study
28	<i>P. b. unicolor</i>	DTU 473	9	3	7/7	8/8	3/3	4/4	3/3	2/2	this study
29	<i>P. b. unicolor</i>	DTU 474	7	3	7/7	9/9	3/3	3/3	2/2	2/2	this study
30	<i>P. b. unicolor</i>	MNHN 1938.0149	7	3	7/7	7/7	3/3	3/3	1/1	1/1	this study
31	<i>P. b. unicolor</i>	MNHN RA-1937.27	7	3	7/7	7/7	3/3	3/3	1/1	1/1	this study
32	<i>P. b. unicolor</i>	SIEZC 20216	3	3	7/8	7/7	3/3	4/4	2/2	1/1	this study

33	<i>P. berdmorei</i> ssp.	NHMUK 62.7.28.8	3	3	?/8	8/8	3/3	3/3	3/2	1/1	<i>this stud</i>
34	<i>P. berdmorei</i> ssp.	MNHN RA-1896.655	11	3	7/8	7/8	3/3	4/4	2/2	1/0	<i>this stud</i>
35	<i>P. berdmorei</i> ssp.	MNHN RA-1896.656	11	1	6/7	6/6	3/3	3/3	1/1	0/1	<i>this stud</i>
36	<i>P. berdmorei</i> ssp.	MNHN RA-1896.657	9	3	7/7	7/7	3/3	4/4	1/1	0/0	<i>this stud</i>
1	<i>P. nuchalis</i>	NHMUK 1912247	?	3	8/8	8/8	3/3	4/4	1/1	1/1	<i>this stud</i>
2	<i>P. nuchalis</i>	FMNH 131635	0	3	8/8	8/7	4/3	5/3	3/3	2/2	<i>this stud</i>
3	<i>P. nuchalis</i>	FMNH 239902	0	1	7/7	7/7	2/3	4/4	3/1	1/1	<i>this stud</i>
4	<i>P. nuchalis</i>	FMNH 239903	0	1	8/8	7/7	4/4	4/4	3/1	1/2	<i>this stud</i>
5	<i>P. nuchalis</i>	FMNH 269040	0	3	8/8	7/7	4/3	4/4	3/3	1/1	<i>this stud</i>
6	<i>P. nuchalis</i>	USNM 070863	0	1	8/7	?	3/3	3/3	1/1	1/1	<i>this stud</i>
7	<i>P. nuchalis</i>	FMNH 131636	0	3	7/7	?	3/3	4/3	1/1	1/1	<i>this stud</i>
8	<i>P. nuchalis</i>	FMNH 269041	0	3	8/8	6/7	3/3	4/3	3/3	1/1	<i>this stud</i>
9	<i>P. nuchalis</i>	ZMH R3971	0	3	8/8	8/7	3/3	4/4	2/2	1/1	<i>this stud</i>

6

Figure 1

Figure 1. Map showing distribution of the subgenus *Pareas* and location of studied populations.

Circles denote localities for which both DNA and morphological data were examined; diamonds denote localities for which only morphological data were available; triangles denote populations for which only DNA data were available; dot in the center of an icon indicates the type locality. **Localities:** (1) Indonesia, Java; (2) Indonesia, West Java, Bogor; (3) Indonesia, West Java; (4) Indonesia, Central Java, Karimundjava Isl.; (5) Indonesia, East Java; (6) Indonesia, Sumatra, Ranau Lake; (7) Indonesia, North Sumatra; (8) Indonesia, Borneo, Central Kalimantan, Moara Terweh; (9) Indonesia, Borneo, East Kalimantan, Kutai N.P.; (10) Malaysia, Borneo, Sarawak; (11) Malaysia, Pahang, Frazers Hills; (12) Malaysia, Terengganu; (13) Malaysia, Kedah, Sungai Sedim; (14) Thailand, Ratchaburi, Suan Phueng; (15) Myanmar, Tanintharyi, Yaephyu; (16) Myanmar, Mon; (17) Myanmar, Mon, Kyaikhto, Kinpon Chaung; (18) Thailand, Chiang Mai, Doi Inthanon N.P.; (19) Thailand, Phitsanulok, Phu Hin Rong Kla N.P.; (20) Laos, Luang Prabang; (21) Laos, Phongsaly; (22) China, Yunnan, Mengla; (23) China, Yunnan, Xishuangbanna; (24) China, Yunnan, Pu'er; (25) Vietnam, Dien Bien, Muong Nhe; (26) Vietnam, Vinh Phuc, Tam Dao N.P.; (27) Laos, Khammouan, Nahin; (28) Vietnam, Quang Binh, Thanh Thach; (29) Cambodia, Kampong Speu; (30) Vietnam, An Giang, Bay Nui; (31) Vietnam, Dong Nai, Trang Bom; (32) Vietnam, Dong Nai, Ma Da (Vinh Cuu); (33) Vietnam, Dong Nai, Cat Tien N.P.; (34) Vietnam, Tay Ninh, Lo Go - Xa Mat N.P.; (35) Vietnam, Binh Phuoc, Bu Gia Map N.P.; (36) Vietnam, Lam Dong, Loc Bao; (37) Vietnam, Lam Dong, Di Linh; (38) Vietnam, Lam Dong, Cat Loc; (39) Vietnam, Lam Dong, Da Huoi; (40) Vietnam, Lam Dong, Bidoup - Nui Ba N.P.; (41) Vietnam, Phu Yen, Song Hinh; (42) Vietnam, Quang Nam, Song Thanh N.P.; (43) Vietnam, Thua Thien-Hue, A Roang, Sao La N.R.; (44) Malaysia, Sarawak, Betong, Saribas; (45) Malaysia, Sarawak, Niah N.P.; (46) Malaysia,

Sarawak, Bintulu; (47) Brunei, Brunei Darussalam; (48) Malaysia, Sabah, Tenom; (49) Indonesia, Sumatra, Riau, Indragiri; (50) Indonesia, Sumatra, Bengkulu, Kepahiang. Base Map created using simplemappr.net.

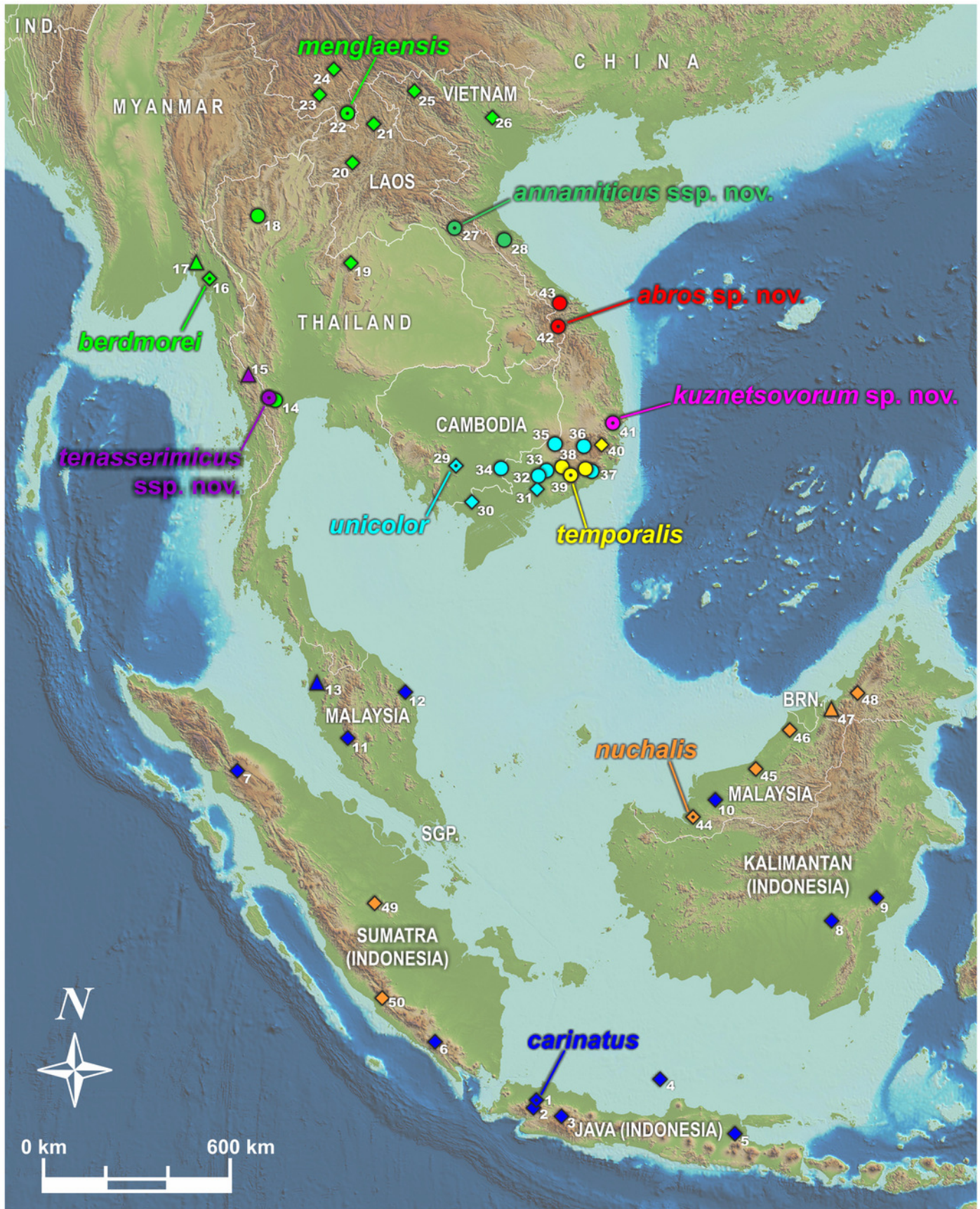


Figure 2

Figure 2. Time tree and biogeographic history of the subfamily Pareinae.

(A) Biogeographic regions used in the present study; (B) BEAST chronogram on the base of 3588 bp-long mtDNA + nuDNA dataset with the results of ancestral area reconstruction using Langrange Dispersal-Extinction-Cladogenesis (DEC) model in RASP. For biogeographic areas definitions, species occurrence data and transition matrices see Supplementary Tables S5 and S6. Information at tree tips corresponds to biogeographic area code (see Fig. 2A), sample number (summarized in Supplementary Table S1), and species name, respectively. Node colors correspond to the respective biogeographic areas; values inside node icons correspond to node numbers (see Supplementary Table S9 and Supplementary Figure S1 for divergence time estimates); values in grey near nodes indicate marginal probabilities for ancestral ranges (S-DIVA analysis), values in blue near nodes correspond to median time of divergence (see Supplementary Table S9); icons illustrate vicariant and dispersal events (see Legend). Base Map created using simplemappr.net.

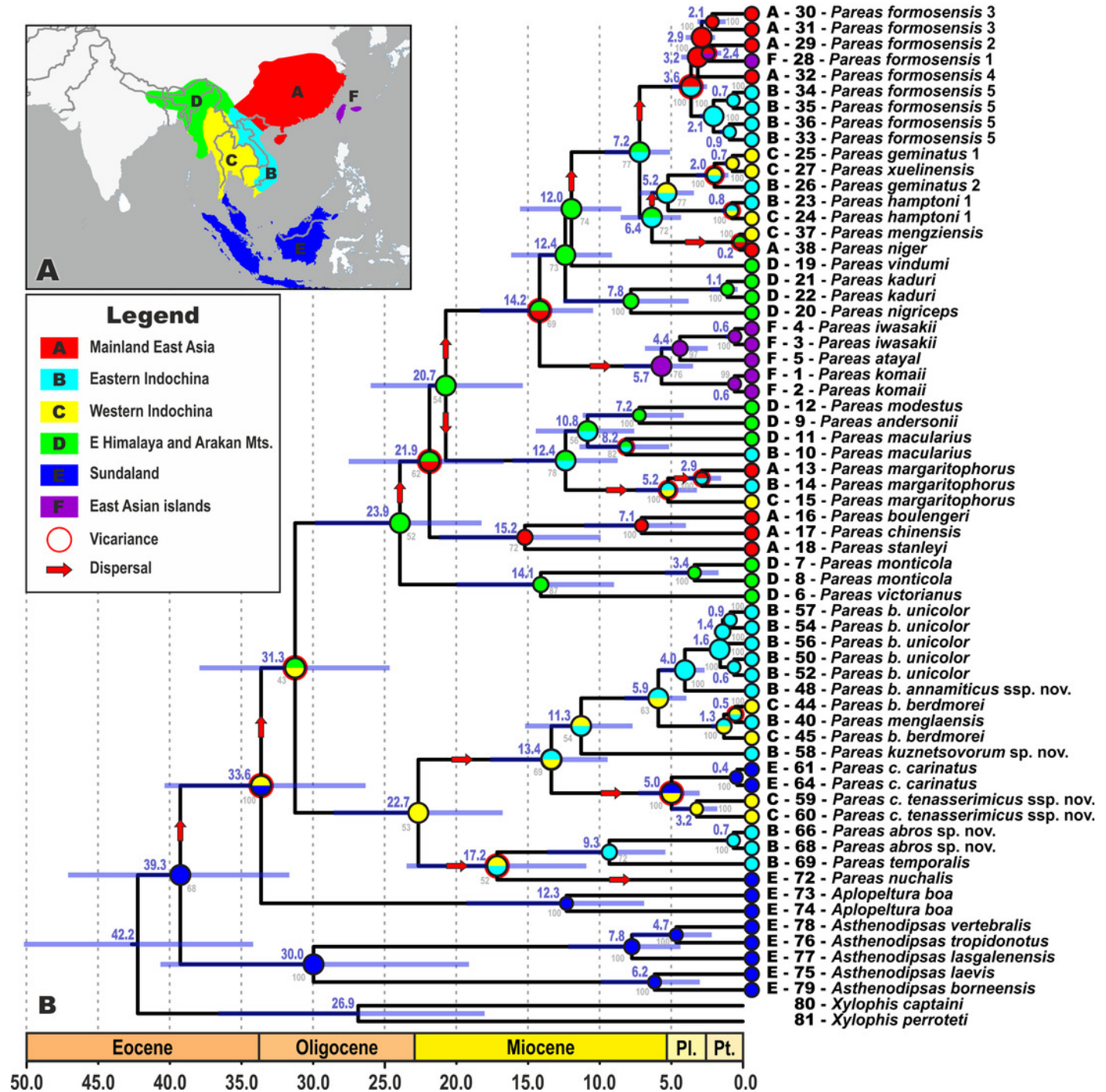


Figure 3

Figure 3. Bayesian inference tree of the subfamily Pareinae derived from the analysis of 1126 bp of *cyt b*, 681 bp of *ND4*, 737 bp of *cmos*, and 1026 bp of *RAG1* gene fragments.

For voucher specimen information and GenBank accession numbers see Supplementary Table S1. Colors denote the taxa of the subgenus *Pareas* and correspond to the color of icons in Figures 1 and 4. Numbers at tree nodes correspond to PP/UFBS support values, respectively. Photos on thumbnails by N. A. Poyarkov (*Pareas abros* **sp. nov.**, *P. temporalis*, and *P. kuznetsovorum* **sp. nov.**), and P. Pawangkhanant (*P. berdmorei annamiticus* **ssp. nov.** and *P. carinatus tenasserimicus* **ssp. nov.**).

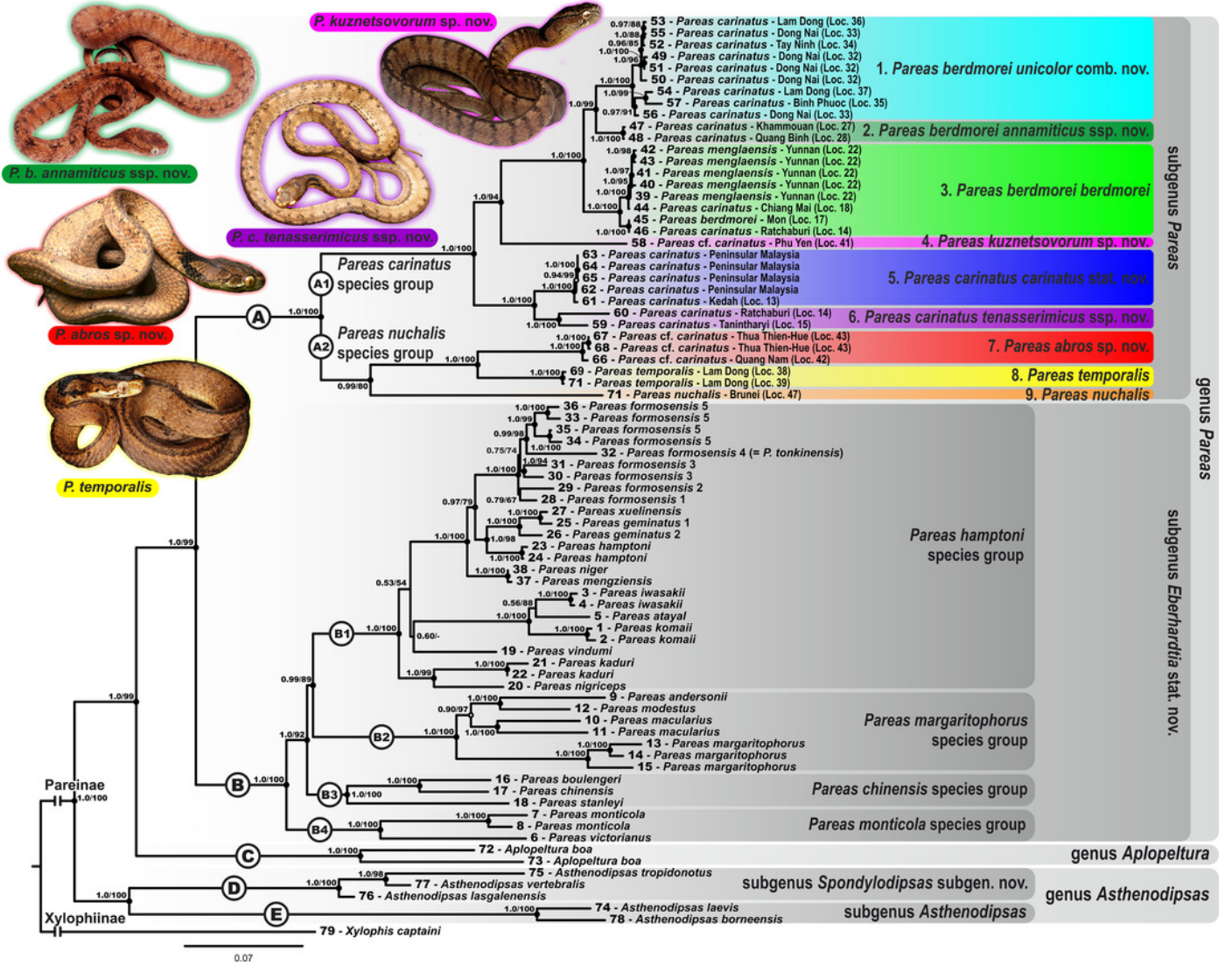


Figure 4

Figure 4. Principal component analysis (PCA) of the species of the subgenus *Pareas* showing ordination along the first two (A) and the first and the third (B) principal components.

Colors denote the taxa of the subgenus *Pareas* and correspond to the color of icons in Figures 1 and 3; dot in the center of an icon indicates the holotype or lectotype of a taxon.

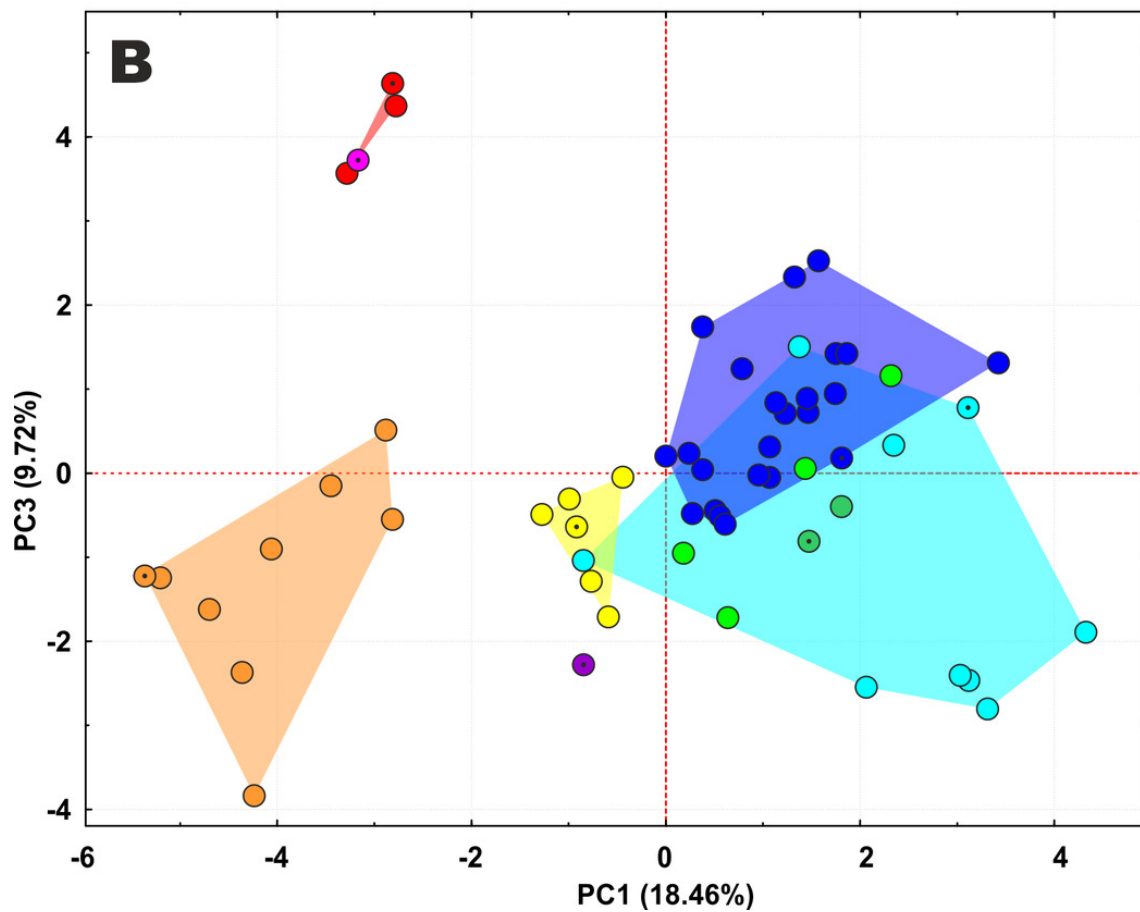
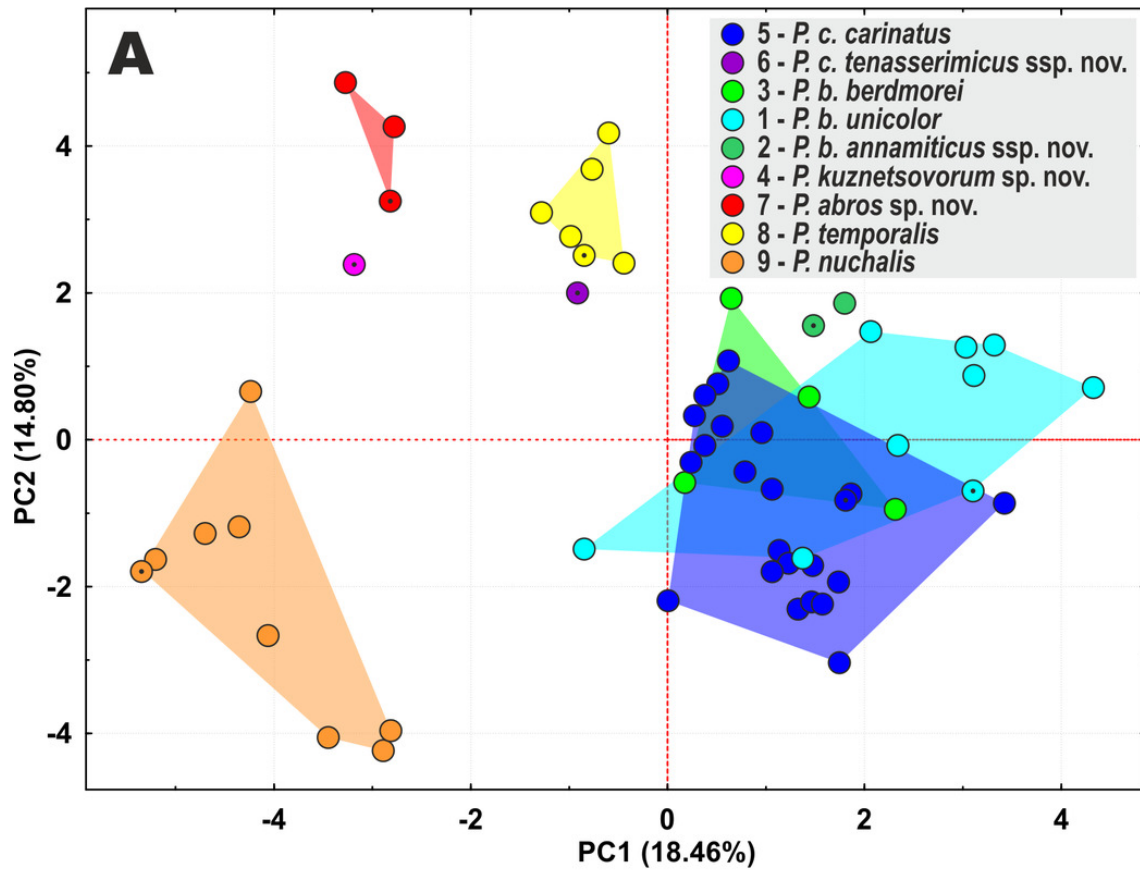
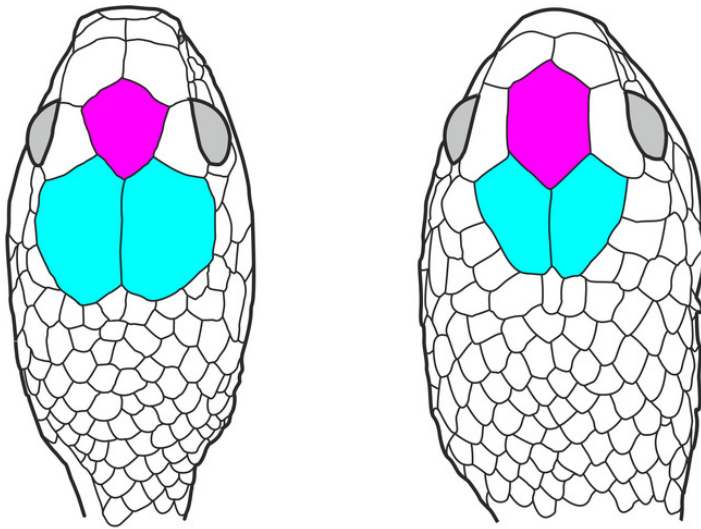
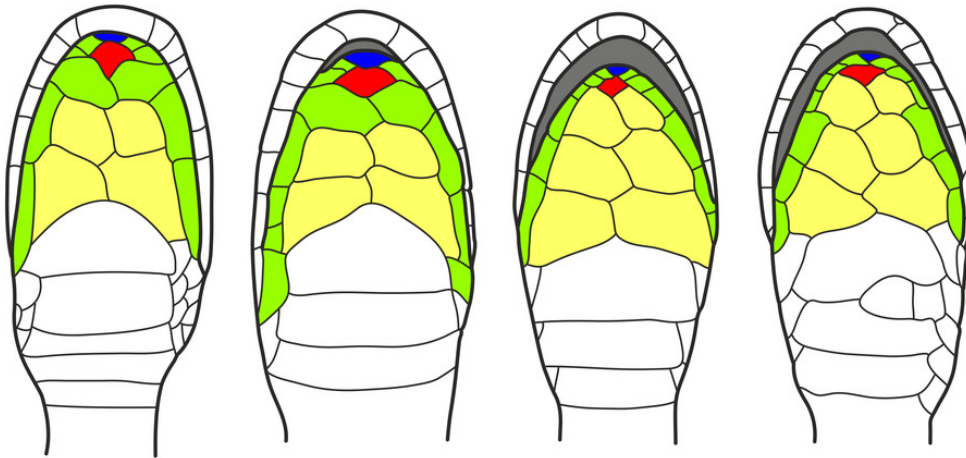
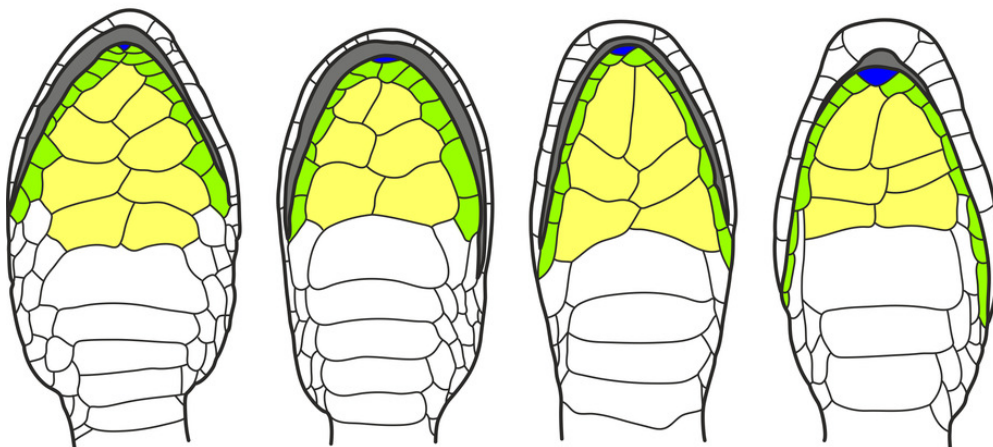


Figure 5

Figure 5. Head scalation of the genera of the subfamily Pareinae.

Dorsal aspect: A - *Pareas (Eberhardtia) formosensis* (FMNH 2555567); B - *Pareas (Pareas) carinatus* (RMNH 954C, lectotype); Ventral aspect: C - *Asthenodipsas (Asthenodipsas) malaccanus* (SMF 32580); D - *Asthenodipsas (Asthenodipsas) laevis* (SMF 81195); E - *Asthenodipsas (Spondylodipsas **subgen. nov.**) vertebralis* (ZMB 65285); F - *Asthenodipsas (Spondylodipsas **subgen. nov.**) tropidonotus* (RMNH 4902B, lectotype); G - *Aplopeltura boa* (ZMB 5397); H - *Pareas (Pareas) carinatus* (ZMB 5397); I - *Pareas (Eberhardtia) formosensis* (ZMB 30585); J - *Pareas (Eberhardtia) margaritophorus* (ZMB 6339). Not to scale. Magenta, cyan, blue, red, green and yellow denote frontal, parietals, mental, inframaxillary, infralabials, and chin shields, respectively. Drawings by N. A. Poyarkov (A–B) and L. B. Salamakha (C–J).

**A****B****C****D****E****F****G****H****I****J**

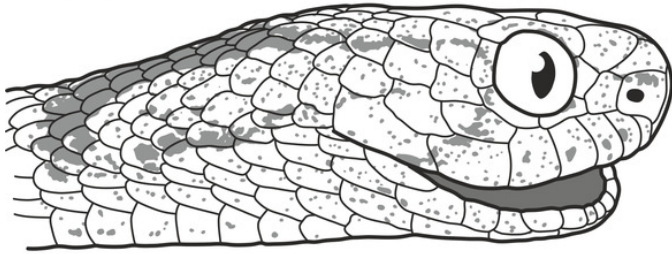
frontal
 parietals
 chin shields
 mental
 inframaxillary
 infralabials

Figure 6

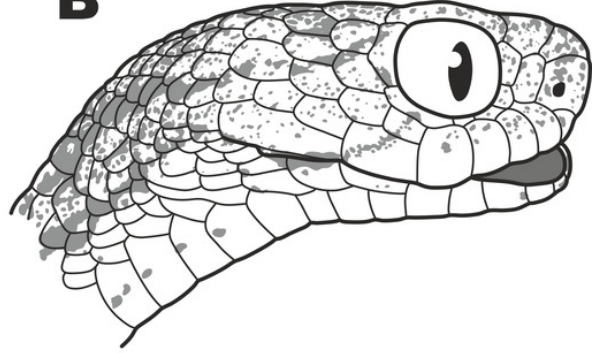
Figure 6. Lateral views of head scalation of taxa of the subgenus *Pareas*.

A - lectotype of *Pareas carinatus* Wagler, 1830 (RMNH 954 C); B - holotype of *P. carinatus tenasserimicus* **ssp. nov.** (ZMMU R-16800); C - lectotype of *Pareas berdmorei* Theobald, 1868 (ZSI 8022); D - holotype of *Pareas menglaensis* Wang, Che, Liu, Ki, Jin, Jiang, Shi & Guo, 2020 (YBU 14124); E - holotype of *P. berdmorei annamiticus* **ssp. nov.** (ZMMU R-16801); F - holotype of *Amblycephalus carinatus unicolor* Bourret, 1934 (MNHN 1938.0149); G - holotype of *Pareas kuznetsovorum* **sp. nov.** (ZMMU R-16802); H - *Pareas nuchalis* (Boulenger, 1900) (FMNH 131635); I - holotype of *Pareas abros* **sp. nov.** (ZMMU R-16393); J - male of *Pareas temporalis* Le, Tran, Hoang & Stuart, 2021 (ZMMU R-13656). Not to scale. Drawings by L. B. Salamakha.

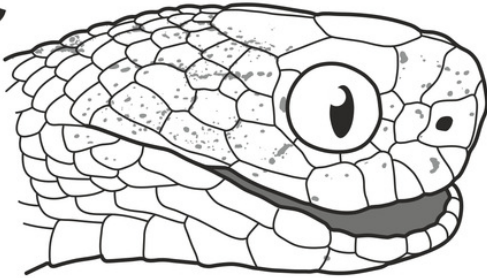
A



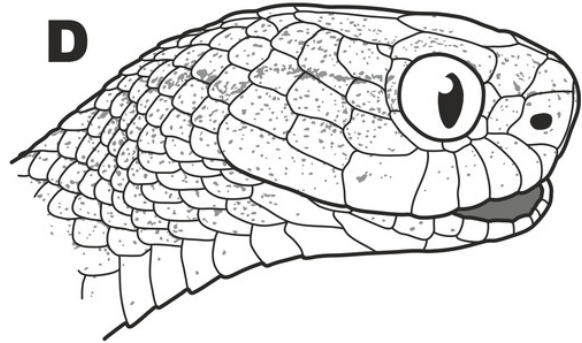
B



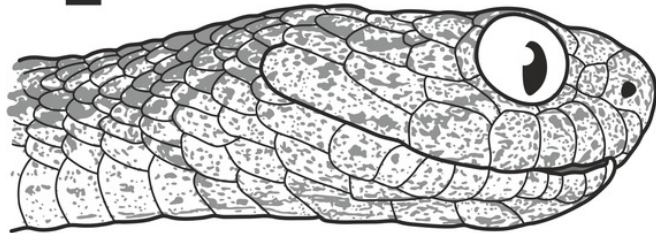
C



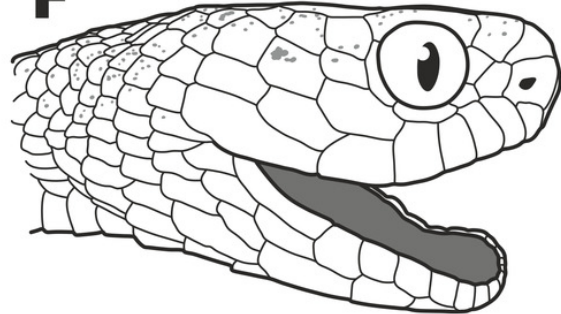
D



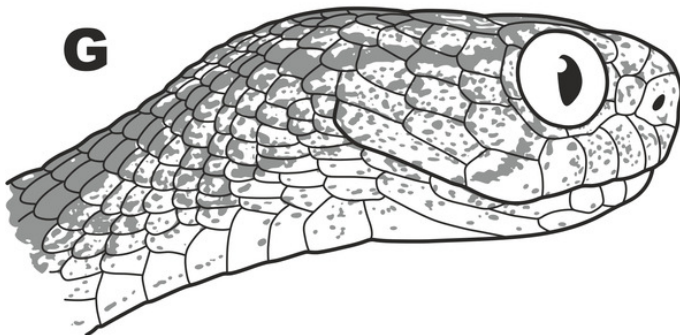
E



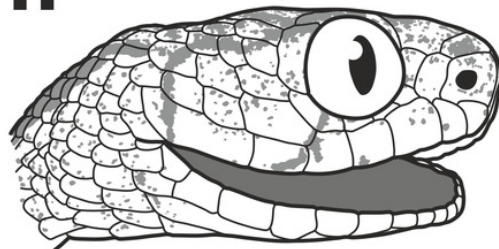
F



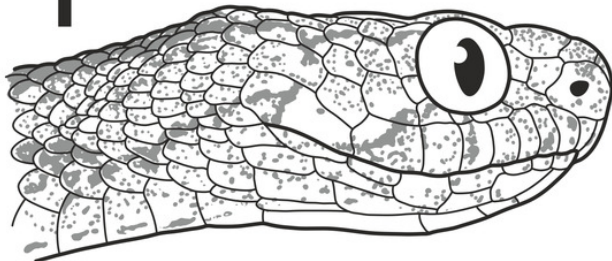
G



H



I



J

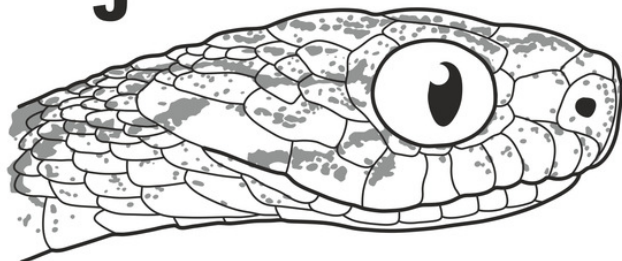


Figure 7

Figure 7. Lectotype of *Pareas carinatus* Wagler, 1830 in preservative (RMNH 954 C, adult male).

A - dorsal view of body; B - ventral view of body; C-F - head in lateral right, lateral left, dorsal, and ventral aspects, respectively. Photos by G. Vogel.

Figure 8

Figure 8. Holotype of *P. carinatus tenasserimicus* ssp. nov. in preservative (ZMMU R-16800, adult male).

A – dorsal view of body; B – ventral view of body; C-F – head in lateral right, lateral left, dorsal, and ventral aspects, respectively. Photos by N. A. Poyarkov.

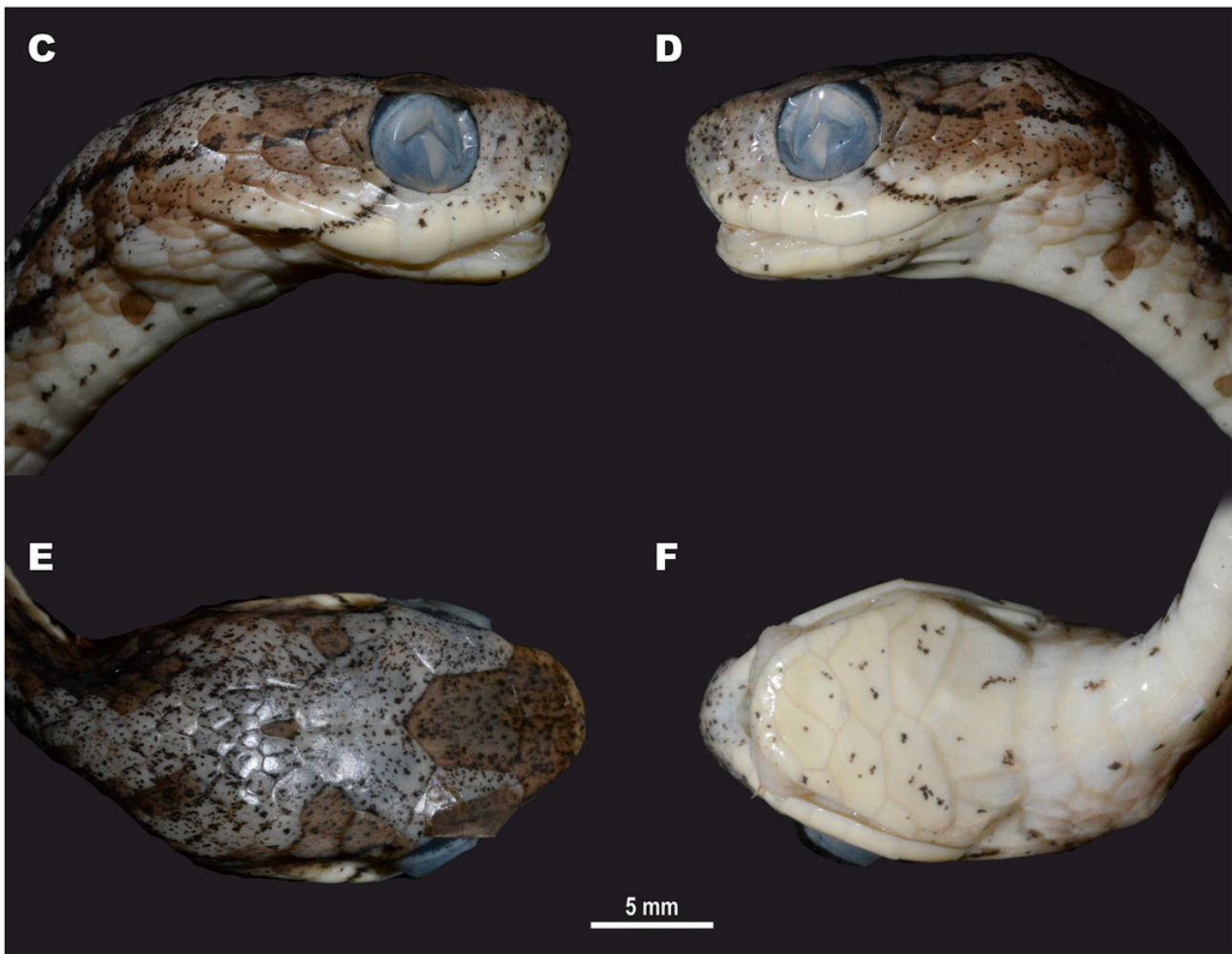


Figure 9

Figure 9. Members of the *Pareas carinatus* complex in life.

A – *P. c. carinatus* from Hala-Bala W.S., Narathiwat Province, Thailand; B, C – *P. c. carinatus* from Gunung Leuser N.P., Bukit Lawang Province, Sumatra, Indonesia; D – *P. c. cf. tenasserimicus* **ssp. nov.** from Kaeng Krachan N.P., Phetchaburi Province, Thailand; E – *P. c. tenasserimicus* **ssp. nov.** from Suan Phueng, Ratchaburi Province, Thailand. Photos by L.A. Neimark (A), Guek Hock Ping aka Kurt Orion (B), H.X.N. Nguyen (C), P. Pawangkhanant (D), and M. Naiduangchan (E).



Figure 10

Figure 10. Lectotype of *Pareas berdmorei* Theobald, 1868 in preservative (ZSI 8022, adult male).

A – general dorsolateral view of body; B – lateral left aspect of head. Photos by I. Das.



Figure 11

Figure 11. Holotype of *Amblycephalus carinatus unicolor* Bourret, 1934 in preservative (MNHN 1938.0149, adult female).

A - dorsal view of body; B - ventral view of body; C-F - head in lateral right, lateral left, dorsal, and ventral aspects, respectively. Photos by G. Vogel.

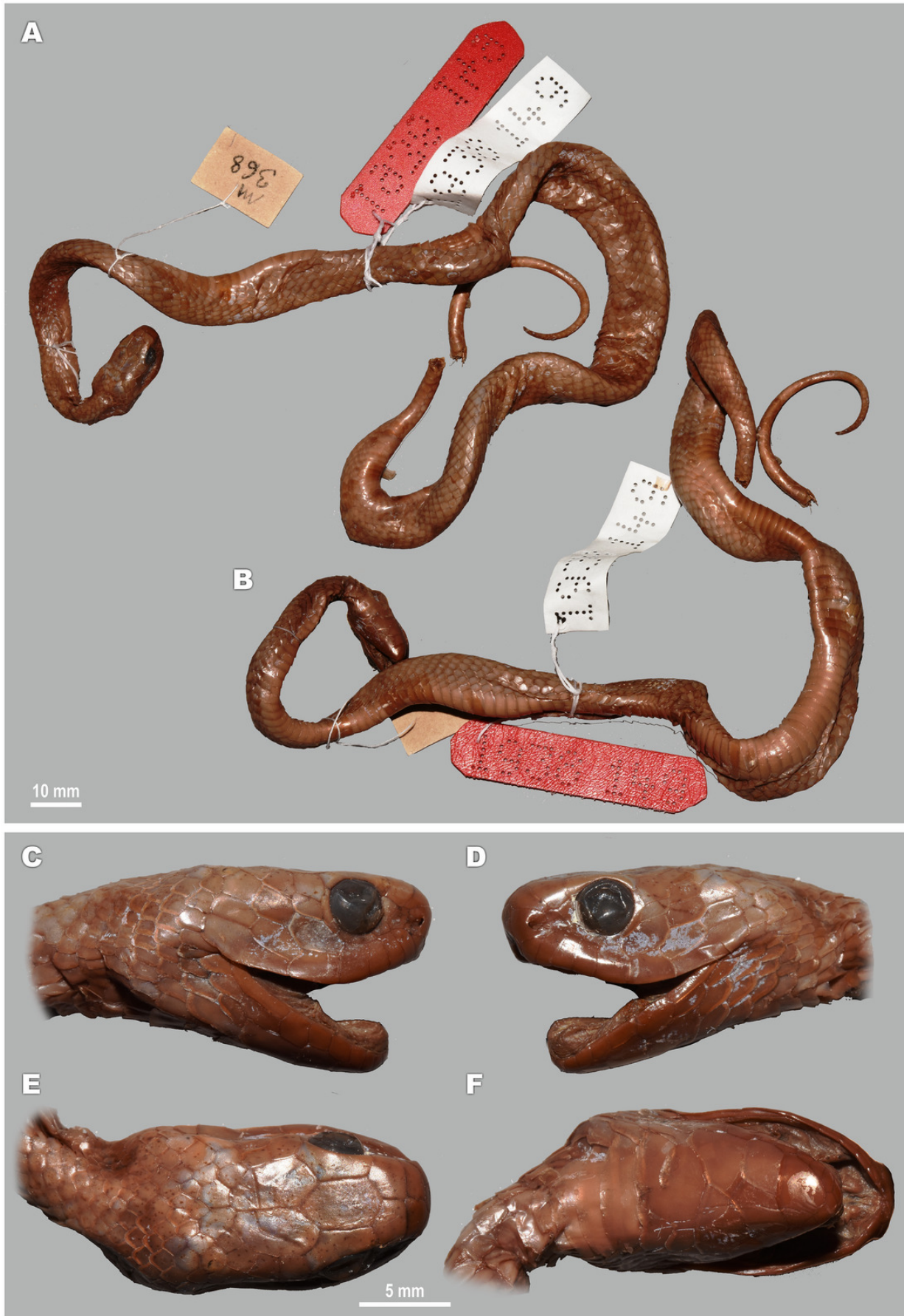


Figure 12

Figure 12. Holotype of *P. berdmorei annamiticus* ssp. nov. in preservative (ZMMU R-16801, adult female).

A – dorsal view of body; B – ventral view of body; C-F – head in lateral right, lateral left, dorsal, and ventral aspects, respectively. Photos by N. A. Poyarkov.

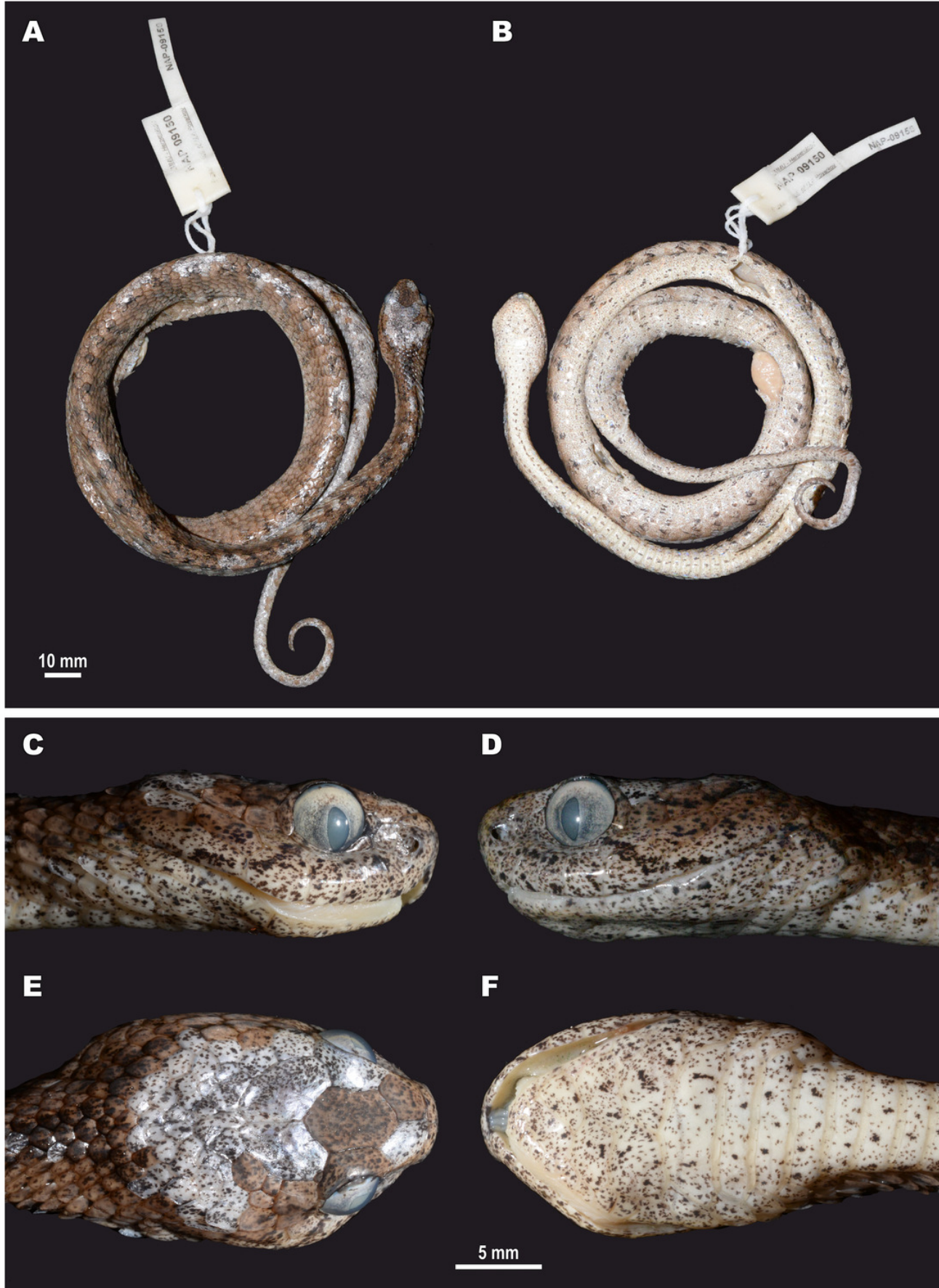


Figure 13

Figure 13. Members of the *Pareas berdmorei* complex in life.

A – *P. b. berdmorei* from Thung Yai Naresuan W.S., Kanchanaburi Province, Thailand; B – *P. b. berdmorei* from Huai Kha Khaeng W.S., Uthai Thani Province, Thailand; C – *P. b. berdmorei* from Phu Hin Rong Kla N.P., Phitsanulok Province, Thailand; D – *P. b. berdmorei* from Jiangcheng, Pu'er City, Yunnan Province, China (close to the type locality of *P. menglaensis*); E – *P. b. unicolor* from Cat Tien N.P., Dong Nai Province, Vietnam; F – *P. b. unicolor* from Loc Bac Forest, Lam Dong Province, Vietnam; G – *P. berdmorei* cf. *annamiticus* **ssp. nov.** from Xe Pian N.P.A., Champasak Province, Laos; H – *P. berdmorei annamiticus* **ssp. nov.** from Nahin District, Khammouan Province, Laos (ZMMU NAP-09150, holotype in life). Photos by P. Pawangkhanant (A–B, H), N.A. Poyarkov (C, E–F), and G. Vogel (D, G).



Figure 14

Figure 14. Holotype of *Pareas kuznetsovorum* sp. nov. in life (ZMMU R-16802, adult male).

A – dorsal view of body; B – ventral view of body; C-F – head in lateral right, lateral left, dorsal, and ventral aspects, respectively. Photos by N. A. Poyarkov.

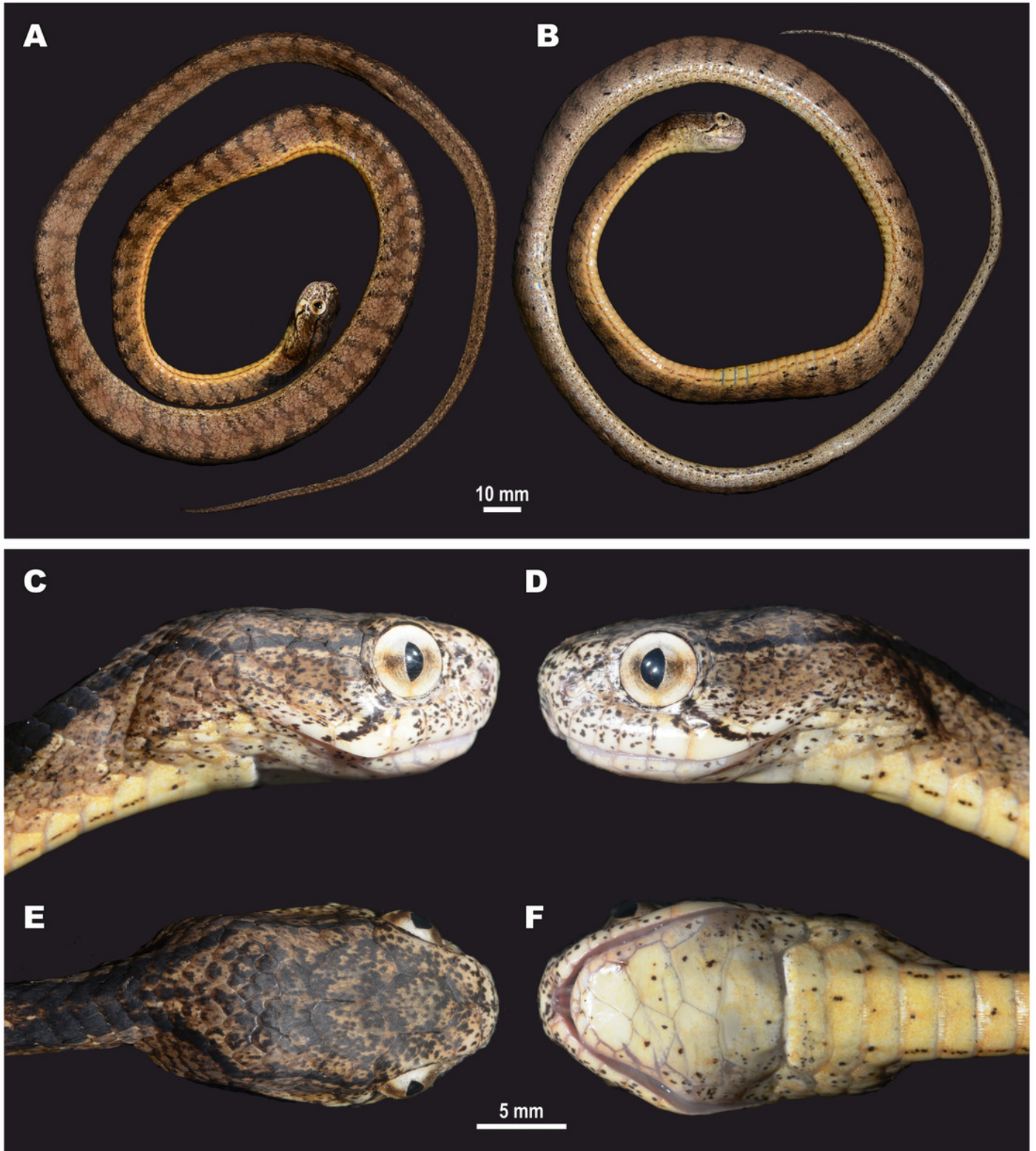


Figure 15

Figure 15. Holotype of *Pareas kuznetsovorum* sp. nov. in life (ZMMU R-16802, adult male) from Song Hinh, Phu Yen Province, Vietnam.

A – general view; B–C – sulcal and asulcal aspects of fully everted hemipenis; D – close-up of midbody showing smooth dorsal scales. Photos by N. A. Poyarkov.

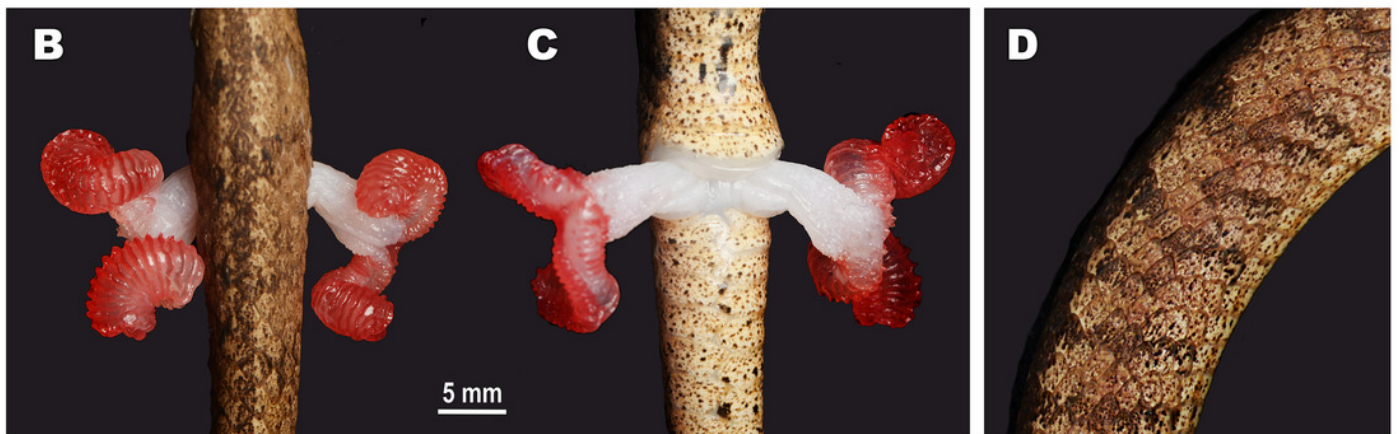


Figure 16

Figure 16. Holotype of *Amblycephalus nuchalis* Boulenger, 1900 in preservative (NHMUK 1901.5.14.2, adult male).

A - dorsolateral view of body; B - ventrolateral view of body; C-F - head in lateral right, lateral left, dorsal, and ventral aspects, respectively. Photos by G. Vogel.



Figure 17

Figure 17. *Pareas nuchalis* in life, adult male from Kota Kinabalu N.P., Kundasang, Sabah, Borneo, Malaysia.

Photo by L.A. Neimark.



Figure 18

Figure 18. Holotype of *Pareas abros* sp. nov. in life (ZMMU R-16393, adult male).

A - lateral left view of body; B - later right view of body; C-E - head in lateral right, ventral, and dorsal aspects, respectively; F - close-up of midbody showing keeled dorsal scales (in eleven rows, five to six of them seen on one side of the body). Photos by N. A. Poyarkov.

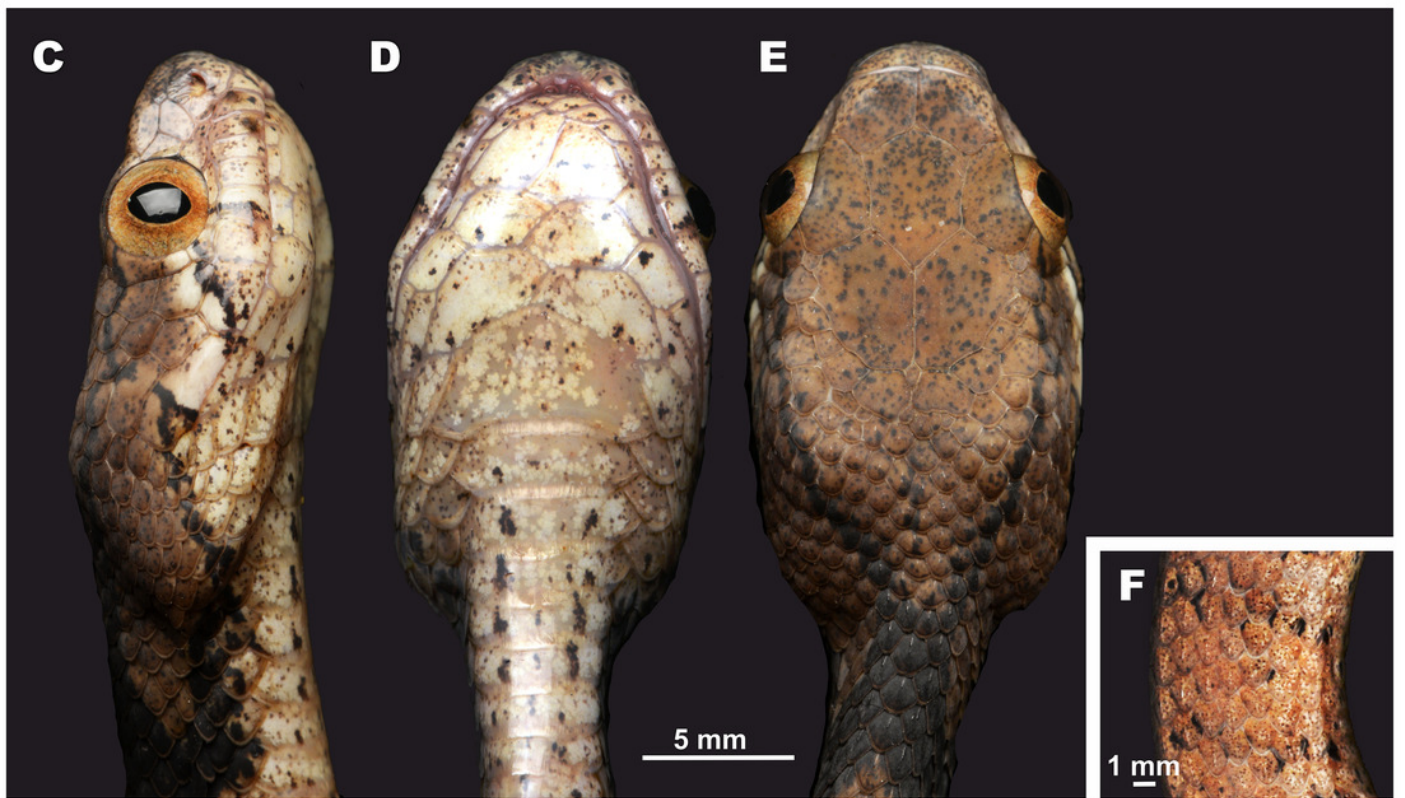
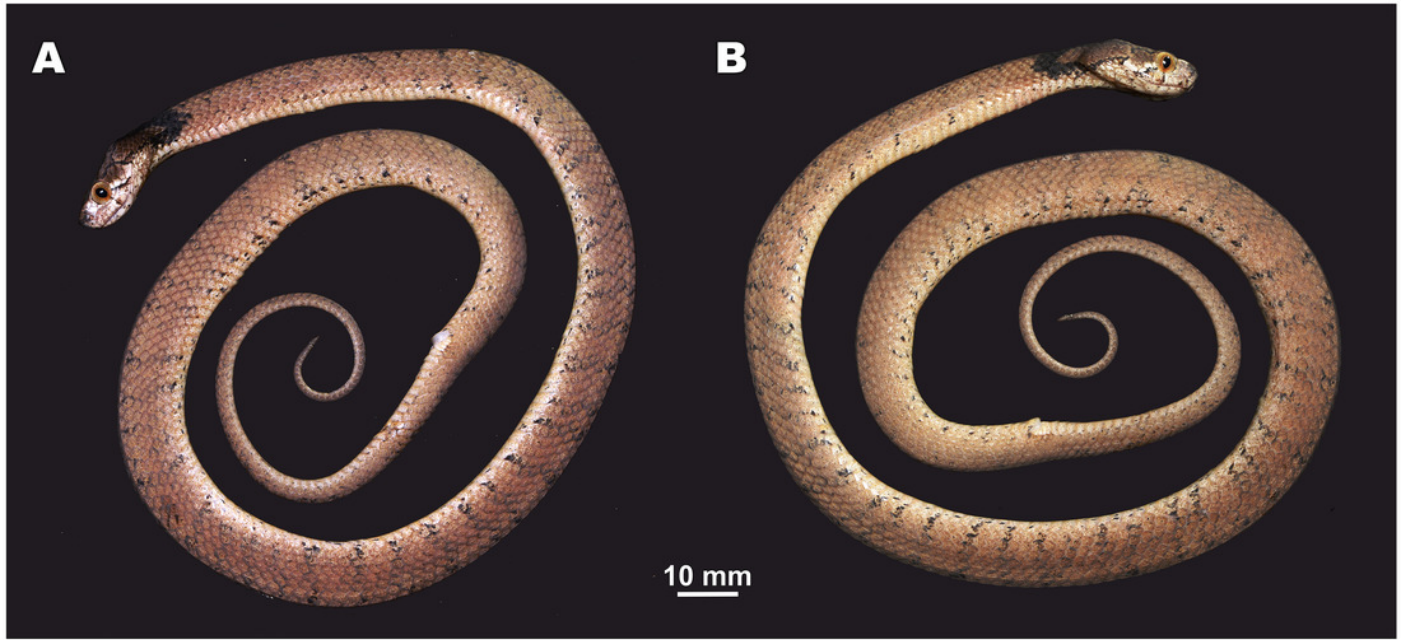


Figure 19

Figure 19. *Pareas abros* sp. nov. in life.

A - male holotype from Song Thanh N.P., Quang Nam Province, Vietnam (ZMMU R-16393); B - male paratype from A Roang, Sao La N.R., Thua Thien - Hue Province, Vietnam (ZMMU R-16392); C - female paratype from A Roang, Sao La N.R., Thua Thien - Hue Province, Vietnam (ZMMU R-14788); D - partially everted hemipenis of ZMMU R-16392 from asulcal (above) and sulcal (below) aspects; E - close-up of midbody of ZMMU R-16392 showing enlarged vertebrals and keeled dorsal scales (in eleven rows). Photos by N. A. Poyarkov.

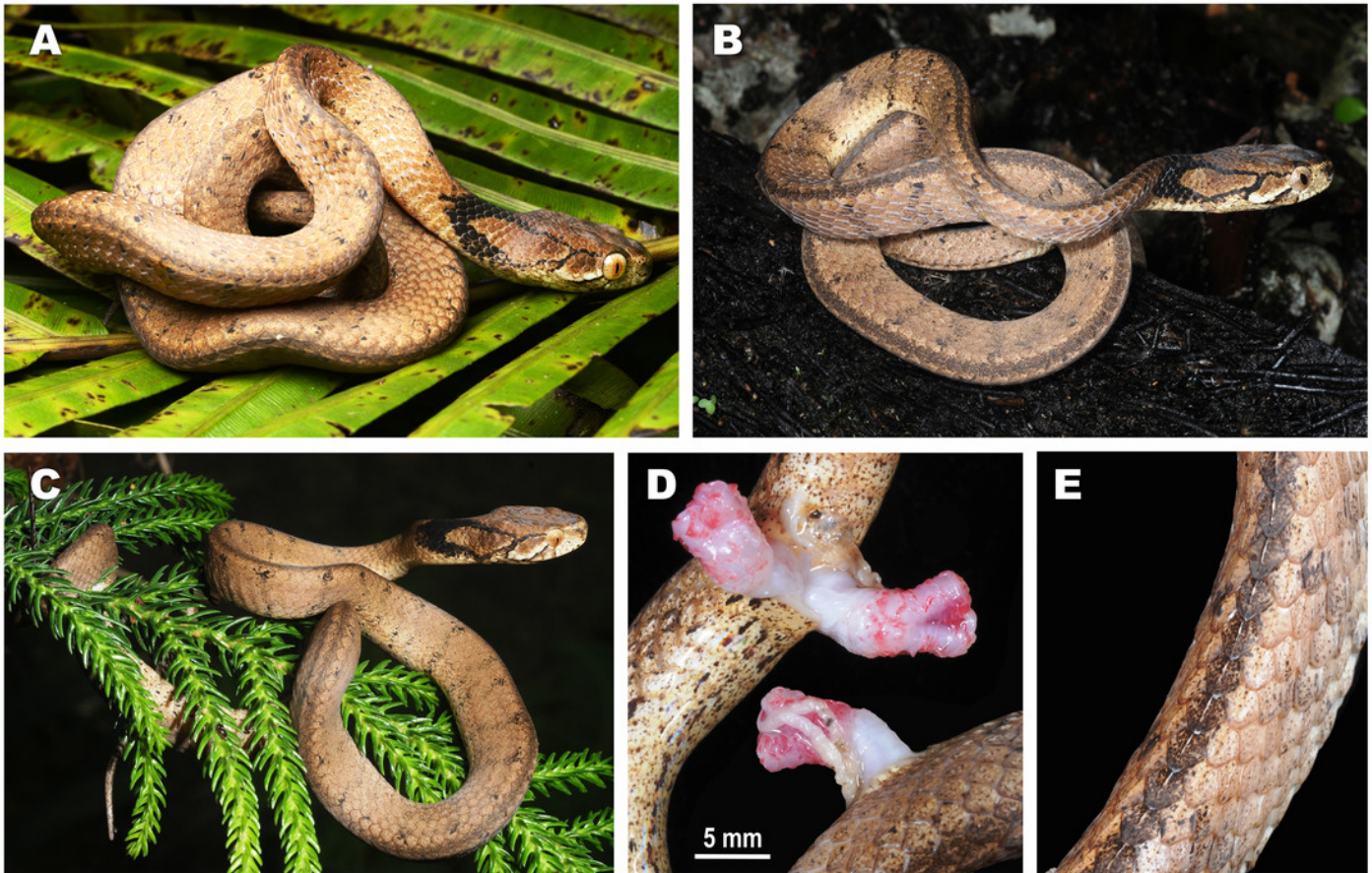


Figure 20

Figure 20. Specimen of *Pareas temporalis* Le, Tran, Hoang & Stuart, 2021 in preservative (ZMMU R-13656, adult male).

A - dorsal view of body; B - ventral view of body; C-E - head in lateral right, ventral, and dorsal aspects, respectively. Photos by G. Vogel.

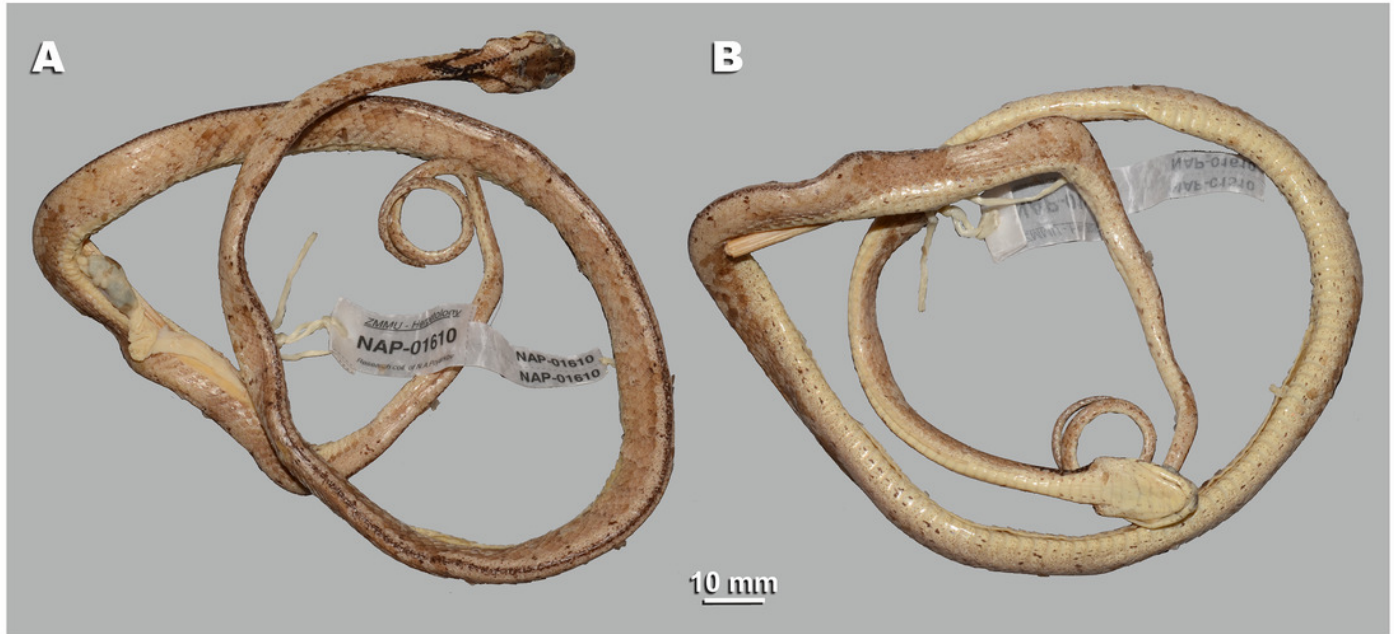


Figure 21

Figure 21. *Pareas temporalis* in life.

A - male specimen from Cat Loc, Lam Dong Province, Vietnam (ZMMU R-13656); B-C - female specimen from Di Linh, Lam Dong Province, Vietnam (SIEZC 20214); D - close-up of midbody of SIEZC 20214 showing all dorsal scales keeled (in 15 rows). Photos by N. A. Poyarkov (A), and L.H. Nguyen (B-D).

